7 Multiple Functions of Notch Signaling during Early Embryogenesis

Silvia L. López

CONTENTS

7.1. HISTORICAL BACKGROUND

The Notch pathway is a key cell-cell communication mechanism utilized during metazoan development. Its outcome depends on cell context: it can inhibit or promote cell fates, cell proliferation, or cell death through ligand-receptor signaling between neighboring cells (Kopan and Ilagan, 2009). The story of Notch began when John S. Dexter, in Thomas Hunt Morgan's laboratory, found a mutant phenotype in *Drosophila* with characteristic serrations at the wings' ends, which he called *Perfect Notched* (Dexter, 1914; Bridges and Morgan, 1916). This was caused by the disruption of a dominant sex-linked gene resulting in male lethality, which received the name *Notch* in subsequent publications (Bridges and Morgan, 1916; Morgan, 1917; Mohr, 1919). In the 1930s, Donald Poulson studied the lethal phenotype and noticed aberrant germ layer development (Poulson, 1937). This was later interpreted as a switch in ectodermal cell fate from dermoblast to neuroblast, since different mutant alleles of *Notch, Delta, mastermind, neuralized, Enhancer of split, almondex*, and *big brain* resulted in nervous system hypertrophy at the expense of the epidermis (Lehmann et al., 1983). These so-called "neurogenic" genes are all involved in the Notch pathway and have vertebrate counterparts (flybase.org; Lehmann et al., 1983; Thurmond et al., 2019).

Seven decades after Dexter's discovery, the fly *Notch* gene was cloned (Artavanis-Tsakonas et al., 1983), and the first vertebrate homologue, *notch1*, was isolated from *Xenopus laevis* (Coffman et al., 1990). Frog experiments using a construct lacking the extracellular domain provided the first clues that the Notch intracellular domain (NICD) mediates signal transduction (Coffman et al., 1993). This truncation resulted in a gain-of-function phenotype that affected germ layer development. Cloning the *Xenopus* gene encoding a ligand, Delta-like-1 (Dll1), demonstrated that Delta/Notch signaling plays a neurogenic role in vertebrates through lateral inhibition, as previously defined in *Drosophila* (Chitnis et al., 1995; Campos-Ortega, 1985; Lewis, 1998). Because of its relative simplicity, primary neurogenesis in *Xenopus* provided an ideal paradigm for Notch pathway research and for unraveling the molecular and cellular bases of vertebrate neural development. Since these ground-breaking studies, the accessibility of *Xenopus* embryos has made them an outstanding model for revealing the role of the Notch pathway in multiple developmental processes and for testing heterologous molecules from different species such as mouse and human, wild-type and mutant forms of pathway components, and to study their function and biochemical modulation *in vivo* (Ali et al., 2014; Hein et al., 2015; Oswald et al., 2016).

7.2. THE NOTCH PATHWAY

Most of what is known about Notch signaling can be categorized in either canonical or non-canonical pathways.

DOI: 10.1201/9781003050230-8

7.2.1. Canonical Notch Signaling

Excellent reviews describe the typical mechanism by which Notch signals, which is summarized in Figure 7.1A (Davis and Turner, 2001; Lai, 2004; Fortini, 2009; Kopan and Ilagan, 2009; Jorissen and De Strooper, 2010; Kovall and Blacklow, 2010; Tanigaki and Honjo, 2010; Groot and Vooijs, 2012; Bray, 2016). In the absence of signaling, a complex containing the DNA-binding protein RBPJ and co-repressors occupies the enhancers of Notch targets to silence them by recruiting histone deacetylases (HDACs) or other chromatin-modifying enzymes. When the mature Notch receptor is bound by a ligand, Delta (Dll), or Jagged (Jag), presented by the sending cell undergoes a conformational change that exposes a cleavage site in its extracellular domain, which is then cleaved by a membrane-tethered ADAM metalloprotease. This renders a membrane-tethered Notch intermediate (Notch extracellular truncation, NEXT), which is cleaved at the transmembrane domain by a γ-Secretase enzyme complex, whose active subunit is Presenilin (Psen). This releases the NICD, which enters the cell nucleus and forms a complex with RBPJ that recruits the co-activator Mastermind-like (MAML), displacing the RBPJ repressor complex and activating Notch-targets. Typically, Notch targets are members of the *hes/hey* gene families encoding bHLH-Orange (bHLH-O) transcriptional repressors.

Hes/Hey bHLH-O transcription factors (TFs) bind to their target DNA sequence through the basic domain, and also achieve transcriptional repression via: (1) a C-terminal tetrapeptide motif WRPW/Y that recruits transcriptional co-repressors of the TLE/Groucho family and (2) the Orange domain, located just C-terminal to the bHLH domain, that controls selection of the bHLH partner for heterodimerization. Hes proteins form homo- or heterodimers with Hey proteins and repress transcription actively or passively. Active repression involves DNA binding to the N box (CACNAG) or the class C site [CACG(C/A)G] and recruitment of TLE/Groucho co-repressors. Passive repression involves heterodimerization with other bHLH factors like E47. The WRPW motif is also necessary for polyubiquitylation, which confers short half-lives to Hes proteins by proteosome degradation, a key feature for their oscillatory expression during somitogenesis (see Section 3.6) (Davis and Turner, 2001; Bertrand et al., 2002; Huang et al., 2014; Kageyama et al., 2007; Imayoshi and Kageyama, 2014). Notably, Hey1 lacks the WRPW motif and does not bind TLE/Groucho (Pichon et al., 2004).

The traditional description of how the Notch pathway is used during development includes the following (Figure 7.1B). (1) In lateral inhibition, Notch prompts binary cell fate choices in cell populations of equal developmental potential. The ligand-sending cell signals to its neighbors, which in response repress ligand expression, "ligand-sending cell fate," and acquire an alternative fate or remain as uncommitted precursors. This usually results in salt-and-pepper patterns of cells of different fates, with roughly regular spacing between specific cell types. (2) In lateral induction, the ligand-sending cell induces ligand expression in its neighbors and instructs them to adopt the same fate. This propagates a cascade of Notch activation through a field of adjacent cells. Also, some cases of boundary formation between two cell populations involve lateral induction (Lewis, 1998; Gazave et al., 2009; Sjöqvist and Andersson, 2019). These models sometimes are insufficient to explain the complex mechanisms controlled by Notch (Favarolo and López, 2018).

7.2.2. Non-Canonical Notch Signaling

Several core components of the canonical Notch pathway also function in what are collectively known as non-canonical pathways; these are likely part of ancestral mechanisms for regulating cell differentiation in metazoans since the canonical pathway did not appear until the bilaterian lineage (Layden and Martindale, 2014). Non-canonical pathways have been described in different cell contexts and a variety of animal models, including (1) activation of Notch targets through NICD without RBPJ participation; (2) activation of Notch targets without NICD participation, with or without RBPJ mediation (Sanalkumar et al., 2010; Tanigaki and Honjo, 2010); (3) interaction with atypical ligands, atypical nuclear cofactors, and other signaling pathways (D'Souza et al., 2010; Heitzler, 2010); and (4) non-nuclear Notch activities, independent of typical ligand interaction and RBPJ-mediated transcription, involving the cytoplasmic tyrosine kinase Abl (Heitzler, 2010) or β-Catenin destabilization (Hayward et al., 2005; Hayward et al., 2008; Sanders et al., 2009; Muñoz-Descalzo et al., 2010; Acosta et al., 2011; Kwon et al., 2011). The latter was first described in *Xenopus* in the context of axis formation (see Section 3.1).

7.3. NOTCH SIGNALING DURING *XENOPUS* EMBRYOGENESIS

The *Xenopus laevis* and *tropicalis* genomes contain four Notch receptor genes (*notch1–4*), three Delta-like ligand genes (*dll1, dlc, dll4*), and two Jagged ligand genes (*jag1, jag2*) (Michiue et al., 2017; Karimi et al., 2018) (Table 7.1) (Figure 7.1). Members of two groups of *hes/hey* genes (*hey1/hey2/hey-L* and *hes1–7*) (Figure 7.2) are regulated by the canonical Notch pathway (Davis and Turner, 2001; Zhou et al., 2012) (Table 7.2). Most of them are up-regulated by Notch, but atypical responses were described for a few *hes1–7* genes (Tables 7.2, 7.3). In addition, cross-regulation between *Xenopus hes/hey* genes was described (Table 7.4).

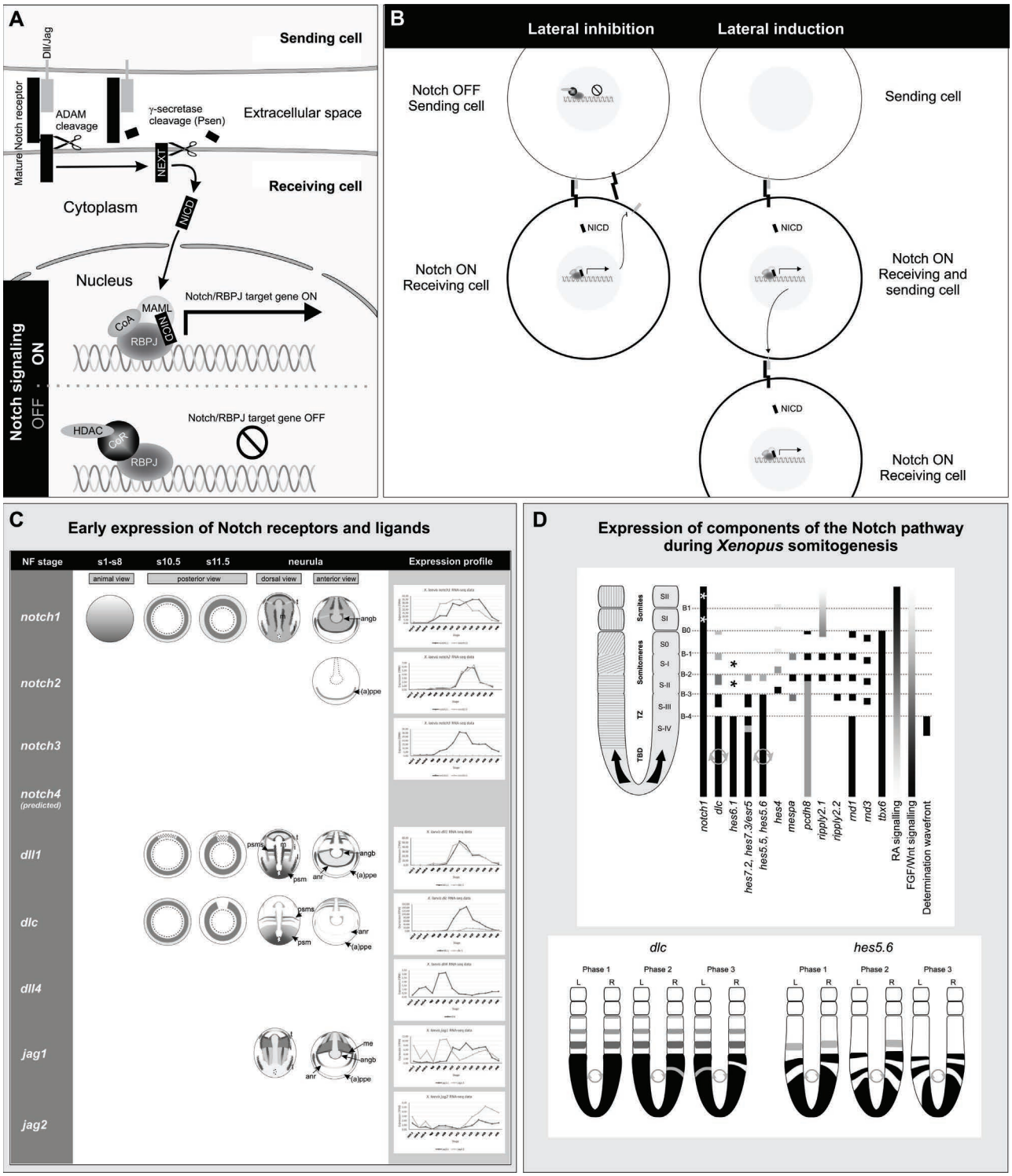

FIGURE 7.1 The canoncial Notch signaling device, expression of Notch receptors and ligands during early embryogenesis, and components of the Notch pathway during somitogenesis in *Xenopus*. (A) Simplified scheme showing the canonical Notch signaling pathway in vertebrates. CoA, co-activators; CoR, co-repressors; see additional abbreviations in the main text. (B) Modes of action of Notch signaling. (C) Early expression patterns of Notch receptors and ligands in *Xenopus*. References for building the expression domain's diagrams (left) are listed in Table 7.1. Quantitative expression profiles from *Xenopus laevis* (average TPM values from Taira and Ueno samples) were plotted with RefSeq data extracted from (Session et al., 2016) (right column). Abbreviations for Figure 7.1C and Figure 7.2: a, anterior; An, animal; anb, anterior neural border; anf, anterior neural fold; ang, anterior neural groove; angb, anterior neural groove border (prospective ventral forebrain and ventral midbrain) (Lahaye et al., 2002); anp, anterior neural plate; anr, anterior neural ridge; (d), deep layer; dbl, dorsal blastopore lip; dmz, dorsal marginal zone; ee, epidermal ectoderm; ego, early gastrula organizer; fp, floor plate; i, intermediate domain of primary neurogenesis; imz, involuting marginal zone; l, lateral domain of primary neurogenesis;

FIGURE 7.1 (Continued)
(l), lateral; lgo, late gastrula organizer; m, domain of primary neurogenesis adjacent to the midline; me, future mesencephalon; mhb, midbrain/hindbrain boundary; ncc, neural crest cells; ncb, neural crest boundaries; nb, neural border; nimz, non-involuting marginal zone; np, neural plate; npe, neural plate edge; (p), posterior; pm, prechordal mesoderm; psms, presomitic mesoderm stripe (indicative of somitogenesis); ppe, pre-placodal ectoderm; psm, pre-somitic mesoderm; prhc, prospective hypochord; prngb, prospective neural groove border; (s), superficial layer; Veg, vegetal; t, trigeminal ganglion. D. Expression of Notch pathway genes during *Xenopus* somitogenesis. Upper diagram: summary of the somitogenesis domains (left) and the expression of Notch pathway genes compared with RA and FGF/Wnt opposite gradients and other relevant segmentation genes discussed in the text (right) (adapted from Sparrow, 2008, with additional information from references listed in Table 7.12 and Kondow et al., 2007; Hitachi et al., 2008; Hitachi et al., 2009; Goda et al., 2009). Before segmentation, *Xenopus* myotomal cells form a parallel array that lies perpendicular to the embryonic long axis and undergoes a 90-degree rotation associated with the appearance of the intersegmental furrow during segmentation (left). A consistent nomenclature for somitogenesis domains and the distinct phases of cyclic gene expression in the presomitic mesoderm (PSM) was conventionally adopted for all vertebrate species (Pourquié and Tam, 2001) (right). In the already segmented paraxial mesoderm, somites are numbered with Roman numerals, with SI the most recently formed one. S0 is the most anterior presumptive somite in the PSM, which is about to be segmented, followed caudally by prospective somites sequentially numbered with negative Roman numerals. Borders between prospective somites (B) are numbered with negative Arabic numerals, with B0 the intersegmental fissure between SI and the PSM (Pourquié and Tam, 2001). The PSM is divided into three regions, according to gene expression patterns. The region encompassing S0 to S-II is known as the somitomere region; S-III and S-IV make up the transition zone (TZ); caudal to the TZ is the tailbud domain (TBD), populated by immature paraxial mesoderm cells (Moreno and Kintner, 2004; Sparrow, 2008). As the embryo elongates caudally, new paraxial cells are produced at the caudal tip of the TBD and are displaced anteriorly (arrows), gradually occupying the TZ, then forming somitomeres (S-III through S0) and finally segregating as a mature somite (S1) from the anterior end of the PSM. Gene expression domains are shown with black/gray bars. Known oscillating behavior is indicated by a circle with double arrows. When the expression of a gene was not studied with enough detail to assign a precise location, asterisks indicate their approximate expression. See Table 7.12 for more details. Lower diagrams: typical expression phases of the oscillatory genes *dlc* and *hes5.6* in the *Xenopus* PSM.

Source: Adapted from Durston et al. (2018), Kirby et al. (2003).

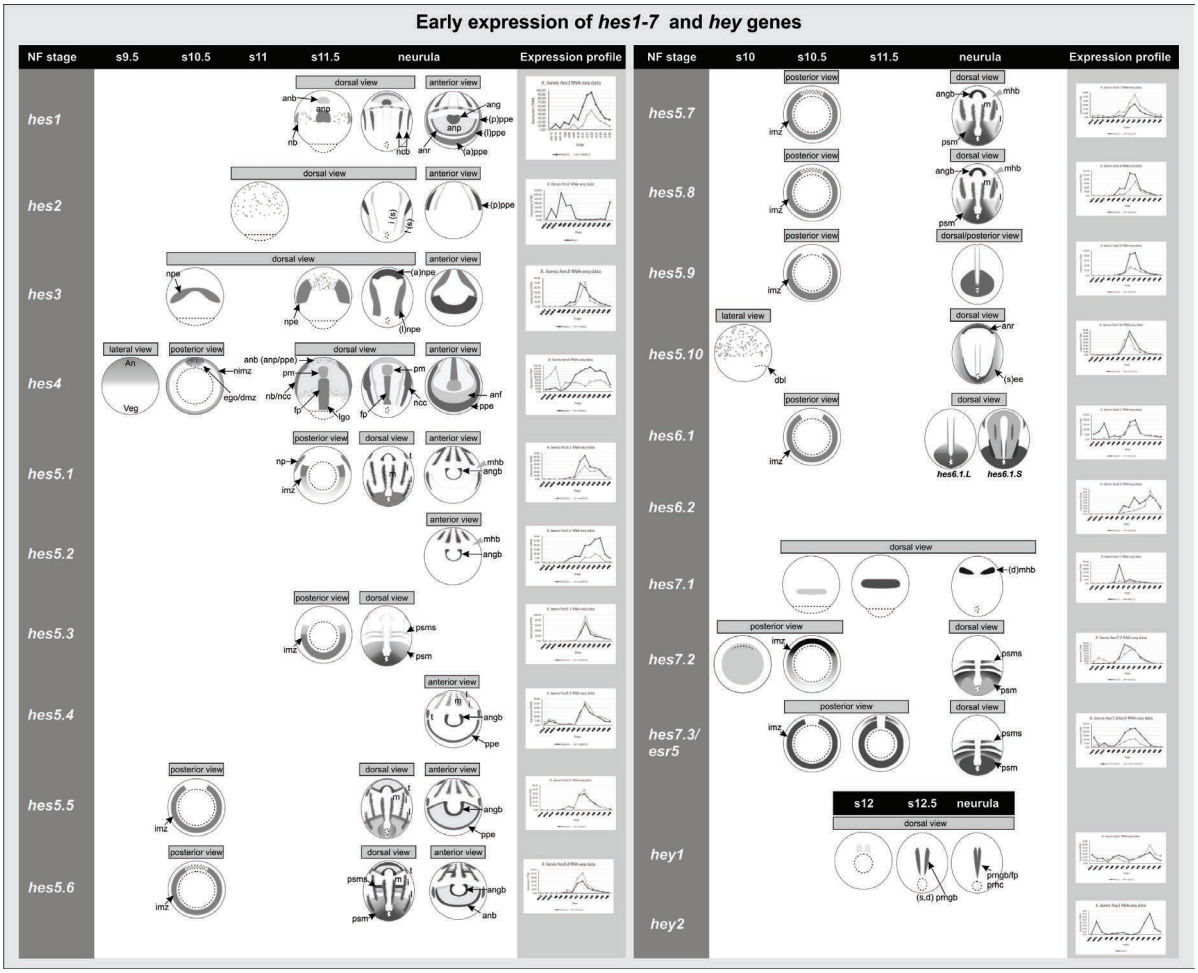

FIGURE 7.2 Early expression patterns of *hes4–7* and *hey* genes in *Xenopus*. References for building the expression domain diagrams (left) are listed in Table 7.2. Quantitative expression profiles from *Xenopus laevis* (average TPM values from Taira and Ueno samples) were plotted with RefSeq data extracted from (Session et al., 2016) (right column). See abbreviations in Figure 7.1 legend.

TABLE 7.1
Main Components of the Notch Pathway in *Xenopus*

Components of the Notch pathway present in *Xenopus tropicalis* and *Xenopus laevis* with current nomenclature were obtained from Michiue et al. (2017) and Xenbase (www.xenbase.org/, RRID:SCR_003280; Karimi et al., 2018). Until very recently, it was believed that only three of the four mammalian orthologues encoding Notch receptors were present in the *Xenopus* genome (Michiue et al., 2017). However, a gene model for *notch4* recently appeared in Xenbase. Besides, the *X. laevis dll4* gene was wrongly identified as a singleton in the transcriptomic analysis of Session et al. (2016; Michiue et al., 2017). Two *rbpj* isoforms were identified in *X. laevis*. Originally, they were termed *XSu(H)1* and *XSu(H)2* (Wettstein et al., 1997; Ito et al., 2007a; Ito et al., 2007b). Transcripts differ in their 5'UTRs, but their predicted protein sequences are almost identical, except for a 20 residue length difference at their N-termini (Wettstein et al., 1997; Ito et al., 2007a). With the availability of the *X. laevis* genome, now it is possible to predict that both are variants from the *RBPJ.S* homeolog. *XSu(H)2* is referred to as *rbpj.S-v2* to distinguish it from the *XSu(H)1* variant (referred to as *rbpj.S-v1*) that was studied elsewhere since Wettstein et al. (1997); it is now clear that *X. laevis* also has an *rbpj.L* homeolog (Michiue et al., 2017). The first (S1 cleavage) of Notch occurs in the secretory pathway, where a furin-like convertase processes the Notch full-length polypeptide. This generates the mature receptor, consisting of a NECD-NTMIC heterodimer (Notch extracellular domain-Notch transmembrane and intracellular domain), with both polypeptides bound by non-covalent interactions. ADAM10 is the best confirmed candidate in cleaving the mature receptor at the S2 site in the extracellular domain, as a consequence of ligand binding (Groot and Vooijs, 2012). Other core components of the pathway are discussed in more detail in the text.

Main Components of the Notch Pathway		*X. tropicalis*	*X. laevis (homeologs)*	Synonyms	Expression (References for Figure 7.1)
Receptors	Notch	*notch1*	*notch1.L* *notch1.S*	*L: LOC108698191* *S: notch, xotch, xnotch, notch-1, xnotch1, x-notch-1*	(Chitnis et al., 1995; Andreazzoli et al., 2003; López et al., 2003; Yan and Moody, 2007; Miazga and McLaughlin, 2009; Castro Colabianchi et al., 2018)
		notch2	*notch2.L* *notch2.S*	*ags2*	(Ogino et al., 2008)
		notch3	*notch3.L* *notch3.S*	*casil, cadasil*	
		notch4	*notch4.L* *notch4.S*	*L: loc108700568* *S: loc100488695*	
Ligands	Delta-like	*dll1*	*dll1.L* *dll1.S*	*X-delta-1*, *delta1*, *delta-1*, *Xdelta-1, XDelta1, x-delta, Delta-1*, *Xdelta1*	(Chitnis et al., 1995; Beck and Slack, 1998; Howell et al., 2002; López et al., 2005; Nichane et al., 2008b; Ogino et al., 2008)
		dlc	*dlc.L* *dlc.S*	*x-delta-2, delta-2, delta2, X-Delta, dll3*	(Jen et al., 1997; Peres and Durston, 2006; Peres et al., 2006; Ogino et al., 2008; Onai et al., 2015)
		dll4	*dll4.L* *dll4.S*	*delta 2*	
	Jagged	*jag1*	*jag1.L* *jag1.S*	*X-Serrate-1, serrate-1, serrate*, *jagged1*	(Kiyota et al., 2001)
		jag2	*jag2.L* *jag2.S*		
Processing	Furin (S1 cleavage, secretory pathway)	*furin*	*furin.L* *furin.S*	*PACE, spc1, xfurin*	
	ADAM-secretase (S2 cleavage)	*adam10*	*adam10.L* *adam10.S*	*xadam10*, *kuz, ad10*, *madm, cd156c*, *kuzbanian*	
	Presenilin (the active subunit of the γ-secretase complex, S3 cleavage)	*psen1*	*psen1.L* *psen1.S*	*L: presenilin-alfa, X-PS-alpha*	
		psen2	*psen2.L* *psen2.S*	*S: presenilin-beta, X-PS-beta*	
Transcription factor	RBPJ	*rbpj*	*rbpj.L* *rbpj.S*	*X-Su(H), XSu(H), Su(H), suppressor of hairless, rbpsuh, CBF1, csl, lag-1, CBF-1* *L: LOC108698058*; *S: X-Su(H)1 and 2*	
Transcriptional co-activator	Mastermind-like (MAML)	*maml1*	*maml1.L* *maml1.S*	*XMam1, Mastermind1, mam1, mam-1, Mastermind*	
		maml2	*maml2.L* *maml2.S*		
		maml3	*maml3.L* *maml3.S*		

TABLE 7.2
Genes of the *hes1–7* and *hey* Groups in the *Xenopus tropicalis* and *Xenopus laevis* Genomes and Their Responsiveness to Notch Signaling

Data for building the list of genes were obtained from Watanabe et al. (2017) and Xenbase (xenbase.org, RRID:SCR_003280; Karimi et al., 2018). The nomenclature proposed by Watanabe et al. (2017) was based on phylogenetic and syntenic analyses that revealed that the old names were misleading. The current nomenclature in Xenbase coincides with that proposed by Watanabe et al. (2017), except for *hes7.3*, which is still named *esr5* in Xenbase. Therefore, this gene is referred to as *hes7.3/esr5* throughout the chapter. Whenever possible, the correspondences of L and S homeologs with old synonyms were checked according to RefSeqs and are indicated. See Table 7.3 for details of experimental evidence of Notch responsiveness. *esr9b* (accession no. AB211547) was considered in Takada et al. (2005) as a possible *esr9* pseudoallele and was called thereafter as *esr9* for simplicity in that publication, leading to confusion with a different gene, *hes5.6.L*, which was also previously called *esr9*. The sequence AB211547 corresponds to Xenbase:XB-GENE-6253435 or *hes5.7.L*. The *X. laevis* gene formerly known as *hes9.1.S* is indeed on the L chromosome and is currently named *hes5.8.L* (Watanabe et al., 2017).

X. tropicalis	X. laevis	Synonyms	Notch Responsiveness	Expression (References for Figure 7.2)
hes1	*hes1.L* *hes1.S*	*hairy1, Xhairy1, hes-1* *L: hes1-a; S:hes1-b*	Positive	(Andreazzoli et al., 2003; Vega-López et al., 2015; Hardwick and Philpott, 2019)
hes2	*hes2.L*	*Xhes2*	Positive	(Sölter et al., 2006; Riddiford and Schlosser, 2016)
hes3	*hes3.L* *hes3.S*		Positive	(Hong and Saint-Jeannet, 2018)
hes4	*hes4.L* *hes4.S*	*Xhairy2, hairy2, H2* *L: hairy2b, Xhairy2b, hes4b, hes4-b; S: hairy2a, XHairy2a, hes4a, hes4-a*	Positive	(Turner and Weintraub, 1994; Tsuji et al., 2003; López et al., 2005; Murato et al., 2007; Nichane et al., 2008b; Nichane et al., 2008a; Murato and Hashimoto, 2009; Aguirre et al., 2013; Vega-López et al., 2015)
hes5.1	*hes5.1.L* *hes5.1.S*	*esr1, esr-1, XESR-1* *L: hes5-like; S: ESR1b*	Positive	(Lamar et al., 2001; Takada et al., 2005; Kuriyama et al., 2006; Blewitt, 2009; Maguire et al., 2012)
hes5.2	*hes5.2.L* *hes5.2.S*	*bHLHb38, esr3. L: esr7, esr-7, hes5.2-a; S: ESR3/7b, hes5.2-b*	Positive	(Nieber et al., 2013; Heeg-Truesdell and LaBonne, 2006)
hes5.3	*hes5.3.L* *hes5.3.S*	*L: esr2, hes3.3*	Positive	(Hayata et al., 2009; Blewitt, 2009; Maguire et al., 2012)
hes5.4	*hes5.4.L* *hes5.4.S*	*hes8*	Positive	(Riddiford and Schlosser, 2016)
hes5.5	*hes5.5.L* *hes5.5.S*	*L: HES-5-like, hes10.L; S: esr10.S, esr10xb, 11A10*	Positive	(Gawantka et al., 1998; Miazga and McLaughlin, 2009; Nieber et al., 2013)
hes5.6	*hes5.6.L* *hes5.6.S*	*L: hes9.1.L, esr9, 8C9; S: hes-5 like*	Positive	(Gawantka et al., 1998; Li et al., 2003; Miazga and McLaughlin, 2009; Riddiford and Schlosser, 2016)
hes5.7	*hes5.7.L* *hes5.7.S*	*esr9, hes9.1-b. L: ESR9b, hes9.1.S; S: HES-5-like vX1*	Positive	(Takada et al., 2005; Taverner et al., 2005; Xenbase community submitted by Nicolas Pollet; Karimi et al., 2018; www.xenbase.org/, RRID:SCR_003280)
hes5.8	*hes5.8.L* *hes5.8.S*	*Xtr: loc100495414* *Xla: L: loc108696616; S: loc108697696, hes5_x2*	Unknown	(Pollet et al., 2005; Xenbase community submitted by Nicolas Pollet; Karimi et al., 2018; www.xenbase.org/, RRID:SCR_003280)
hes5.9	*hes5.9.L* *hes5.9.S*	*Xtr: loc733709* *Xla: L: loc108696614; S: loc108697697, hes5_x1*	Unknown	(Kjolby and Harland, 2017)
hes5.10	*hes5.10.L* *hes5.10.S*	*esr6e, esr-6e. L: hes3.1.L; S: hes3.1.S*	Positive Atypical response to RBPJ	(Chalmers et al., 2002; Chen et al., 2005; Xenbase community submitted by Naoto Ueno; Karimi et al., 2018; www.xenbase.org/, RRID:SCR_003280)
hes6.1	*hes6.1.L* *hes6.1.S*	*XHes6, Xhes-6. L: clone 29B3–2; S: clone 10C6*	Negative	(Koyano-Nakagawa et al., 2000; Cossins et al., 2002; Hufton et al., 2006; Murai et al., 2007; Murai et al., 2011; Kjolby and Harland, 2017)
hes6.2	*hes6.2.L* *hes6.2.S*		Negative, Positive	
hes7.1	*hes7.1.L* *hes7.1.S*	*HES-related 1, XHR1*	Positive	(Shinga et al., 2001; Takada et al., 2005)
hes7.2	*hes7.2.L* *hes7.2.S*	*esr4, ESR-4, enhancer-of-split-related 4, ESR 4*	Positive	(Gawantka et al., 1998; Taverner et al., 2005; Peres et al., 2006; Xenbase community submitted by Naoto Ueno; Karimi et al., 2018; www.xenbase.org/, RRID:SCR_003280)
hes7.3/esr5	*hes7.3.L/esr5.L* *hes7.3.S/esr5:S*	*L: esr5, x-esr5, Xesr5, ESR 5*	Negative, Positive	(Taverner et al., 2005; Blewitt, 2009; Kinoshita et al., 2011; Kjolby and Harland, 2017; Janesick et al., 2017)
hey1	*hey1.L* *hey1.S*	*hrt1, XHRT1, chf2, hrt-1, hesr1, herp2, oaf1, bc8*	Positive	(Pichon et al., 2002)
hey2	*hey2.L*	*hesr2, gridlock*	Unknown	

TABLE 7.3
Experimental Evidence for the Responsiveness of *hes1–7* and *hey* Genes to the Notch Pathway in *Xenopus*

No references were found for *hes5.8, hes5.9*, and *hey2* regulation by the Notch pathway in *Xenopus*, and therefore they are not listed in this table. Abbreviations for Tables 7.3 to 7.12: AP, anterior-posterior; aPM, anterior prechordal mesoderm; ANB, anterior neural border; bHLH, basic helix-loop-helix; ChIP, chromatin immunoprecipitation; CHX, cycloheximide (an inhibitor of protein synthesis); Dex, dexamethasone; DIMZ, dorsal involuting marginal zone; *dll1STU*, antimorph of *dll1*, lacking the intracellular domain (Chitnis et al., 1995); DML, dorsal midline; DMZ, dorsal marginal zone; DN, dominant-negative; DBM, DNA binding mutant; DNIMZ, dorsal non-involuting marginal zone; E1A constructs, protein of interest fused to the activation domain of the human type 5 adenovirus E1a protein; EnR constructs, protein of interest fused to the *Drosophila* Engrailed repressor domain; ER-constructs, hormone-inducible forms of proteins with nuclear functions under the control of the ligand-binding domain of the human estrogen receptor. These recombinant fusion proteins translocate to the cell nucleus when estradiol (E2) is added to the culture medium at the desired NF stage; FP, floor plate (ventral midline of the neural tube); GO, gastrula organizer; GR-constructs, hormone-inducible forms of proteins with nuclear functions under the control of the ligand-binding domain of the human glucocorticoid receptor. These recombinant fusion proteins translocate to the cell nucleus when Dex is added to the culture medium at the desired NF stage; GR-*NICD1*–22: hormone-inducible form of the *X. laevis* Notch1 intracellular domain (Wettstein et al., 1997); HDAC, histone deacetylase; HUA, hydroxyurea and aphidicolin (strong inhibitors of cell proliferation); ICD, intracellular domain; IMZ, involuting marginal zone; ISH, *in situ* hybridization; MHB, midbrain/hindbrain boundary; MO, antisense morpholino oligonucleotide; NB, neural border; NCCs, neural crest cells; NF, Nieuwkoop and Faber stage of development in *Xenopus*; NICD, Notch intracellular domain (NICD constructs are constitutively active); NIMZ, non-involuting marginal zone; *notch1-ΔE*, *notch1* construct without most of the extracellular domain, constitutively active; pH3, phosphorylated form of histone H3 (marker of cell proliferation); PN, primary neurogenesis; PPE, pre-placodal ectoderm; pPM, posterior prechordal mesoderm; PSM, presomitic mesoderm; RA, retinoic acid; RAR, retinoic acid receptor; *RBPJ,* recombination signal binding protein for immunoglobulin kappa J region, transcription factor that mediates canonical Notch signaling; *RBPJ-Ank*: constitutively active form of the transcription factor RBPJ, consisting of the *X. laevis* Notch1 ankyrin repeats fused to the C-terminus of *X. laevis* RBPJ (Wettstein et al., 1997); *RBPJDBM*, DNA binding mutant form of *X. laevis* RBPJ that binds to NICD but lacks the ability to bind target sites in the DNA and acts as a dominant-negative protein by forming non-functional complexes (Wettstein et al., 1997); sq, semiquantitative; TBD, tailbud region of the presomitic mesoderm; TF, transcription factor; TZ, transition zone of the presomitic mesoderm; VMZ, ventral marginal zone; Δ, deletion; ↑up-regulation, expansion, or increase; ↓down-regulation, reduction, or decrease.

Gene	Regulated by	Regulation/Details	Gain-of-Function	Loss-of-Function (Dominant-Negative/Antagonist/Morpholino)
hes1	*dll1/ notch/ RBPJ*	Positive in pronephros and neural plate.	GR-*RBPJ-Ank*, Dex NF18: ↑*hes1* in pronephros (Taelman et al., 2006). GR-*RBPJ-Ank*, Dex unstated stage: ↑*hes1* neural plate domains (Vega-López et al., 2015).	*RBPJDBM* ↓ *hes1* in pronephros (Taelman et al., 2006). *dll1STU* ↓*hes1* in neural plate domains (Yan et al., 2009; Vega-López et al., 2015).
hes2	*notch1/ RBPJ*	Positive in NB.	*NICD1* or *RBPJ-Ank*: ectopic *hes2* restricted to the lateral border of the neural plate (Sölter et al., 2006).	
hes3	*notch1*	Positive.	*NICD1:* ↑*hes3* (NF18, microarray) (Vasiliu et al., 2015).	
hes4	*dll1/ notch1/ RBPJ*	Positive in NB/NCC.	*NICD1:* ↑NB *hes4* domain (gastrulation, ISH) (López et al., 2005). *GR-RBPJ-Ank* or *GR-NICD1–22:* Dex, unstated stage: ↑ NCC *hes4* domain (neural plate stage) (Vega-López et al., 2015). Dex NF12: ↑ NCC *hes4* domain (neural fold stage) (Glavic et al., 2004).	*GR-RBPJDBM* (Dex NF12): ↓*hes4* NCC domain at neural fold stage (Glavic et al., 2004). *dll1STU*: ↓*hes4* in NCC (neural plate stage) (Vega-López et al., 2015).
	notch/ RBPJ	No regulation in NCC.	*GR-RBPJ-Ank* (Dex NF11): did not affect the NCC *hes4* domain at neural plate stage (Nichane et al., 2008a).	*GR-RBPJDBM* (Dex NF11): did not affect the NCC *hes4* domain at neural plate stage (Nichane et al., 2008a).

(*Continued*)

TABLE 7.3 (Continued)

Experimental Evidence for the Responsiveness of *hes1–7* and *hey* Genes to the Notch Pathway in *Xenopus*

Gene	Regulated by	Regulation/Details	Gain-of-Function	Loss-of-Function (Dominant-Negative/Antagonist/Morpholino)
	dlc/notch/ RBPJ	Positive in somitogenesis. *dlc* and *hes4:* complementary expression patterns in somitomeres, consistent with an inductive role of *dlc* on *hes4* through Notch activation in neighboring cells (Jen et al., 1997).		*dlc-tr* or *RBPJDBM: s*uppressed the segmental *hes4* prepattern in somitomeres (Jen et al., 1997). *dlc* MO: ↓*hes4* (ISH, tailbud stage) (Peres et al., 2006).
	notch/ RBPJ *hes4* 3'UTR	Positive. A paired RBPJ motif in the proximal promoter and a minimal 25 bp sequence in the 3'UTR, are necessary for *hes4* expression in neural tissue, pronephros, and anterior PSM, but are insufficient for *hes4* expression in the FP. 3UTR confers global instability to *hes4* mRNA, except in the anterior PSM. *In vivo* gene reporter, tailbud stage (Davis et al., 2001). Notch1 is associated with the RBPJ site of the *hes4* genomic loci (ChIP assay, NF25) (Sakano et al., 2010).		
	dll1/ notch1/ RBPJ	Positive in DML precursors during gastrulation.	*NICD1:* ↑*hes4*+ population of FP precursors in the GO and *hes4* FP domain in neurulae (López et al., 2005). *dll1* overexpression*:*↑*hes4*+ population of FP precursors in the GO (López et al., 2005).	*RBPJ*DBM: ↓*hes4*+ population of FP precursors in the GO and *hes4* FP in neurulae (López et al., 2005).
	dll1/ notch1	Positive in ectoderm.	*NICD1:* ↑*hes4* in animal caps (RT-PCR, NF20) and cell-autonomously in ectoderm (ISH, NF20) (Cui, 2005).	*dll1STU:* prevented the induction of *hes4* by *neurog2* in animal caps (RT-PCR, NF20) (Cui, 2005).

hes5.1	*dll1/ notch1/ RBPJ/ maml1*	Positive. An HDAC inhibitor enhanced *hes5.1* response to induction by *dll1* in neuralized animal caps, supporting the hypothesis that activation by Dll1/Notch disrupts the formation of the repressor complex containing RBPJ and HDAC-1 that maintains Notch-target genes repressed in the absence of Notch signaling (Kao et al., 1998). Paired RBPJ binding site proximal to the TATA box, necessary but not sufficient for neural expression *in vivo* (Lamar and Kintner, 2005).	*NICD1*: ↑*hes5.1* in animal caps (NF10.5, sqRT-PCR) (Kinoshita et al., 2011) and whole embryos (NF18, 28, microarray) (Vasiliu et al., 2015). (RT-qPCR, sometime between NF9.5–10) (Mir et al., 2008). Induced ectopic *hes5.1* in neural and non-neural ectoderm (neural plate stage) (Deblandre et al., 1999). *dll1* overexpression, *RBPJ-Ank* or *NICD1* but not *RBPJ*: ↑*hes5.1* in neuralized or naive animal caps (neurula stage) (Wettstein et al., 1997; Lamar et al., 2001; Lahaye et al., 2002; Pichon et al., 2002). The RAM23 domain and ankyrin repeats (Ank) of NICD1 were essential for this induction, with some contribution of sequences downstream of the Ank repeats (Wettstein et al., 1997). *hGR-NICD1(22)* or GR-*RBPJ*-Ank (Dex 1 hr.) +/− CHX: ↑*hes5.1* in neuralized animal caps (Wettstein et al., 1997). *hGR-NICD1(22)* or *hGR-RBPJ-Ank*, Dex 30 min: ↑*hes5.1* in neuralized animal caps (Lahaye et al., 2002). *hGR-RBPJ-Ank*, Dex 1 hr +/− CHX: ↑*hes5.1* in naive animal caps (Lahaye et al., 2002). *RBPJ.S v2-Ank* ↑ *hes5.1* in naive animal caps (RT-sqPCR) (Ito et al., 2007b). *RBPJ* overexpression: inhibited *hes5.1* induction by *dll1* in neuralized animal caps (similar to *RBPJDBM*) (Wettstein et al., 1997).	*RBPJDBM:* suppressed *NICD1*'s ability to induce *hes5.1* in naive animal caps (neurula stage) (Lahaye et al., 2002; Pichon et al., 2002) and *dll1*'s or *neurog2*'s ability to induce *hes5.1* in neuralized animal caps (Wettstein et al., 1997; Lamar et al., 2001). *hes5.1* was downregulated in embryos derived from *RBPJDBM*-injected oocytes (RT-qPCR, sometime between NF9.5–10) (Mir et al., 2008). *RBPJ.S v2DBM:* ↓*hes5.1* in naive animal caps (RT-sqPCR) (Ito et al., 2007b). *DN-maml1:* ↓*hes5.1* in domains of PN (Katada and Kinoshita, 2003).
	jag1	Positive during PN.	*jag1* overexpression but not *jag1*ICD: ↑ *hes5.1* in neuralized animal caps (Kiyota and Kinoshita, 2004).	
hes5.2	*notch1/ RBPJ*	Positive in the ectoderm/neuroectoderm. Paired RBPJ binding site proximal to the TATA box (Lamar and Kintner, 2005).	*NICD1:* induced ectopic *hes5.2* in neural and non-neural ectoderm (Deblandre et al., 1999): ↑*hes5.2* in neuralized animal caps (NF14–15) (Sölter et al., 2006) and whole embryos (NF18, NF28, microarray) (Vasiliu et al., 2015).	
hes5.3	*notch1*	Positive.	*NICD1:* ↑*hes5.3* (NF18, NF28, microarray) (Vasiliu et al., 2015).	
hes5.4	*notch1/ RBPJ*	Positive in placodes.	*NICD1:* ↑*hes5.4* in placodes and adjacent non-neural ectoderm, even in the absence of function of the PPE genes *six1/eya1* (ISH, neural plate stage) (Riddiford and Schlosser, 2017).	*RBPJDBM:* ↓*hes5.4* in neural plate and placodes (ISH, neural plate stage) (Riddiford and Schlosser, 2017).

(*Continued*)

TABLE 7.3 (Continued)

Experimental Evidence for the Responsiveness of *hes1–7* and *hey* Genes to the Notch Pathway in *Xenopus*

Gene	Regulated by	Regulation/Details	Gain-of-Function	Loss-of-Function (Dominant-Negative/Antagonist/Morpholino)
hes5.5	*notch1*	Positive.	*NICD1:* ↑*hes5.5* (NF18, 28; microarray) (Vasiliu et al., 2015).	
	RBPJ	Positive in the nervous system. A paired RBPJ binding site proximal to the TATA box is necessary but not sufficient for neural expression *in vivo* (Lamar and Kintner, 2005).		
	notch1/ RBPJ	Positive in the IMZ.	*GR-RBPJ-VP16* or *GR-NICD1* (Dex NF10): ↑IMZ *hes5.5* domain (gastrula, ISH) (Miazga and McLaughlin, 2009).	*GR-RBPJ-EnR* (Dex NF10): ↓IMZ *hes5.5* domain (gastrula, ISH) (Miazga and McLaughlin, 2009).
hes5.6	*notch1*	Positive.	*NICD1:* ↑*hes5.6* (NF18, 28; microarray) (Vasiliu et al., 2015).	
	notch1/ RBPJ	Positive during gastrulation/IMZ.	*GR-RBPJ-VP16* or *GR-NICD1* (Dex NF10): ↑IMZ *hes5.6* domain (gastrula, ISH) (Miazga and McLaughlin, 2009).	*GR-RBPJ-EnR* (Dex NF10): ↓IMZ *hes5.6* domain (gastrula, ISH) (Miazga and McLaughlin, 2009).
			NICD1: ↑*hes5.6* (mid-gastrula, RT-qPCR, NF11) (Castro Colabianchi et al., 2018).	*notch1* MO: ↓*hes5.6*; rescued by *NICD1* (RT-qPCR, NF11) (Castro Colabianchi et al., 2018)
hes5.7	*notch1*	Positive.	*NICD1:* ↑*hes5.7* (NF28, microarray) (Vasiliu et al., 2015).	
hes5.10	*notch1/* atypical response to *RBPJ*.	Positive in the non-neural ectoderm.	*NICD1:* ↑*hes5.10* throughout the non-neural ectoderm (NF14) (Deblandre et al., 1999); ↑*hes5.10* (NF18, NF28, microarray) (Vasiliu et al., 2015).	*RBPJDBM:* ↑*hes5.10* in the inner cells of isolated ectoderm (NF11, RNAse protection) (Deblandre et al., 1999).
hes6.1	*notch1/ RBPJ*	Negative in the neural plate.	*NICD1:* ↓*hes6.1* (a positive regulator of neurogenesis) in the neural plate and did not appear to affect expression in PSM at neurula stage (Koyano-Nakagawa et al., 2000), although some expansion in the PSM staining in Figure 3A of this work is noticed.	*RBPJDBM:* ↑*hes6.1*+ cell population in the neural plate [data not shown in (Koyano-Nakagawa et al., 2000)].
hes7.1	*notch1*	Negative regulation in MHB establishment (non-canonical pathway?).	*NICD1:* ↓*hes7.1* at the MHB (NF13) (Takada et al., 2005).	*RBPJDBM:* did not affect *hes7.1* expression at the MHB (Takada et al., 2005).
	notch1	Positive.	*NICD1:* ↑*hes7.1* (NF28, microarray) (Vasiliu et al., 2015).	
hes7.2	*dlc/ notch/ RBPJ*	Positive in somitogenesis.	*dlc* overexpression or *RBPJ-Ank:* expanded *hes7.2* into the gaps of the somitomeric region (ISH late neurula/early tailbud) (Jen et al., 1999).	*RBPJDBM:* ↓*hes7.2* in the somitomeric, TZ, and TBD regions (ISH late neurula/early tailbud) (Jen et al., 1999; Peres et al., 2006).
			dlc overexpression or *NICD1*: loss of the stripped *hes7.2* pattern in the somitomeric region (ISH, neurula) (Peres et al., 2006).	*dlc* MO: ↓ *hes7.2* (ISH, neurula) (Peres et al., 2006).
	notch1	Positive.	*NICD1:* ↑*hes7.2* (NF28, microarray) (Vasiliu et al., 2015).	

hes7.3/esr5	*dlc/ notch/ RBPJ*	Positive in somitogenesis.	*dlc* overexpression or *RBPJ-Ank:* expanded *hes7.3/esr5* expression into the gaps of the somitomeric region (ISH late neurula/early tailbud) (Jen et al., 1999).	*RBPJDBM:* ↓*hes7.3/esr5* in the somitomeric region and the TZ but not in the TBD (ISH late neurula/early tailbud) (Jen et al., 1999).
	notch1	Positive.	*NICD1:* ↑*hes7.3/esr5* (NF28, microarray analysis) (Vasiliu et al., 2015).	
	notch1/ hes5.1	Negative during mesoderm induction.	*NICD1:* unable to induce *hes7.3/esr5* in naive animal caps. *NICD1* or *hes5.1:* inhibited the induction of *hes7.3/esr5* by the mesodermal inducer *nodal2* in animal caps (NF10.5, sqRT-PCR). *hes5.1* overexpression*:* ↓*hes7.3/esr5* in the IMZ (NF10.5, ISH) (Kinoshita et al., 2011).	*hes5.1 ΔWRPW:* ↑*hes7.3/esr5* in animal caps mesodermalized by *nodal2* (NF10.5, sqRT-PCR) (Kinoshita et al., 2011).
hey1	*notch1/ RBPJ*	Positive.	*RBPJ-Ank* or *NICD1*: ectopic *hey1* in whole embryos and ectodermal explants (neurula) (Pichon et al., 2002).	*RBPJDBM:* ↓*NICD1*'s ability to induce ectopic *hey1* in whole embryos and ectodermal explants (Pichon et al., 2002).
	notch1/ RBPJ	Positive (head, somites, pronephros).	GR-*NICD1* or GR-*RBPJ-VP16*, Dex NF11–13 or NF15–19, ISH NF24–30: ↑*hey1* in all domains, except in the pronephros with the early Dex treatment (↓*hey1*) (Rones et al., 2002).	GR-*RBPJDBM*, Dex NF11–13 or NF15–19 ISH NF24–30: ↓*hey1* (Rones et al., 2002).
	notch1	Positive.	*NICD1:* ↑*hey1* (NF18, NF28, microarray analysis) (Vasiliu et al., 2015).	

TABLE 7.4
Cross-Regulation between *hes* and *hey* Genes in *Xenopus*

See abbreviations in Table 7.3 legend.

Gene	Regulated by	Regulation/Details	Gain-of-function	Loss-of-function (Dominant-negative/Antagonist/Morpholino)
hes1	*hes4*	Negative in ectoderm (Koyano-Nakagawa et al., 2000).	*hes4* overexpression: ↓*hes1* in whole embryos and animal caps (neural plate stage). Effect in animal caps reversed by co-injection of *hes6.1* mRNA (Koyano-Nakagawa et al., 2000).	*hes4-ΔWRPW-Gal4:* ↑*hes1* in animal caps (Koyano-Nakagawa et al., 2000)
	hes6.1	Inhibits *hes1* post-transcriptionally and induces it indirectly (Koyano-Nakagawa et al., 2000). Hes6.1 protein binds Hes1 *in vitro* and in embryos, antagonizing Hes1 ability to suppress PN in a TLE/Groucho-independent way (Koyano-Nakagawa et al., 2000; Murai et al., 2011).	*hes6.1* overexpression: ↑*hes1* in animal caps and whole embryos (neural plate stage). Inhibited *hes4's* ability to repress *hes1* in animal caps. The induction of *hes1* is explained by the blockade of the *hes1/hes4* auto-regulatory negative feedback loop (Koyano-Nakagawa et al., 2000).	*hes6.1*DBM: ↑*hes1* in whole embryos (neural plate stage) like *hes6.1* overexpression. Therefore, *hes6.1* does not need to bind DNA to induce *hes1*. (Koyano-Nakagawa et al., 2000).
	hey1	Hey1 and Hes1 heterodimerize in embryos, enhancing the binding of Hey1 to a class B E-box oligonucleotide (Taelman et al., 2004).		
hes4	*hes5.1*	Positive in ectoderm	*hes5.1* overexpression: ↑*hes4* in animal caps (unknown stage, RT-PCR) (Cui, 2005)	
	hes6.1	Inhibits *hes4* post-transcriptionally and induces it indirectly (Koyano-Nakagawa et al., 2000). Hes6.1 binds Hes4 *in vitro* and in embryos, antagonizing its ability to repress *hes1* in a TLE/Groucho-independent way (Koyano-Nakagawa et al., 2000).	*hes6.1* overexpression: ↑*hes4* in whole embryos (neural plate stage). The induction of *hes4* is explained by the blockade of the *hes1/hes4* auto-regulatory negative feedback loop (Koyano-Nakagawa et al., 2000).	*hes6.1*DBM: ↑*hes4* in whole embryos (neural plate stage) like *hes6.1* overexpression. Therefore, *hes6.1* does not need to bind DNA to induce *hes4*. (Koyano-Nakagawa et al., 2000).
hes5.1	*hes4*	Negative in the ectoderm, ventral mesoderm, and anterior neural plate.	*hes4* overexpression: blocked *hes5.1* induction by *neurog2* in animal caps and by *NICD1* in VMZ explants (NF unknown, RT-PCR); ↓anterior neural *hes5.1* expression (ISH, neurula) (Cui, 2005).	*hes4-ΔWRPW:* ↑*hes5.1* in animal caps and VMZ explants; rescued the repression of *hes5.1* by *hes4* in VMZ explants (NF unknown, RT-PCR); weakly ↑*hes5.1* anterior neural domain (ISH, neurula) (Cui, 2005).
	hes6.1	Positive during PN.	*hes6.1* overexpression: ↑*hes5.1* PN domains [data not shown in (Koyano-Nakagawa et al., 2000)].	
	hes7.1	Represses *hes5.1* (probably directly) during the establishment of the presumptive MHB.	*hes7.1* overexpression: ↓*hes5.1* (neural plate stage) (Takada et al., 2005).	*GR-hes7.1-VP16* (Dex NF10.5–11) +/– CHX: ↑*hes5.1* domains at neural plate stage (Takada et al., 2005).

				hes7.1 MO: filled the MHB gap with *hes5.1* expression (PN medial stripes) and anteriorly expanded the *hes5.1* PN intermediate stripes (Takada et al., 2005).
	hes7.3/esr5	Negative during mesoderm induction.		*hes7.3/esr5-ΔWRPW:* ↑*hes5.1* in animal caps mesodermalized by *nodal2* (NF10.5, sqRT-PCR) and in the MZ (NF10.5, ISH) (Kinoshita et al., 2011).
hes5.2	*hes6.1*	Positive during PN.	*hes6.1* overexpression: ↑*hes5.2* PN domains [data not shown in (Koyano-Nakagawa et al., 2000)].	
	hes7.1	Represses *hes5.2* (probably directly) during the establishment of the presumptive MHB.	*hes7.1* overexpression: ↓*hes5.2* (neural plate stage) (Takada et al., 2005).	*GR-hes7.1-VP16* (Dex NF10.5–11) +/− CHX: ↑*hes5.2* domains at neural plate stage (Tak[a]da et al., 2005).
hes5.4	*hes5.4*	Auto-repression		*hes5.4* MO*:* ectopic *hes5.4* in the neural plate (Riddiford and Schlosser, 2017).
hes5.7	*hes7.1*	Represses *hes5.7* (probably directly) during the establishment of the presumptive MHB.	*hes7.1* overexpression: ↓*hes5.7* (neural plate stage) (Takada et al., 2005).	*GR-hes7.1-VP16* (Dex NF10.5–11) +/− CHX: ↑*hes5.7* domains at neural plate stage (Takada et al., 2005). *hes7.1* MO: filled the MHB gap with *hes5.7* expression (medial stripes of PN) and anteriorly expanded the *hes5.7* PN intermediate stripes (Takada et al., 2005).
hes7.1	*hes5.1*	Negative during MHB specification	*hes5.1* overexpression: ↓*hes7.1* (MHB, ISH at neural plate stage (Takada et al., 2005)	
	hes7.1	Auto-repression (probably direct) during the establishment of the presumptive MHB.		*GR-hes7.1-VP16* (Dex NF10.5–11) +/− CHX: ↑*hes7.1* domains at neural plate stage (Takada et al., 2005).
hes7.2	*hes7.3/esr5*	Negative in somitogenesis. Negative feedback loop of Notch pathway	*hes7.3/esr5* overexpression: ↓*hes7.2* in the PSM (Jen et al., 1999)	*hes7.3/esr5-ΔWRPW*: derepressed *hes7.2* in the TZ in the PSM (Jen et al., 1999).
hes7.3/esr5	*notch1/* *hes5.1*	Negative during mesoderm induction	*NICD1:* unable to induce *hes7.3/esr5* in naive animal caps. *NICD1* or *hes5.1* overexpression: ↓*hes7.3/esr5* induced by the mesodermal inducer *nodal2* (animal caps, NF10.5, sqRT-PCR). *hes5.1* overexpression: ↓*hes7.3/esr5* in the IMZ (NF10.5, ISH) (Kinoshita et al., 2011).	*hes5.1-ΔWRPW:* ↑*hes7.3/esr5* (animal caps mesodermalized by *nodal2*, NF10.5, sqRT-PCR) (Kinoshita et al., 2011).

7.3.1. Establishing the Dorsal-Ventral Axis

The polarity of the initial dorsal-ventral (DV) axis is controlled by two antagonistic centers: the ventral center (VC) secretes morphogens (BMP4, Wnt8a) that induce ventral-posterior fates, and the dorsal center (DC) secretes antagonists and expresses repressors of ventral morphogens, protecting the dorsal region from being ventralized and posteriorized thus promoting dorsal-anterior fates. These centers have been characterized in amphibians (De Robertis, 2009) and fish (Thisse and Thisse, 2015). The DC is evident at the blastula stage and consists of: (1) the Nieuwkoop center (NC) in vegetal cells and (2) the Blastula Chordin- and Noggin-expressing (BCNE) center in marginal zone and animal cells. The BCNE gives rise to most of the brain and the organizer and secretes the neural inducers Noggin, Chordin, and Nodal3, which trigger brain induction shortly after mid-blastula transition (Wessely et al., 2001; Kuroda et al., 2004).

While the molecular establishment of the DC has been well documented (see Chapters 4 and 6), the early events leading to the establishment of the VC were largely unknown; our work found that Notch1 is involved (Acosta et al., 2011; Castro Colabianchi et al., 2018). The first clue was that NICD1 down-regulated *chordin* and *nodal3* in the BCNE. Strikingly, *RBPJDBM* did not affect their early expression, but *notch1* knock-down in ventral cells expanded their domains. This indicated that a ventral *notch1* activity restricts the BCNE to the dorsal side through an *RBPJ*-independent pathway (Acosta et al., 2011). Indeed, NICD1 destabilized a β-Catenin mutant lacking the GSK3 phosphorylation sites, whereas *notch1* knock-down increased its levels and ventrally expanded the domain in which β-Catenin was nuclear in the blastula, indicating that maternal *notch1* contributes to confining nuclear β-Catenin to the dorsal side. Moreover, when analyzed at tailbud or tadpole stages, *NICD1* mRNA injection resulted in a ventralized phenotype, whereas *notch1* knock-down, but not *RBPJDBM*, favored dorsal-anterior development. Notably, NICD1 blocked secondary axis induction by ventral injection of *ctnnb1* (β-*catenin*) mRNA, indicating that Notch1 has ventralizing properties because it interferes with the β-Catenin dorsalizing activity (Acosta et al., 2011).

Although our functional experiments revealed a ventral, non-canonical *notch1* activity, it was not clear if this were due to an asymmetric *notch1* mRNA distribution or regulation of Notch1 activity. We found that both *notch1* mRNA and protein are enriched in the ventral region of *Xenopus* embryos from fertilization to mid-blastula, with an opposite distribution of nuclear β-Catenin (Castro Colabianchi et al., 2018), consistent with the proposed role for Notch1 in destabilizing β-Catenin. This ventral enrichment of *notch1* mRNA and protein is the earliest localized sign of ventral development described so far in vertebrates, preceding the ventral localization of *wnt8a*, *bmp4*, and *ventx* mRNAs and dorsal localization of nuclear β-Catenin. Importantly, we noticed nuclear Notch1 in ventral cells during cleavage and mid-blastula stages, suggesting that besides the non-canonical role in destabilizing β-Catenin, Notch1 could be poised to trigger transcriptional activity. Through a gene reporter assay, we found that *RBPJ*-dependent transcriptional activity was higher on the ventral side at the onset of gastrulation. Functional experiments involving NICD1, full-length *notch1*, *RBPJDBM*, and *notch1* knock-down showed that *notch1* is necessary for the proper expression of VC genes such as *wnt8a*, *ventx*, and *bmp4*. Canonical, RBPJ-dependent Notch1 activities are mainly involved in controlling their expression, but non-canonical Notch1 activities might also contribute indirectly through β-Catenin destabilization and the known complex crosstalk between the DC and the VC (Castro Colabianchi et al., 2018). Interestingly, animal-dorsal expression of *foxi1*, which is necessary for ectoderm development, is independent of Wnt/β-Catenin signaling and is restricted to the dorsal region through a Notch1/RBPJ-dependent mechanism (Mir et al., 2008). Overall, this work supports the hypothesis that asymmetric Notch1 activity, including both canonical and non-canonical components, is involved in dorsal-ventral axis formation.

We proposed that Notch1 participates in forming the initial DV axis via a dual, ventralizing role (Figure 7.3A): (1) promoting the VC mainly through the canonical Notch/RBPJ pathway and (2) restricting the DC by destabilizing maternal β-Catenin independent of its phosphorylation by GSK3 and RBPJ. Through this non-canonical pathway, Notch1 ensures the elimination of β-Catenin from the ventral side that escapes from the GSK3-dependent degradation route. By inhibiting the early Wnt/β-Catenin pathway, Notch1 contributes to preventing hyperdorsalization and controls brain size by restricting the BCNE (Acosta et al., 2011; Castro Colabianchi et al., 2018). Interestingly, in mammalian embryonic stem cells, membrane-bound Notch1 associates with hypophosphorylated β-Catenin, decreasing its levels through the endocytic/lysosomal degradation pathway (Kwon et al., 2011). This finding reinforces the conclusions of our work, the first to study this non-canonical Notch pathway in embryonic axis formation in vertebrates.

7.3.2. Germ Layer Formation

In invertebrates, Notch signaling is a key pathway for the induction of the germ layers, whereas in vertebrates, germ layer induction and specification are controlled by several TFs and signaling pathways (Favarolo and López, 2018). In *Xenopus*, the presumptive array of germ layers can be roughly predicted along the animal-vegetal axis of the egg (Figure 7.3B). At cleavage stages, the animal cells approximate the ectoderm, the vegetal cells approximate the endoderm, and the intervening equator or marginal zone (MZ) mostly contributes to the mesoderm (Dale and Slack, 1987; Moody, 1987a; Moody, 1987b). Thus, the MZ, which is composed of an involuting (IMZ) and a non-involuting (NIMZ) region (Keller and Danilchik, 1988), constitutes a transition area between germ layers whose limits need to be defined

during gastrulation (Figure 7.3B–D). Individual MZ cells of the early gastrula simultaneously express markers of two or three germ layers, and segregation is gradually refined as cells progressively and asynchronously commit to one germ layer (Wardle and Smith, 2004).

7.3.2.1. Refining Germ Layer Boundaries

In *Xenopus*, the boundaries between germ layers are refined by Notch signaling. In early gastrulae, *notch1* is expressed in both the IMZ and NIMZ (López et al., 2003; Miazga and McLaughlin, 2009), whereas *dll1* and *dlc* are only in the IMZ. The *dlc* domain forms a complete ring (Peres et al., 2006), whereas the *dll1* domain has a gap in the organizer region (López et al., 2005); subsequently, *dlc* also shows this gap (Peres et al., 2006). *dll1* is expressed in the pre-involuted IMZ but does not persist after involution (Wittenberger et al., 1999) (López et al., 2005) (Figure 7.1C) (Table 7.5). *rbpj.S-v2* transcripts are abundant just before gastrulation (Wettstein et al., 1997; Ito et al., 2007b), and its protein seems to regulate Notch function because it is required for *hes5.1* expression (Table 7.4) and is essential for gastrulation movements and mesoderm specification (Table 7.5) (Ito et al., 2007a). However, lineage tracing showed that perturbed Notch signaling did not transform one germ layer completely into another; only cells near the presumptive boundaries are competent to respond to Notch signaling (Contakos et al., 2005; Revinski et al., 2010). Therefore, the Notch pathway is not essential for the formation of germ layers in *Xenopus* but rather refines their segregation (Revinski et al., 2010).

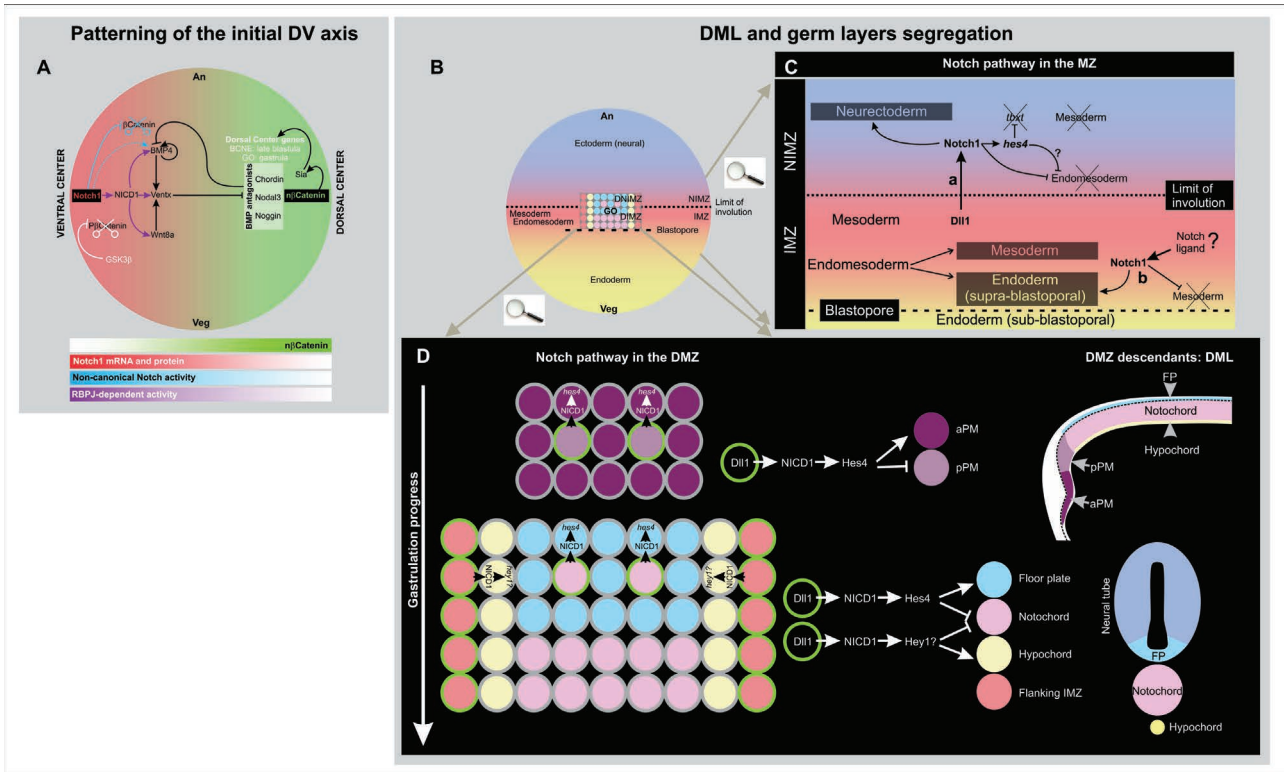

FIGURE 7.3 Notch plays early roles during patterning of the initial DV axis and during gastrulation in the germ layer and DML segregation. (A) Maternal *notch1* mRNA and Notch1 protein are enriched in the ventral region, exerting a ventralizing role by: (1) promoting ventral center development, mainly through the canonical Notch/RBPJ pathway and (2) preventing dorsal center development in the ventral side through a non-canonical pathway, independently of RBPJ, by destabilizing maternal βCatenin protein that escapes GSK3β-dependent phosphorylation (Pβcatenin) (modified from (Castro Colabianchi et al., 2018). (B–D) During gastrulation, Notch1 is required for the segregation of germ layers throughout the marginal zone (MZ), including dorsal midline (DML) components (adapted from (Favarolo and López, 2018) and aPM, pPM, and notochord arrangement in the DML based on (Yamaguti et al., 2005). (B) Diagram of a gastrulating embryo in dorsal view, showing the arrangement of presumptive germ layers (color-coded) along the An-Veg axis, the transition zone between them (marginal zone, MZ) (magnified in C), and the dorsal MZ containing the gastrula Organizer (GO) at the center, populated by the DML precursors (color-coded), magnified in D. IMZ, involuting marginal zone; NIMZ, non-involuting marginal zone; DIMZ, dorsal involuting marginal zone; DNIMZ, dorsal non-involuting marginal zone. (C) Dll1 from the IMZ activates the Notch1 pathway on the neighboring NIMZ cells, favoring neuroectoderm at the expense of mesodermal fates (a: type A decision), thus refining the limit of involution. In the IMZ, Notch1 promotes endomesoderm segregation, favoring endodermal at the expense of mesodermal fates (b, type B decision); the involved ligand is unknown. Inhibited markers and germ layers are crossed out. (D) In the DIMZ, Dll1 expressed in isolated cells activates Notch1/*hes4* in their neighbors, first favoring aPM at the expense of pPM and then favoring floor plate (FP) fates at the expense of the notochord, stopping involution. Dll1 from MZ cells flanking the DMZ activates Notch1 signaling, promoting hypochordal fate at the expense of the notochord. Because of its expression pattern, *hey1* is a good candidate for intervening in this choice.

TABLE 7.5
Core Components of the Notch Pathway in the Development of Germ Layers and the Dorsal Midline in *Xenopus*

See abbreviations in Table 7.3 legend.

Gene	Expression Role/Details	Gain-of-Function	Loss-of-Function (Dominant-Negative/Morpholino)
notch1	*notch1* is expressed in the IMZ and NIMZ during gastrulation (López et al., 2003; Miazga and McLaughlin, 2009). **Germ layers:** Balanced Notch1 signaling is required for delimiting the three germ layers and normal morphogenetic movements during gastrulation. Cell-fate choice upon activation of Notch signaling does not depend on proliferation during gastrulation. **DML:** Among the DML precursors, *notch1* favors FP and hypochord development at the expense of the notochord.	**Germ layers:** *notch1ΔE* +/– HUA at gastrula stage, analysis at tailbud stage: ↑epidermal, neural, and muscle tissues (Coffman et al., 1993). *notch1ΔE* (animal caps): ↑ectodermal response to neural induction; prolonged ectodermal competence for mesodermal induction beyond the onset of gastrulation (Coffman et al., 1993). Mouse NICD1, analysis at tailbud stage: ↓myosin (muscle differentiation marker) (Kopan et al., 1994). *GR-NICD1*, Dex NF2, but not Dex NF12: ↑neural plate (*sox2;* late neurula, NF18/19) and muscle tissues (12/101 marker; tailbud, NF25) (Glavic et al., 2004). GR-*NICD1* or GR-*RBPJ*-VP16, Dex NF10 or 12, analysis at late neurula/tailbud stages: ↑endodermal ↓mesodermal derivatives (Contakos et al., 2005). GR-*RBPJ*-VP16, Dex NF14, analysis at late neurula/tailbud stages: ↓endodermal ↑mesodermal derivatives (Contakos et al., 2005). *NICD1*, analysis at gastrula stages: DMZ-directed injection: delayed blastopore formation and closure; ↓mesoderm (*tbxt*), ↑neural ectoderm (*sox2*) ↑supra-blastoporal endoderm (*sox17*). Dorsal/animal-directed injection: *tbxt* domain expanded but more diffuse, probably due to ectopic prolonged competence for mesodermal induction in the ectoderm (Revinski et al., 2010). **DML:** *notch1ΔE* +/– HUA at gastrula stage: ↓notochord (tailbud stage) (Coffman et al., 1993). *NICD1*: Analysis at gastrula stage: ↓GO mesoderm (*chrd),* ↑presumptive FP (*hes4*) (López et al., 2003), (López et al., 2005). Analysis at neurula stage: ↓notochord (*chrd, tbxt*), ↑FP (*shh, foxa4*) (López et al., 2003). Analysis at tadpole stages: ↑hypochord (vegf,*spon1*, NF25,38) (Peyrot et al., 2011). *GR-NICD1*/time-controlled experiments with Dex: higher susceptibility to ↑FP and ↓notochord in the first than in the second half of gastrulation (López et al., 2003)	**Germ layers:** GR-*RBPJDBM*, Dex NF 10 or 12, analysis at late neurula/tailbud stages: reduced endodermal, expanded mesodermal derivatives (Contakos et al., 2005). GR-*RBPJDBM*, Dex NF14, analysis at late neurula/tailbud stages: expanded endodermal, reduced mesodermal derivatives (Contakos et al., 2005). *notch1* MO (dorsal injections), analysis at gastrula stage: delayed blastopore formation and closure, expanded the mesoderm (*tbxt*), animally shifted the neural-ectoderm (*sox2*), reduced the supra-blastoporal endoderm (*sox17*) (Revinski et al., 2010). **DML:** *notch1* MO: expanded the notochord (*chrd*+ cells, neurula stage) (López et al., 2003).

psen	**DML:** ϒ-secretase is necessary to keep the morphogenetic movements at a normal pace during gastrulation.		DAPT (ϒ-secretase inhibitor): delayed the convergent-extension movements typical of the notochordal cells during gastrulation (Revinski et al., 2010).
RBPJ	Both *RBPJ.S* variants (see Table 7.1) are expressed ubiquitously from the unfertilized egg to the tailbud stage, but *RBPJ.S-v2* transcripts are more abundant before gastrulation (Wettstein et al., 1997) (Ito et al., 2007b). **Germ layers:** *RBPJ*-dependent signaling favors the development of endoderm-derived cell types and disfavors the development of mesoderm-derived cell types during gastrulation but plays the opposite role since the neural plate stage. A critical time window that comprises gastrulation and ends at the onset of neurulation was described in particular for cardiac mesoderm specification, which is disfavored by Notch/RBPJ signaling during this period.	**Germ layers:** GR-*RBPJ-VP16*, analysis at late neurula and tailbud stages: Dex NF10 or 12: ↑markers of endodermal-derived cell types, ↓markers of mesodermal-derived cell types (paraxial, intermediate, and cardiac mesoderm). Dex NF14: ↓markers of endodermal-derived cell types, slightly ↑markers of intermediate mesoderm-derived cell types. Cardiac mesoderm unaffected (Contakos et al., 2005). GR-*RBPJ-VP16* (Dex NF10) +/- ER-*RBPJDBM* (E2 at NF10, 14, 15, 16); ISH of the cardiac field marker *nkx2.5* at tailbud stage: the loss of *nkx2.5* induced by activating Notch/RBPJ signaling at the onset of gastrulation was rescued by blocking Notch/RBPJ during gastrulation. This rescuing ability was gradually lost after the onset of neurulation (Miazga and McLaughlin, 2009). GR-*RBPJ*-VP16 (Dex NF10): ↓*gata4* (mid-gastrula) (Miazga and McLaughlin, 2009).	**Germ layers:** GR-*RBPJDBM*, analysis at late neurula and tailbud stages: Dex NF10 or 12: ↓markers of endodermal-derived cell types, ↑markers of mesodermal-derived cell types (paraxial, intermediate, and cardiac mesoderm). Dex NF14: ↑markers of endodermal-derived cell types, ↓markers of intermediate mesoderm-derived cell types. Cardiac mesoderm unaffected (Contakos et al., 2005) GR-*RBPJDBM* (Dex NF10), ISH analysis at NF11–11.5: precocious induction of heart field markers (*nkx2–5, gata4, tbx5)* (Miazga and McLaughlin, 2009). *RBPJDBM*, analysis at gastrula stage: mild expansion of *tbxt* (pan-mesodermal) and *myf5* (presumptive paraxial mesoderm) domains, variable ↓ and animal shift of *sox2*, variable results of *sox17* expression (endoderm) (Revinski et al., 2010). *RBPJDBM*, analysis at neural plate stage: mild tendency to ↑paraxial mesoderm markers *myf5* and *myoD* and ↓neural marker *sox2* (Revinski et al., 2010). *RBPJ.S v2* MO: abnormal gastrulation, neural fold disorganization, ↓mesodermal markers *tbxt, myod1, ventx1.2, chrd*, but not *gsc* (RT-sqPCR, NF 10.5). ↓*tbxt* in the IMZ (ISH). This effect was not rescued by *NICD1* or *DN-hes5.1* (Ito et al., 2007a). *RBPJ.S-v1* MO: no morphological defects, no changes in molecular markers (Ito et al., 2007a). Probably due to compensation by the other homeolog as neither MO used in this study is predicted to knock-down *RBPJ.L.* **DML:** *RBPJDBM:* ↑*chrd+* in the GO and *chrd+* notochord expression in neurula; ↓FP (*foxa4+/shh+* cells) (neurula)(López et al., 2003); ↓hypochord (*vegf, spon)* (NF28/35) (ISH) (Peyrot et al., 2011).

(*Continued*)

TABLE 7.5 (Continued)

Core Components of the Notch Pathway in the Development of Germ Layers and the Dorsal Midline in *Xenopus*

Gene	Expression Role/Details	Gain-of-Function	Loss-of-Function (Dominant-Negative/Morpholino)
dll1	Onset in the IMZ at early gastrula (NF10.5, ISH), with a gap of lower expression in the GO, with scattered *dll1*+ cells (López et al., 2005). Expression in the pre-involuted IMZ does not persist in involuted cells (Wittenberger et al., 1999; López et al., 2005). **Germ layers:** Dll1 signaling from pre-involuted IMZ activates Notch signaling in the NIMZ, promoting neural-ectodermal and inhibiting endomesodermal fates (Revinski et al., 2010). **DML:** Within the GO, Dll1 promotes FP development at the expense of notochordal fate.	**DML:** *dll1*, dorsal overexpression; analysis at gastrula stage: ↑FP precursors (*hes4*), ↓notochordal precursors (*chrd*) in the GO (López et al., 2005).	**Germ layers:** *dll1STU* (dorsal injection), analysis at gastrula stage: ↓*tbxt* in its normal domain, displaced by expanded supra-blastoporal endoderm (*sox17*) that took its place; ↓neural ectoderm (*sox2*) because of the animal shift and expansion of the presumptive mesoderm (*tbxt)* (Revinski et al., 2010). *dll1* MO (lateral injection), analysis at gastrula stage: impaired blastopore closure, ↓circumblastoporal *tbxt* expression (only a vegetal view was shown). Both effects were rescued by co-injection of *NICD1* mRNA (Kinoshita et al., 2011). **DML:** *dll1STU*, dorsal injection; analysis at gastrula stage: ↑notochordal precursors (*chrd*), ↓FP precursors (*hes4*) in the GO (López et al., 2005).
dlc	Onset in the IMZ at early gastrula (NF10.5, ISH) in a complete circumblastoporal ring; a lower expression gap appears at NF11 at the GO (Peres et al., 2006). Necessary for *hox* genes expression in the IMZ. There are restrictions, at least for *hox* genes, to respond to Dlc signaling outside the IMZ (see Table 7.12 for additional information).	*dlc* overexpression*:* did not affect *hoxc6* and *hoxd1* in the IMZ and could not expand them outside their normal region (ISH, gastrula stage) (Peres et al., 2006).	*dlc* MO: ↓*hoxb4, hoxc6, hoxb9*, and *bmp4* in the IMZ (ISH, gastrula stage); *tbxt* expression unaffected in the IMZ (ISH, late gastrula) (Peres et al., 2006).

Constitutively active Notch1 constructs and time-controlled Notch1/RBPJ activation or blockade resulted in a variety of changes in markers of ectodermal-, neural-, mesodermal-, and endodermal-derived cell types at neurula and tail-bud stages (Tables 7.5, 7.9), indicating that the response to Notch1/RBPJ signaling changes over time. We perturbed the Notch pathway in several ways to address a possible role in controlling the boundaries between germ layers, analyzing the consequences during gastrulation when they segregate, and also in early neurulation (Revinski et al., 2010) (Table 7.5). Activation and blockade delayed gastrulation, indicating that Notch1 activity is tightly balanced to keep morphogenetic movements at a normal pace. Germ layers were specified, but they did not develop properly because their MZ boundaries were shifted. Consequently, cells at the boundaries allocated incorrectly and changed their specification to the incorrect germ layer. In *NICD1* mRNA-injected embryos, the presumptive neural ectoderm and supra-blastoporal endoderm were expanded at the expense of mesoderm, whereas *notch1* knock-down produced the opposite changes (Revinski et al., 2010). Both *dll1STU* (Revinski et al., 2010) and *dll1* knock-down (Kinoshita et al., 2011) inhibited the pan-mesodermal marker *tbxt* in its normal circumblastoporal domain. In embryos injected with *dll1STU*, this was accompanied by the animal displacement of the *tbxt* domain as expanded supra-blastoporal endoderm (*sox17*-positive) took its place. The neural ectoderm (*sox2* expressing) also was reduced in response to this animal-ward expansion of the presumptive mesoderm (Revinski et al., 2010).

We proposed that *notch1* is involved in the segregation between neural ectoderm, mesoderm, and endoderm by controlling their boundaries in the MZ (Revinski et al., 2010) (Figure 7.3B,C) in the following ways. (1) Refining the limit of involution between the IMZ and the NIMZ favored neural ectoderm at the expense of mesoderm (type A decisions). (b) In the IMZ, by refining mesoderm segregation from the supra-blastoporal endoderm, favoring endoderm over mesoderm (type B decisions). Strikingly, *dll1STU* shifted the limit of involution animal-wards, favoring endomesodermal development over neural ectoderm, but *notch1* knock-down expanded the mesoderm at the expense of both endoderm and neural ectoderm; perturbing Notch/RBPJ signaling during gastrulation had a similar effect (Contakos et al., 2005). This indicates that Dll1 is involved in type A but not in type B decisions. According to this model, pre-involuted IMZ cells present Dll1 to the neighboring cells on the other side of the limit of involution, thus preventing them from adopting the same fate (endomesoderm) by triggering the Notch pathway, which instead promotes neural ectoderm specification (Revinski et al., 2010). Interestingly, in animal caps assays, Notch1ΔE alone weakly induced neural ectoderm but strongly enhanced ectodermal competence for neural induction (Coffman et al., 1993). Therefore, Dll1 signaling from pre-involuted IMZ might enhance the competence of their neighbors above the limit of involution to respond to neural inducers and become neural instead of mesoderm, sharpening the boundary between both populations. Once the mesodermal cells involute, they no longer express Dll1, ending this activity. While it appears that Dll1 controls the limit of involution (type A decisions), it remains unknown which *notch1*-dependent mechanisms underlie mesodermal versus endodermal (type B) decisions. More work is needed to discern the possible role of the diverse Dll/Jag ligands and non-canonical Notch pathways in the segregation of germ layers.

7.3.2.2. Which Notch Targets Are Involved in Germ Layer Segregation?

The IMZ expresses several *hes* genes during gastrulation (Figure 7.2). Most of their patterns are similar to that of *dll1*, but the dorsal *hes5.1* and *hes5.3* boundaries are more distant from the organizer, and *hes7.2* is more abundant in the organizer. Only *hes4* is broadly expressed in the NIMZ, but *hes5.10* (at early gastrula) and *hes2* (at mid-gastrula) are expressed in scattered cells (Figure 7.2). Except for *hes5.8* and *hes5.9*, whose regulation by Notch signaling has not been studied, all the *hes5* genes expressed in the MZ, as well as *hes2*, *hes4*, and *hes7.2*, are positively regulated by Notch in several contexts, although a few of them were tested for Notch responsiveness in the MZ. In contrast, *hes6.1* and *hes7.3/esr5* are down-regulated in the neural plate and the IMZ, respectively (Tables 7.2, 7.3). Interestingly, *hes5.10* is later expressed throughout the non-neural ectoderm and responds positively to NICD1, although it is not clear whether RBPJ is involved (Deblandre et al., 1999). The early expression of *hes6.1, hes7.2*, and *hes7.3/esr5* in the IMZ might be related to their role during somitogenesis (see Section 3.6). Only a few of the *hes* genes expressed in the MZ have been experimentally tested for their role in the MZ (*hes4, hes5.1, hes5.6*, *hes6.1*, *hes7.3/esr5*) (Table 7.6). One clear candidate for positioning the limit of involution is *hes4*, which first is broadly expressed in the presumptive ectoderm of the blastula, then progressively confined to the boundary with the mesoderm during gastrulation, accumulating transcripts in the whole NIMZ with highest levels dorsally in a pattern complementary to *tbxt* (pan-mesoderm) (López et al., 2005; Aguirre et al., 2013). *hes4* might be one of the Notch targets involved in type A decisions because: (1) the *hes4* NIMZ domain was expanded by NICD1 (López et al., 2005) and down-regulated by blockade of Notch1/RBPJ signaling (unpublished results); (2) *hes4* overexpression blocked gastrulation movements, impeding MZ cell involution; (3) *hes4* overexpression repressed *tbxt* throughout the entire IMZ (López et al., 2005; Cui, 2005; Aguirre et al., 2013); and (4) *hes4* knock-down expanded the *tbxt* domain toward the animal pole, indicating that it is required for the correct placement of the ectoderm-mesoderm boundary (Aguirre et al., 2013) (Figure 7.3B,C) (Tables 7.5, 7.6).

Overexpression and dominant-negative experiments indicate that *hes7.3/esr5* promotes and *hes5.1* inhibits mesoderm specification and they repress each other (Kinoshita et al., 2011) (Tables 7.4, 7.6). In animal cap explants, NICD1 induced *hes5.1* but not *hes7.3/esr5* (Kinoshita et al., 2011) (Tables 7.2, 7.3), Nodal2 induced *hes7.3/esr5* but not *hes5.1*,

TABLE 7.6
hes/hey Genes in the Development of Germ Layers and the Dorsal Midline in *Xenopus*

See abbreviations in Table 7.3 legend.

Gene	Role/Details	Gain-of-Function	Loss-of-Function (Dominant-Negative/Morpholino)
hes1	Represses *myod1*, probably directly, downstream of mesodermal induction.	*hes1* overexpression, mesodermalized animal caps: ↓*tbxt* (pan-mesoderm) and *myoD* (paraxial mesoderm) but not GO mesodermal markers (*chrd*, *gsc*). Inhibition of *myoD* downstream of *tbxt* (Umbhauer et al., 2001). *hes1* overexpression, whole embryos: delayed gastrulation, trunk defects; ↓*myoD* but not *chrd* (gastrula) through the DNA-binding and repressor domains (Umbhauer et al., 2001).	*hes1-VP16* or *GR-hes1-VP16* (Dex 2 hs after NF11) +/– CHX, animal caps: ↑*myoD* but not *tbxt*, suggesting a direct regulation of *myod*.
hes4	**Germ layers:** *hes4* is normally expressed in the NIMZ since late blastula stage and restricts mesoderm specification to the IMZ during gastrulation. **DML:** As a mediator of Notch1 signaling in DML development, blocks the involution of *hes4*+ GO cells, favoring their incorporation into the dorsal NIMZ (notoplate/future FP) at the expense of the notochord. Both *hes4* homeologs are required for FP development (López et al., 2005; Aguirre et al., 2013). Required for aPM specification by restricting pPM and notochord specification (Yamaguti et al., 2005). *hes4* acts as a cell-autonomous repressor in the aPM, restricting contiguous cell fates, contributing to regionalize the axial mesoderm. It is also able to induce dorsal genes in a non-cell-autonomous way through the activity of the WRPW motif, to ensure an organizer environment (Murato et al., 2006).	**Germ layers:** *hes4.S* overexpression*:* ↓*tbxt* (pan-mesoderm) throughout the IMZ (López et al., 2005; Cui, 2005; Aguirre et al., 2013). **DML:** *hes4.S*, dorsal overexpression: ↓notochord specification (*chrd, tbxt)* in the GO; ↑FP precursors in gastrulae and neurulae (*foxa4*+ cells in GO and notoplate, *shh*+ cells in notoplate) (López et al., 2005). *hes4.L*, dorsal overexpression: ↓*chrd* (pPM, notochord), *not* (notochord), *dkk1*, and *hex* (anterior endoderm) in the GO; head defects (Yamaguti et al., 2005). *hes4.S*, ventral overexpression: ↓*tbxt*, induced ectopic GO markers (*chrd, foxa4)*, but these cells were unable to involute during gastrulation (López et al., 2005); induced a headless secondary axis (Aguirre et al., 2013). *hes4.L*, ventral overexpression: ↓ventral mesoderm specification (*ventx*); induced ectopic GO markers and a headless secondary axis (Yamaguti et al., 2005).	**Germ layers:** *hes4.L+S* MO: animal expansion of *tbxt* (pan-mesoderm) throughout the MZ. *hes4.S* might be more relevant in restricting *tbxt* expression to the IMZ (Aguirre et al., 2013). **DML:** *hes4.S* MO, dorsal injection: ↑notochordal precursors' population in the GO and notochord in neurulae (*chrd*, *tbxt*); ↓FP precursors population in gastrulae and neurulae (*foxa4+* cells in GO and notoplate, *shh*+ cells in the notoplate). Reversed the effects of *NICD1* on DML markers (López et al., 2005). *hes4.L* MO or *hes4.S* MO: ↓FP *shh* (Murato et al., 2006). *hes4.L* MO: ↑aPM (*chrd*) and notochord (*chrd*, *not*) at the expense of the anterior pPM (*gsc*) (ISH NF14); did not affect anterior endodermal markers nor *ventx* (ventral mesoderm) (early gastrula stage) (Yamaguti et al., 2005).
hes5.1	Inhibits mesoderm specification.	*hes5.1* overexpression: ↓*tbxt* in mesodermalized animal caps (Ito et al., 2007a) and the IMZ at early gastrula (NF10.5, ISH) (Kinoshita et al., 2011).	*hes5.1 ΔWRPW:* ↑*tbxt* at early gastrula (NF10.5, ISH) (Kinoshita et al., 2011).

hes5.6	**Germ layers:** Possible regulation of the timing of cardiac field specification (Miazga and McLaughlin, 2009). **DML:** Possible role in DML development.	**Germ layers:** GR-*hes5.6*-VP16 (Dex NF10): ↓*gata4* (mid-gastrula) (Miazga and McLaughlin, 2009). **DML:** *hes5.6*, dorsal overexpression: ↑*chrd* (GO) (Taelman et al., 2004).	
hes6.1	Required for presumptive paraxial mesoderm specification, involving recruitment of TLE/Groucho co-repressors but not DNA binding.	*hes6.1* overexpression*:* ↑*tbxt* (pan-mesoderm), *myod1* (presumptive paraxial mesoderm), and *wnt8a* (lateral/ventral mesoderm) but did not affect the GO marker *chrd*. Expansion was restricted to the nearby MZ (ISH, gastrula). ↑*tbxt* and *wnt8a* but not *chrd* or endodermal markers (animal caps, RT-qPCR). Mesodermal induction by *hes6.1* mainly required FGF but also Nodal signaling (RT-qPCR, ISH) (Murai et al., 2007).	*hes6.1DBM:* same effects on mesoderm as *hes6.1* overexpression (gastrula). *hes6.1 ΔWRPW:* mesodermal markers unaffected (gastrula). *hes6.1* MO: ↓*myod1, myf5* (presumptive paraxial mesoderm) in the IMZ (without affecting *tbxt*, *wnt8a, chrd,* or the endodermal marker *sox17)*. This effect was rescued by *hes6.1* or *hes6.1DBM* but not by *hes6.1 ΔWRPW* (ISH, mid-gastrula) (Murai et al., 2007).
hes7.3/esr5	Necessary for mesoderm specification.	*hes7.3/esr5* overexpression*:* ↑*tbxt* in the IMZ at early gastrula (NF10.5, ISH) (Kinoshita et al., 2011).	*hes7.3/esr5 ΔWRPW:* ↓*tbxt* at early gastrula (NF10.5, ISH) (Kinoshita et al., 2011).
hey1	Possible role in the segregation of DML precursors, repressing notochordal fates. Hey1 does not bind the co-repressor TLE/Groucho, as it lacks the typical WRPW motif of bHLH-O repressors (Pichon et al., 2004). For *chrd* downregulation, Hey1 acts as a DNA binding repressor, requiring the Orange domain and the C-terminal region for dimerization. Hey1 heterodimerizes *in vivo* with Hes1 and Hes4 and weakly with Hes2, but it does not bind Hes5.5 or Hes5.6 (Taelman et al., 2004).	*hey1* overexpression*:* stopped gastrulation, ↓*chrd* (GO), *tbxt* (pan-mesoderm; IMZ), and *not* in the notochord and GRP. It did not affect *not* in the notoplate but induced ectopic *not* in the limit of involution, outside the GO (Taelman et al., 2004). GR-*hey1* (Dex NF12): FP not affected at tailbud stage (Taelman et al., 2004). An earlier induction with Dex will be useful to address possible effects during DML segregation.	*hey1DBM:* did not repress *chrd* (Taelman et al., 2004).

and Hes5.1 reduced *hes7.3/esr5* induction by Nodal2. Therefore, it was proposed that a mutually antagonistic relationship between *hes5.1* and *hes7.3/esr5* controls the balance of mesoderm specification within the IMZ (Kinoshita et al., 2011). It will be interesting to determine whether *hes5.1* also mediates endodermal versus mesodermal choices.

hes5.5 and *hes5.6* are positively regulated by canonical Notch-RBPJ in the IMZ (Miazga and McLaughlin, 2009). While the function of *hes5.5* in this tissue has not been studied, Notch regulates the timing of heart field specification, possibly through *hes5.6* (Tables 7.5, 7.6) (Miazga and McLaughlin, 2009). While *hes6.1* is negatively regulated by Notch/RBPJ in the neural plate, it is not known whether this pathway controls *hes6.1* expression in the IMZ during gastrulation, although it is a direct Wnt/β-Catenin target and requires input from zygotic Wnt/β-Catenin signaling (Hufton et al., 2006; Kjolby and Harland, 2017). *hes6.1* favors paraxial mesoderm development (but not general mesoderm induction) by sequestering TLE/Groucho co-repressors, thus relieving *myod1* from repression in mesodermal precursors (Cossins et al., 2002; Murai et al., 2007) (Table 7.6).

7.3.3. Dorsal Midline Tissues

Cells that derive from the dorsal MZ/organizer region constitute the vertebrate dorsal midline (DML), an essential signaling center for development of the surrounding tissues. The DML gives rise to several derivatives: (1) the prechordal endomesoderm (PEM), a key signaling center for anterior neural development that emerges from the deep cells of the organizer to form the prechordal plate; (2) the notoplate (Figure 7.3B,D), which gradually converges and extends during gastrulation to form the floor plate (FP) of the neural tube; (3) the notochord; and (4) the dorsal midline of the endoderm, in *Xenopus* known as the gastrocoel roof plate (GRP), which functions as a left-right organizer. During neurulation, some GRP cells incorporate into the notochord and somites, while bilateral GRP rows gradually fuse into the hypochord, ventral to the notochord (Keller and Danilchik, 1988; Minsuk and Keller, 1997; Kiecker and Niehrs, 2001; Shook et al., 2004; López and Carrasco, 2006) (Figure 7.3D). Gene marker studies revealed that the precursors of these various derivatives are intermingled at the beginning of gastrulation but gradually segregate (Bouwmeester et al., 1996; Artinger et al., 1997; Yamaguti et al., 2005); this process is highly influenced by the Notch pathway.

Components of the Notch pathway are differentially expressed in the multipotent DML precursors that either involute (as the IMZ) or remain on the surface as the NIMZ, that is, notoplate (López et al., 2003; López et al., 2005). *hes4* is expressed in the dorsal NIMZ and then in the notoplate and FP. *dll1* is expressed in a compact domain throughout the IMZ, except for the organizer region, where only scattered cells express *dll1* and also *hes4* prior to involution. Once these dorsal IMZ cells involute, only *hes4* expression continues, restricted to the prechordal mesoderm but absent from the notochord. In fact, *hes4* is the only *hes1–7* gene expressed in the *Xenopus* DML during gastrulation and neurulation (Figure 7.2) (Tsuji et al., 2003; López et al., 2005; Yamaguti et al., 2005).

We perturbed the Notch pathway in several ways to address its role during DML development, including *hes4* overexpression and knock-down, constitutive NICD1 activation, time-controlled GR-NICD1 activation, blocking the whole *notch1* pathway by knock-down, the RBPJ-dependent pathway with *RBPJDBM*, Dll1 signaling with *dll1STU*, and Notch processing with *psen1* knock-down. Our results indicated that during gastrulation, *notch1/psen1/RBPJ/hes4* signaling favors notoplate over notochord fate (López et al., 2003; López et al., 2005) (Tables 7.5, 7.6). Other authors showed that Notch promotes hypochord over notochord by injecting *NICD1* and *RBPJDBM* (Peyrot et al., 2011) (Table 7.5). As the PEM mesodermal population segregates during gastrulation into two subdomains, *hes4* and *gsc* are expressed in the anterior prechordal mesoderm (aPM), whereas *chordin* is expressed in the posterior prechordal mesoderm (pPM) (Yamaguti et al., 2005). It was proposed that *hes4* initially ensures an organizer environment by inducing early organizer genes through a non-cell-autonomous activity that depends on the WRPW domain. Then, *hes4* is required for aPM specification, as it inhibits contiguous fates through a cell-autonomous repressive activity, restricting pPM and notochord (Yamaguti et al., 2005; Murato et al., 2006) (Table 7.5).

Based on these studies, we propose a model for how the Notch pathway allocates dorsal MZ descendants into the different DML tissues (Figure 7.3B,D). First, DML precursors choose between aPM or pPM fates. Dll1 from scattered cells in the organizer induces *hes4* in neighboring cells, which represses pPM fates, thus promoting aPM. As gastrulation proceeds and more posterior cells involute, multipotent precursors in the mid- and late organizer choose between FP, notochord, or hypochord fates. Dll1 from scattered cells in the boundary between the dorsal NIMZ and the pre-involuted IMZ interacts with the Notch1 receptor on the surrounding cells, activating *hes4* to repress the genes that promote notochord development and impede their involution so they gradually incorporate into the notoplate. By this mechanism, *dll1* executes a cell fate switch that favors notoplate development at the expense of notochord. Dll1 presented by the IMZ cells flanking the organizer activate Notch1 signaling in a pair of bilateral rows of dorsal IMZ cells, favoring hypochord over notochord; the down-stream mechanism is unknown, since *hes4* is not expressed by hypochord precursors. In addition, *notch1/hes4* expand the expression of *foxa4*, a positive notoplate/FP regulator (López et al., 2003; López et al., 2005), whereas *foxa4* knock-down suppress *hes4* in the FP (Murgan et al., 2014), suggesting they establish a positive feedback loop. The expression of *hey1*, which is positively regulated by Notch/RBPJ (Pichon et al., 2002; Rones et al., 2002) (Tables 7.2, 7.3), matches the time and spatial profile of hypochord development, with initial bilateral stripes in the GRP that later fuse at the midline

(Pichon et al., 2002; Shook et al., 2004) (Figure 7.2). Since *hey1* is also expressed in scattered cells in the involuted dorsal IMZ at early gastrula (see clone XL097h17 in Taverner et al., 2005), it will be interesting to study if it promotes hypochordal fates over notochord. *hey1* is also expressed in the FP during neurulation, but neither time-controlled *hey1* overexpression at late gastrula nor *hey1* knock-down affected FP development when analyzed at tailbud stages (Taelman et al., 2004). There is evidence that *hey1* might suppress neurogenesis in the FP by antagonizing proneural genes, thereby maintaining FP identity. Interestingly, *neurog2* overexpression revealed FP's potential to differentiate into neurons, and *hey1* overexpression suppressed primary neurogenesis in the neural plate. However, neither *hey1* knock-down alone nor combined with *hes4.L* knock-down induced ectopic neurogenesis in the FP, indicating that additional inhibitors might be required to inhibit neurogenesis (Taelman et al., 2004).

7.3.4. Primary Neurogenesis

Differentiation of multipotent neural progenitors into the diverse nervous system cell types is an orchestrated process ensuring that neurons and glia appear at the right time and place during development. Key players in this process are Notch pathway components and several bHLH proteins. Those encoded by "proneural" genes—members of the Neurogenin and Achaete-scute families—heterodimerize with the bHLH factor E47, bind the E box (CANNTG), and activate transcription, promoting competence for neuronal differentiation. Downstream, other bHLH transcriptional activators promote the determination of neurons (NeuroD family) or oligodendrocytes (Olig family). Notch-regulated Hes proteins typically repress proneural gene expression or activity, maintaining neural precursors in a proliferative and undifferentiated state, and allow astrocyte differentiation (Davis and Turner, 2001; Bertrand et al., 2002; Huang et al., 2014; Kageyama et al., 2007; Imayoshi and Kageyama, 2014).

Anamniotes develop through a larval period that requires a simple neuronal circuitry for swimming and escape reflexes to be functioning around hatching (Roberts, 1989). In *Xenopus*, a first wave of primary neurogenesis, which begins at late gastrula and peaks at neural plate stages, generates three bilateral pairs of longitudinal stripes of "primary neurons": motoneurons, interneurons, and sensory neurons that are responsible for these larval behaviors (Chitnis et al., 1995). Study of primary neurogenesis in *Xenopus* significantly contributed to the discovery of the molecular and cellular basis of vertebrate neurogenesis and provided an accessible paradigm to study the Notch pathway (Tables 7.7, 7.8). The neurogenesis gene regulatory network (GRN) built from this work is initially controlled by the balanced expression of "prepattern genes," such as those encoding Gli and Zic TFs (Lee et al., 1997; Marine et al., 1997; Brewster et al., 1998; Nakata et al., 1998). By refining proneural gene expression, the prepattern TFs roughly outline regions in the neural plate in which primary neuronal differentiation can or cannot occur; this confers neuronal differentiation competence to restricted domains (Zimmerman et al., 1993; Ma et al., 1996).

Proneural genes induce *notch1* and *dll1*, whose expression in the posterior neural plate begins around late gastrula in overlapping stripes that prefigure the placement of the primary neurons (Turner and Weintraub, 1994; Chitnis et al., 1995; Ma et al., 1996; Chitnis and Kintner, 1996) (Figure 7.1C). *notch1* is expressed by most cells in the proneural domain, whereas *dll1* is restricted to a subset of them (Chitnis et al., 1995; Ma et al., 1996; Chalmers et al., 2002). Primary neurogenesis is circumscribed by Notch-dependent lateral inhibition: the selected neuronal precursor expresses Dll1, which binds Notch1 in neighboring cells, activating the Notch/Psen/RBPJ/Maml pathway, resulting in the induction of Hes1–7 bHLH-O repressors that inhibit proneural genes and thereby repress neuronal fate in the neighbors (Chitnis et al., 1995; Ma et al., 1996; Bellefroid et al., 1996; Wettstein et al., 1997; Perron et al., 1999; Paganelli et al., 2001; Katada and Kinoshita, 2003; López et al., 2003; Nichane et al., 2008b; Revinski et al., 2010; Riddiford and Schlosser, 2017) (Tables 7.3, 7.4, 7.8). A negative feedback loop is established in the neuronal precursors that suppresses *dll1* expression in their neighbors through NICD1. The neuronal precursors continue to express proneural genes, which induce the bHLH-determination factor *neurod1*. Once *neurod1* is activated, the cells become refractory to lateral inhibition and undergo terminal differentiation into neurons (Chitnis et al., 1995; Chitnis and Kintner, 1996; Olson et al., 1998; Sjöqvist and Andersson, 2019). Another pathway for preventing lateral inhibition is through the upregulation of the zinc-finger TF myt1 by Neurog2 (Bellefroid et al., 1996). In other scenarios, when proneural TFs reach a certain threshold, they induce Ebf2 in selected progenitors, which stabilizes commitment to a neuronal fate by enhancing *dll1* expression and reinforcing *neurod1* expression (Dubois et al., 1998). *neurod1* appears to feed back to directly potentiate *dll1* expression, as it promotes ectopic *dll1* in whole embryos and induces *dll1* in animal caps in the absence of protein synthesis (Seo et al., 2007).

7.3.4.1. Notch Ligands

In the neural plate, *dll1* expression is stronger posteriorly, and *jag1* expression is stronger anteriorly (Table 7.7) (Figure 7.1C) (Kiyota et al., 2001). Jag1 normally restricts the differentiation of primary neurons, and combined *dll1* and *jag1* expression is indispensable for the normal primary neurogenesis pattern (Kiyota et al., 2001) (Table 7.7). Interestingly, Dll1 and Jag1 contain sequences encoding a putative nuclear localization signal. Moreover, GFP fusion proteins of both ligands naturally underwent proteolitic cleavage during gastrulation, releasing their intracellular domains (ICDs), which were detected in nuclei. However, only Jag1-ICD-GFP persisted in cell nuclei and repressed primary neurogenesis without activating *hes5.1* (Kiyota and Kinoshita, 2004). It was proposed that Jag1 inhibits primary

TABLE 7.7
Core Components of the Notch Pathway Involved in *Xenopus* Neurogenesis

See abbreviations in Table 7.3 legend. *ascl2*, *neurog1*, and *neurog2* are bHLH proneural genes; *neurod1* and *neurod4* encode bHLH neuronal determination TFs; *ebf2* encodes an HLH TF, positive regulator of neurogenesis; *pak3* acts downstream of proneural genes, withdrawing progenitors from the cell-cycle and promoting neuronal differentiation; *myt1* encodes a zinc-finger TF, positive regulator of neurogenesis; *tubb2b*, terminal neuronal differentiation marker; *sox2* and *sox3*, neural plate markers.

Gene	Expression Role/Details	Gain-of-Function	Loss-of-Function (Dominant-Negative/Morpholino/Antagonist)
notch1/psen1/RBPJ	*notch1* is expressed by most or all cells in the proneural domains since late gastrula (Chitnis et al., 1995). Inhibits PN in neural plate and placodes. RBPJ directly binds the RAM23 region of NICD1 (Wettstein et al., 1997), and this complex activates transcription of Notch target genes.	*notch1ΔE* or *NICD1:* ↓PN (neural plate and placodes); *NICD1:* ↓*dll1, neurog2, neurod4*, *myt1, pak3* (Chitnis et al., 1995; Ma et al., 1996; Bellefroid et al., 1996; Perron et al., 1999; Souopgui et al., 2002; Riddiford and Schlosser, 2017). *NICD1:* blocked ectopic neurogenesis induced by *neurod4, ascl2*, or *neurog2*; unable to block ectopic neurogenesis induced by *neurod1* or by co-injection of either proneural gene together with *myt1* (Chitnis and Kintner, 1996; Ma et al., 1996; Bellefroid et al., 1996; Perron et al., 1999). *notch1ΔE:* blocked terminal neuronal differentiation induced by *neurog2* but not by *neurod1* (Olson et al., 1998). *RBPJ* overexpression: weakly ↓PN (Wettstein et al., 1997). *psen1* overexpression:↑PN (Paganelli et al., 2001). See *hes5.1, hes5.4, hes6.1* in Table 7.3.	*notch1* MO: ↑PN (NF15, ISH) (López et al., 2003). *RBPJ^{DBM}:* ↑density of *neurog2*+, *dll1*+ cells, and primary neurons; reversed the inhibition of PN produced by *dll1* overexpression (Wettstein et al., 1997). DAPT (γ-secretase inhibitor): ↑PN (Revinski et al., 2010). See *hes5.1*, *hes6.1* in Table 8.3.
dll1	"Salt-and-pepper" expression begins at late gastrula, restricted to a subset of cells in the proneural domains, scattered within the deep layer of the neural ectoderm, preceding the onset of *neurod1* and *tubb2b.* Marks future neurons around the time they are committed to a neuronal fate (Chitnis et al., 1995; Ma et al., 1996; Chalmers et al., 2002). Within the proneural domains, Dll1 inhibits PN in neighboring cells by lateral inhibition, involving down-regulation of *dll1* (but not of *jag1*) in the receiving cells. Not involved through lateral inhibition in delaying or restricting anterior neurogenesis at neural plate stage.	*dll1* overexpression: ↓PN (Chitnis et al., 1995) without affecting *jag1* (Kiyota et al., 2001); ↓*myt1* (Bellefroid et al., 1996). See *hes5.1* in Table 7.3.	*dll1STU:* ↑PN even when proliferation was blocked with HUA; effect confined to proneural domains, reversed by *dll1* overexpression (Chitnis et al., 1995). ↑density of *neurog2*+, *myt1*+ cells in the proneural domains (Ma et al., 1996; Bellefroid et al., 1996). ↑density of supernumerary neurons induced by *ebf2* overexpression (Dubois et al., 1998). *dll1* MO: ↑PN (Nichane et al., 2008b). *dll1STU:* unable to promote neurogenesis in neuralized animal caps of anterior character overexpressing *ascl2* (NF16) (Papalopulu and Kintner, 1996). Unable to rescue the inhibition of neurogenesis in the trigeminal placode produced by *rax* overexpression (whole embryos) (Andreazzoli et al., 2003).

dlc	Expression in the pair of medial stripes of PN (Peres and Durston, 2006). In the neural plate, *dlc* is necessary for terminal neuronal differentiation in the medial stripe of PN.		*dlc MO:* ↓primary neurons (ISH *tubb2b*, NF21) without affecting *neurog2* in the medial stripe (ISH, NF21) (Peres and Durston, 2006).
jag1	Expressed in the ANB, in a pair of transversal, bilateral stripes corresponding to the future mesencephalon, trigeminal placodes, and two pairs of bilateral AP stripes in the posterior neural plate, one presumably corresponding to the developing intermediate neurons and the other in-between the medial and intermediate *dll1* stripes (Kiyota et al., 2001). *jag1* inhibits PN. This does not rely on *dll1* down-regulation.	*jag1* overexpression*:* ↓PN without affecting *dll1*; prevented the increase of PN induced by *dll1STU* (Kiyota et al., 2001). *jag1ICD:* translocated to the nucleus, ↓PN (Kiyota and Kinoshita, 2004). See *hes5.1* in Table 7.3.	*DN-jag1* (lacking the intracellular domain): ↑PN; this was rescued by *dll1* in a dose-dependent manner (Kiyota et al., 2001).

neurogenesis through Notch-canonical trans-signaling, involving *hes5.1* activation in receiving cells, and through Jag1-ICD cis-signaling, perhaps acting as a transcriptional regulator not involving *hes5.1* (Kiyota et al., 2001; Kiyota and Kinoshita, 2004).

In the posterior neural plate, another member of the *delta* gene family, *dlc*, which is only expressed by the medial stripes (Figure 7.1C), appears to be necessary for terminal differentiation of primary neurons (Peres and Durston, 2006) (Table 7.7).

7.3.4.2. Which *hes1–7* Genes Are Involved in Primary Neurogenesis?

There is a synexpression group transcribed in primary neurogenesis domains, including *hes6.1* and multiple *hes5* genes (Figure 7.2). Of these, *hes5.1*, *hes5.2*, and *hes5.4–5.7* are positively regulated by Notch signaling in some cases through paired RBPJ binding sites (Tables 7.2, 7.3). *hes5.5* needs direct additional input from proneural bHLH factors, whereas *hes5.1* is indirectly up-regulated by them. Therefore, Notch/RBPJ signaling is necessary for the expression of *hes5* genes in proneural domains *in vivo*, but they also require regulation by additional inputs. In contrast, *hes4*, which is expressed in other domains and is directly regulated by Notch through RBPJ binding sites, was not up-regulated by *neurog2* overexpression (Lamar and Kintner, 2005).

So far, gain- and loss-of-function experiments show that *hes2*, *hes4*, *hes5.1*, *hes5.4*, *hes1*, *hes5.5, hes5.6*, and *hey1* are able to suppress primary neurogenesis but in different domains of the neural plate (Table 7.8). *hes1*, *hes2*, and *hes4* are involved in the development of the neural border and/or its descendants (see subsequently) and, as well as *hey1*, they are up-regulated by Notch (Tables 7.2, 7.3). *hes4* and *hey1* are expressed in the midline of the neural plate (future floor plate), while *hes2* is expressed in the superficial layer of the intermediate and lateral primary neuron stripes (Figure 7.2), where neural precursors continue to proliferate (Sölter et al., 2006).

hes6.1 is expressed in scattered cells in the medial and lateral primary neuron domains (Figure 7.2). Interestingly, it is repressed by Notch/RBPJ signaling and is required for expression and activity of *neurog2* and the neuronal determination gene *neurod1*, thus relieving neuronal precursors from Notch-mediated lateral inhibition (Koyano-Nakagawa et al., 2000; Murai et al., 2011) (Tables 7.2, 7.3, 7.8). Moreover, *neurog2* and *neurod1* induced *hes6.1* in the absence of protein synthesis in animal caps (Seo et al., 2007), suggesting they directly activate *hes6.1*, establishing a positive feedback loop. It was proposed that Hes6.1 promotes primary neurogenesis through direct protein-protein antagonistic interactions with other Hes factors (e.g. Hes1, Hes4) that inhibit neuronal differentiation and by sequestering TLE/Groucho co-repressors that antagonize bHLH-O Hes proteins that directly repress proneural and neuronal determination genes (Murai et al., 2011).

7.3.4.3. Regulation of the Cell-Cycle

There is evidence that Notch1 might inhibit the withdrawal of neuroblasts from mitosis and prevent their differentiation through the negative regulation of *p21-activated kinase 3 (pak3)* (Souopgui et al., 2002). However, either blocking Dll1 or excessive Notch1/RBPJ signaling inhibited mitosis in the neural plate (Vernon et al., 2006). Experiments with mouse P19 cells and *Xenopus* embryos showed a differential sensitivity of the *dll1* and *neurod1* promoters to the Cdk-dependent phosphorylation status of Neurog2: while the *dll1* promoter can be activated by hypo-phosphorylated Neurog2 (in cells undergoing cycle lengthening) or by phospho-Neurog2 (in rapidly cycling progenitors), the *neurod1* promoter can only be activated by hypo-phosphorylated Neurog2. Hypo-phosphorylated Neurog2 was able and phospho-Neurog2 was unable to promote neuronal differentiation in the presence of NICD1, indicating that the Cdk-dependent Neurog2 phosphorylation status also determines its post-transcriptional sensitivity to Notch signaling (Hindley et al., 2012). Therefore, it was proposed that hypo-phosphorylated Neurog2 shifts the balance from progenitor maintenance to neuronal differentiation. Similarly, studies employing the proneural mouse Ascl1 in *Xenopus* mitotic and interphase egg extracts and *Xenopus* embryos undergoing primary neurogenesis indicate that the Cdk-dependent phosphorylation status of Ascl1 regulates its post-translational sensitivity to Notch signaling. Hypo-phosphorylated Ascl1 probably escapes Notch-mediated lateral inhibition through up-regulation of Myt1 (Ali et al., 2014). Hes1 is phosphorylated by CyclinB/Cdk1 and CyclinA/Cdk2 *in vitro*, suggesting it may be controlled by phosphorylation in the G2/M phase (Hardwick and Philpott, 2015). Phosphorylation by proline-directed kinases destabilizes Hes1 protein and decreases its inhibitory activity on PN *in vivo* (Hardwick and Philpott, 2019).

7.3.5. Neural Plate Border and Midbrain-Hindbrain Boundary

Neural induction subdivides the embryonic ectoderm into neural and non-neural regions, with an intervening transition zone known as the neural plate border (NB) zone. This zone gives rise to neural crest cells (NCCs) and cranial placodes and is positioned by intermediate BMP levels as well as local FGF and Wnt signaling that induce a number of NB specifier genes (Stuhlmiller and García-Castro, 2012; Pla and Monsoro-Burq, 2018; Grocott et al., 2012; Saint-Jeannet and Moody, 2014; Steventon et al., 2014). Members of the Notch pathway and *hes1–7* genes are expressed throughout the development of the NB and its derivatives (Figure 7.2) (Tables 7.9, 7.10). *dll1* is restricted to the NB by the counterbalanced activities of a positive regulator, Irx1, and a negative regulator, Snai1 (Glavic et al., 2004), and *hes4* expression in the NB laterally restricts the neural plate (Maharana and Schlosser, 2018). Interestingly, *hes3* can promote neural plate fate at the expense of NCC and cranial

TABLE 7.8

Role of *hes/hey* Genes in *Xenopus* Neurogenesis and Epidermal Differentiation

See abbreviations in Table 7.3 legend and marker details in Table 7.7 legend.

Gene	Role/Details	Gain-of-Function	Loss-of-Function (Dominant-Negative/Morpholino)
hes1	Inhibits neurogenesis by abolishing the activity of proneural/neuronal differentiation bHLH TFs and keeping neural progenitors in a proliferative state, independently of binding to TLE/Groucho co-repressors. Hes1 binds to N-box *in vitro* (Koyano-Nakagawa et al., 2000) and does not block the ability of Neurog2 to bind DNA or its coactivator E12 *in vitro* (Murai et al., 2011).	*hes1* overexpression: ↑*sox2* [not shown in (Nichane et al., 2008a)], induced ectopic *dll1* [not shown in (Nichane et al., 2008b)], ↓PN by abolishing *Neurog2* and *Neurod1* activity (Murai et al., 2011). mir-9 MO and *hes1* target protector MO: ↓neurogenesis (NF30), ↑proliferation (Bonev et al., 2011).	*hes1*-ΔWRPW: did not suppress PN (Murai et al., 2011).
hes2	Inhibits PN by repressing proneural gene transcription and other mechanisms such as binding to proneural bHLH proteins like NeuroD. In the retina, *hes2* promotes gliogenesis and inhibits neurogenesis through a DNA-binding mechanism. Immunoprecipitation in animal cap explants: XHes2 interacts with XNeuroD1, XNeuroD4, XHes1, and XHes6 but not with other bHLH proteins tested, including XNeurog2 (Sölter et al., 2006).	*hes2:* mRNA overexpression: ↓PN, ↓ *neurog2* (Sölter et al., 2006). Local overexpression by *in vivo* DNA lipofection in the developing retina: ↑glial population at the expense of neurons (Sölter et al., 2006).	*Hes2-ΔW-VP16:* mRNA: induced ectopic primary sensory neurons and *neurog2* (Sölter et al., 2006). *In vivo* lipofection of Hes2-ΔW-VP16 DNA: ↓glial population, ↑some neuronal types (Sölter et al., 2006). *hes2DBM:* did not affect retinal fates; DNA binding domain necessary for promoting gliogenesis in the retina (Sölter et al., 2006). *hes2 MO:* ↑*neurog2* in presumptive otic placode. *In vivo* lipofection of *hes2* MOs ↓glial population in the retina (Sölter et al., 2006).
hes4	Inhibits PN. Hes4 protein binds to N-box *in vitro* (electrophoretic mobility shift assay) (Koyano-Nakagawa et al., 2000).	*hes4* overexpression*:* ↓PN (*tubb2b*, neural plate stage) (Glavic et al., 2004) (Cui, 2005); ↓*neurog2* and *neurod1* in the anterior neural plate (Andreazzoli et al., 2003; Cui, 2005); ↑*dll1* independently of DNA binding (neural plate stage) (Nichane et al., 2008b); blocked the induction of *tubb2b* by *neurog2/noggin* in animal caps (NF unknown, RT-PCR) (Cui, 2005). *hGR-hes4* (Dex NF18): ↓PN (ISH *tubb2b*, neurula stage) (Taelman et al., 2006).	*hes4* MO: ↑ *neurog2, myt1*, and *dll1;* ↑PN in the trigeminal placode (early neurula) (Nagatomo and Hashimoto, 2007; Murato and Hashimoto, 2009); ↓proliferation, ↑apoptosis (late neurula) (Nagatomo and Hashimoto, 2007); ↓*dll1* (neural plate stage) (Nichane et al., 2008b).
hes5.1	Inhibits PN probably by repressing bHLH proneural genes through DNA binding and recruitment of the co-repressor TLE/Groucho. The DNA binding domain and the WRPW motif are necessary for inhibiting PN and preventing ectopic neurogenesis induced by the bHLH TF Atoh7 (Schneider et al., 2001).	*hes5.1* overexpression: ↓PN, even in the presence of the bHLH TF Atoh7 (ISH, neural plate stage) (Schneider et al., 2001).	*hes5.1 ΔWRPW:* ↑PN [data not shown in (Ito et al., 2007a)]. *hes5.1 ΔWRPW* or *hes5.1 ΔN* (basic domain deleted): did not prevent ectopic PN induced by the bHLH TF Atoh7 (ISH, neural plate stage) (Schneider et al., 2001).
hes5.4	During placodal development, *hes5.4* restricts the neurogenesis cascade upstream of proneural genes. Required for the expression of the neural progenitor gene *sox3* and neuronal differentiation downstream of proneural genes.	*hes5.4* overexpression: ↓*neurog1, neurog2*, *neurod1*, and *tubb2b* in the neural plate and placodes; ↓ neural marker *sox3* in placodes (ISH, neural plate) (Riddiford and Schlosser, 2017).	*hes5.4* MO: ↑*hes5.4*, *neurog1, neurog2, dll1*, and *pou4f1.2* placodal domains with occasional reductions of these markers; ↓placodal *sox3, neurod1*, and *tubb2b* (Riddiford and Schlosser, 2017).

(*Continued*)

TABLE 7.8 (Continued)
Role of *hes/hey* Genes in *Xenopus* Neurogenesis and Epidermal Differentiation

Gene	Role/Details	Gain-of-Function	Loss-of-Function (Dominant-Negative/Morpholino)
hes5.5	Inhibition of PN. Does not interact *in vitro* with Hey1 (Taelman et al., 2004).	GR-*hes5.5* (Dex NF12 or NF18): ↓PN (ISH neurula stage) (Taelman et al., 2004; Taelman et al., 2006).	
hes5.6	Inhibition of PN. Does not form homodimers *in vivo* nor heterodimerizes with other bHLH-O proteins (Hes1, Hes4, Hes5.6, Hey1). Heterodimerizes *in vivo* with bHLH proteins that promote neurogenesis (Neurog2, Neurod1, Neurod4) (IP assay from *Xenopus* embryo extracts) (Taelman et al., 2004).	GR-*hes5.6* (Dex NF12 or NF18): ↓PN (ISH neurula stage) (Taelman et al., 2004; Taelman et al., 2006).	
hes5.10	Inhibits differentiation of epidermal multiciliate cells in the inner layer of the non-neural ectoderm through a Dll1/Notch-dependent lateral inhibition mechanism. Possibly participates in the inhibition of neurogenesis in the outer layer of the ectoderm through a different mechanism.	*hes5.10* overexpression: ↓density of multiciliate cells in the epidermis (tailbud stage); ↓*dll1* in animal caps (mid-gastrula) (Deblandre et al., 1999); ↓*neurod1* and PN without affecting *neurog2* or neural specification; acts downstream of *neurod1*, because it prevented ectopic neurogenesis but not ectopic *neurod1* induced by *neurog2* (Chalmers et al., 2002).	*hes5.10DBM:* ↑density of multiciliate cells in the epidermis (tailbud stage), ↑*dll1* in animal caps (mid-gastrula) (Deblandre et al., 1999). *hes5.10* MO: unable to induce ectopic PN in the deep layer (Chalmers et al., 2002).
hes6.1	*hes6.1* promotes PN by antagonizing other Hes proteins that suppress neuronal differentiation. It does so in a post-transcriptional, TLE/Groucho-independent, and DNA binding-independent way (Koyano-Nakagawa et al., 2000; Murai et al., 2011). However, the full promotion of PN requires TLE/Groucho binding (Murai et al., 2011). See Table 7.4 for the regulation of *hes1* and *hes4* by *hes6.1*.	*hes6.1* overexpression: ↑*neurog2* domains (Koyano-Nakagawa et al., 2000) and primary neuron differentiation (Cossins et al., 2002) throughout the posterior neural plate; ↑*dll1*, *hes5.1*, and *hes5.7* domains, indicating that the increase in neuronal differentiation does not involve transcriptional repression of genes of the lateral inhibition program (Koyano-Nakagawa et al., 2000). Hes6.1 did not affect the binding of Neurog2 to its E12 coactivator during *in vitro* binding to E-box. Hes6.1 did not directly interact with Neurog2 (immunoprecipitation assay). Hes6.1 directly binds and impairs the ability of Hes1 to repress PN through a TLE/Groucho-independent mechanism (Murai et al., 2011).	*hes6.1* MO: ↓*tubb2b, neurog2*, and *neurod1* (neural plate stage); prevented the induction of ectopic neurons by *neurog2* or *neurod1* (Murai et al., 2011). *hes6.1* ΔWRPW: did not rescue the inhibition of PN produced by *hes6.1* MO (Murai et al., 2011). *hes6.1DBM:* promoted PN like *hes6.1* overexpression, indicating that DNA binding is not required for this activity (Cossins et al., 2002).
hey1	Possible role in suppressing neurogenesis in the FP by antagonizing proneural genes, contributing to promote or maintain FP identity. Additional inhibitors might be required to maintain neurogenesis inhibited in FP. Hey1 does not bind the co-repressor TLE/Groucho, as it lacks the typical WRPW motif of bHLH-O repressors (Pichon et al., 2004). For inhibition of PN, Hey1 acts as a DNA binding repressor, requiring the Orange domain and the C-terminal region for dimerization. Hey1 heterodimerizes *in vivo* with Hes1 and Hes4 and weakly with Hes2, but it does not bind Hes5.5 or Hes5.6. It weakly binds bHLH proteins that promote neuronal differentiation (Neurod1 and Neurod4) but does not bind the proneural protein Neurog2 (Taelman et al., 2004).	*hey1* or GR-*hey1* (Dex NF12 or NF18): ↓PN (Taelman et al., 2004; Taelman et al., 2006). *hey1* blocked *neurog2*'s ability to induce ectopic neurogenesis (Taelman et al., 2004).	*hey1DBM:* did not inhibit PN and could not block *neurog2*'s ability to induce ectopic neurogenesis (Taelman et al., 2004). *hey1* MO +/- *hes4.L* MO: did not induce ectopic neurogenesis in the FP. (Taelman et al., 2004). Note: MO sequences were not reported in this study. *hey1.L+S* MO: *tubb2b* unaffected (ISH in tailbuds) (Taelman et al., 2006).

placodes, suggesting it also participates in setting the neural plate/NB boundary, although this could not be confirmed by *hes3* knock-down, perhaps due to compensation by other *hes* genes (Hong and Saint-Jeannet, 2018).

7.3.5.1. The Role of *hes4* in NB and NCC Development

hes4 is expressed in prospective NCC territories, along with *notch1* (Glavic et al., 2004; Vega-López et al., 2015), and appears to act through partially counteracting pathways to promote and restrict *foxd3* expression to NCC (Maharana and Schlosser, 2018).

Neural induction subdivides the ectoderm into neural and non-neural regions. The transition zone is the neural border, from which neural crest cells, placodes, the bordering non-neural ectoderm, and dorsal neural tube segregate (Stuhlmiller and García-Castro, 2012; Pla and Monsoro-Burq, 2018). The pre-placodal ectoderm (PPE) forms a horseshoe-shaped domain surrounding the neural plate at its anterior end and later segregates into individual placodes (Stuhlmiller and García-Castro, 2012; Grocott et al., 2012; Saint-Jeannet and Moody, 2014; Steventon et al., 2014; Pla and Monsoro-Burq, 2018). NCC development begins during gastrulation, when the NB is induced and stabilized and progresses through sequential steps, with the NB-TFs controlling the onset of NCC induction within the NB at the end of gastrulation and during the neural plate stage. This is followed by NCC specification, which occurs through a multistep process during neurulation and involving the activation of a new set of genes encoding specific NCC transcription factors (NCC-TFs), which are not shared with contiguous populations. These NCC-TFs are activated in a stereotyped sequence, with an early step (activation of *sox9* since NF11; *snai2* and *foxd3* since NF12–12.5) and a maturation step, with the activation of late NCC-TFs (*sox10* from NF13–14, *twist1*). NCC migration begins at the end of neurulation (once the neural folds fuse at the midline, transforming the neural plate into the neural tube) and continues during organogenesis, during which post-migratory NCCs colonize target tissues and organs, where they differentiate into multiple cell types (Pegoraro and Monsoro-Burq, 2013; Pla and Monsoro-Burq, 2018).

There are conflicting interpretations concerning the role of *hes4* in NB/NCC development and its regulation by Notch signaling in these tissues (Tables 7.9, 7.10). Although *hes4* is already expressed in the NB at mid-gastrula (Tsuji et al., 2003) and is considered an NB specifier *in vivo*, this TF alone can not initiate NCC specification in animal cap explants (Milet et al., 2013). Analysis at advanced neurula stages indicated that Dll1 signals to presumptive NCC through Notch1/RBPJ inducing *hes4*, which represses *bmp4* to ensure optimal BMP signaling levels for NCC specification (Glavic et al., 2004). Others showed that during NCC specification, *hes4* restricts *dll1* in NCC for the survival and maintenance of precursors in a mitotic, undifferentiated state (Nagatomo and Hashimoto, 2007). Strikingly, another group showed that the NCC *hes4* domain was unaffected in neurulae following activation or blockade of the RBPJ-dependent pathway at mid-gastrula and noticed that *hes4* and *dll1* domains partially overlap in the anterior, lateral neural plate. They proposed that Dll1 favors NCC precursor proliferation rather than controlling the balance between primary neurons and NCC fates. Through a DNA-binding independent mechanism, *hes4* transiently and indirectly induces *dll1* expression, leading to NCC proliferation and differentiation. Through a cell-autonomous, DNA-binding-dependent mechanism, *hes4* up-regulates early NB genes and is required for NCC survival and maintenance in an undifferentiated state (Nichane et al., 2008a; Nichane et al., 2008b). More recently, other authors showed that in the pre-migratory NCC territory, *hes1* and *hes4* are positively regulated by Dll1/Notch/RBPJ whereas BMP down-regulates *hes4* (Nagatomo and Hashimoto, 2007; Vega-López et al., 2015). These authors propose that *hes1* and *hes4* are required for several processes during NCC development. First, both promote NCC specification at the expense of neural plate and epidermis independent of cell proliferation; then Hes4 acts as a transcriptional repressor during NCC specification and is later required for their survival during neurulation; finally, *hes4* is required cell-autonomously to initiate NCC migration and their differentiation into the cranial skeleton.

Wnt and FGF signaling are necessary for *hes4* expression, whereas BMP down-regulates it in the presumptive NCC at neural plate stages (Nichane et al., 2008a; Vega-López et al., 2015). Others identified three *hes4* expression phases during NB/NCC development. First, during NB induction (early gastrula), *hes4* expression is insensitive to BMP signaling but requires down-regulation of the Wnt pathway. Then, during NCC induction (mid-gastrula), it requires Wnt and down-regulation of BMP signaling. Finally, both pathways are required for *hes4* expression during NCC maintenance in early neurula (Steventon and Mayor, 2012). FGF signaling was proposed to regulate *hes4* and *dll1* in the NB through Stat3.1, which is phosphorylated by FGF/FGFR4. Whereas low Stat3.1 activity up-regulates *hes4*, high Stat3.1 activity promotes *dll1* expression and Dll1/Notch signaling (Nichane et al., 2010). Overall, it is clear that *hes4* is required for NCC development in *Xenopus*, but controversies still exist about the underlying mechanisms (for discussion, see Vega-López et al., 2015). Time-dependent opposite responses to the same experimental Notch perturbation, which were observed in other contexts in *Xenopus* (Contakos et al., 2005; Revinski et al., 2010), might underlie the conflicting results between different studies. Some reviews regard Notch signaling as an important source for NCC maintenance rather than as a key player in NB induction during gastrulation (Stuhlmiller and García-Castro, 2012; Pla and Monsoro-Burq, 2018). Curiously, most studies analyzed the effects of perturbing Notch signaling on *hes4* too late to address if this pathway plays an early role in establishing the NB *hes4* domain (Table 7.9). However, we observed a clear expansion of the NB *hes4* domain at mid-gastrula after constitutive Notch1 activation beginning at cleavage stages (López et al., 2005), suggesting that Notch participates in the establishment of

TABLE 7.9
Core Components of the Notch Pathway in *Xenopus* Neural Border and Its Descendants

krt12.4, non-neural ectoderm marker; *nkx1–2*, posterior NB MARKER (Kurata and Ueno, 2003); *sox2*, *sox3*, *soxd*, neural plate markers; *foxe3*, positive regulator of lens fate (Ogino et al., 2008); *pax3*, *msx1*, *zic1*, NB markers (Nichane et al., 2008b). For additional abbreviations, see main text and Table 7.3 legend.

Gene	Expression	Gain-of-Function	Loss-of-Function (Dominant-Negative/Morpholino)
notch1/RBPJ	*notch1* expression: NB, neural plate, and ectoderm (Coffman et al., 1993). Prospective NCC territories (neural plate stage) (Glavic et al., 2004).	**NB, NCC:** *notch1ΔE:* ↓*twist1, nkx1–2*, non-neural ectoderm (*krt12.4*) (neural plate stage, ISH) (Coffman et al., 1993; Kurata and Ueno, 2003); ↓branchial arches (tadpole) (Coffman et al., 1993). *NICD1:* ↑NB marker ***hes4*** (gastrula, ISH) (López et al., 2005), neural plate marker *sox2* (neural plate stage, ISH) (Revinski et al., 2010). *GR-NICD1* or *GR-RBPJ-Ank* (Dex NF12): ↑presumptive NCC (*snai2, foxd3*, ***hes4***); ↓*bmp4* (non-neural ectoderm) (late neurula) (Glavic et al., 2004). *GR-RBPJ-Ank* (Dex NF11): ***hes4***NCC domain unaffected (neural plate stage, ISH) (Nichane et al., 2008a). **PPE:** *NICD1:* ↑*hes5.4* in placodes and adjacent non-neural ectoderm, even in the absence of *six1/eya1* function (ISH, neural plate stage) (Riddiford and Schlosser, 2017). **Lens placode (*notch1 /notch2* ?):** GR-*RBPJ*-VP16 (Dex NF15): ectopic *foxe3* restricted to the anterior ectoderm (NF22–24) (Ogino et al., 2008). GR-*RBPJ*-VP16 or *NICD1* + GR-*otx2* (Dex NF15): massive ectopic *foxe3* (NF22–24) (Ogino et al., 2008).	**NB, NCC:** *RBPJ^{DBM}* ↓neural plate *(sox2)* (neural plate stage, ISH) (Revinski et al., 2010). *notch1* MO: ↓presumptive neural plate (*sox2*) (late gastrula); ↑neural plate (*sox2*) (neural plate stage) (ISH) (Revinski et al., 2010). *GR-RBPJDBM* (Dex NF12): ↓presumptive NCC (*snai2, foxd3*, ***hes4***); ↑*bmp4* domain (late neurula) (Glavic et al., 2004). GR-RBPJDBM (Dex NF11): ***hes4***NCC domain unaffected (neural plate stage, ISH) (Nichane et al., 2008a) **PPE:** *RBPJDBM:* ↓*hes5.4* in neural plate and placodes (ISH, neural plate stage) (Riddiford and Schlosser, 2017). **Lens placode (*notch1 /notch2* ?):** GR-*RBPJ*DBM/Dex NF15: ↓*foxe3*, impaired lens development (NF22–24) (Ogino et al., 2008).
notch2	PPE (neural plate stage) (Murato and Hashimoto, 2009; Maharana and Schlosser, 2018).		
dll1	Anterior neural border (ANB), surrounding the presumptive NCC at early neurula stage. (Glavic et al., 2004).	**NB, NCC:** *dll1* overexpression*:* ↑NCC (*snai2*, *sox10*) without affecting NB (*pax3*, *msx1*), neural plate (*soxd, sox3*), or placodal marker *six1* (Nichane et al., 2008b).	**NB, NCC:** *dll1STU:* ↓NCC (*snai2, foxd3*, ***hes4***); ↑*bmp4* (late neurula) (Glavic et al., 2004); ↓neural plate (*sox2*) (late gastrula, early neurula; ISH) (Revinski et al., 2010). *dll1* MO: ↓NCC (*snai2*, *sox10*) (neural plate stage) (Nichane et al., 2008b). **Lens placode:** *dll1STU:* Head defects, ↓*foxe3* (Ogino et al., 2008)
dlc	Similar to *dll1* but at lower levels. Expressed in an arc corresponding to the ANB; later resolves into *dlc*+ cranial placodes (Glavic et al., 2004; Peres and Durston, 2006).		**NCC, placodes:** *dlc* MO*:* migration failure of NCC and placodal cells (Peres and Durston, 2006). *dlctr*: ↓*foxe3* (NF23) (Ogino et al., 2008).
jag1	ANB, surrounding the presumptive NCC at early neurula stage (Glavic et al., 2004).		

the NB through the positive regulation of the NB-specifier *hes4*, which receives multiple regulatory inputs from other pathways. Moreover, Notch1 can suppress *nkx1–2* in presumptive NCC; this gene encodes a transcriptional repressor thought to inhibit neural fate to allow NCC induction (Kurata and Ueno, 2003).

7.3.5.2. The Role of *hes* Genes in PPE Development

Notch signaling and genes of the *hes1–7* group are also involved in cranial placode development (Tables 7.9, 7.10). Six1 and its co-activator Eya1 are crucial regulators of placode development (Brugmann et al., 2004; Riddiford and Schlosser, 2016). *hes4* is required for establishing the preplacodal ectoderm; the expression of *notch2*, *six1*, and *eya1* in this tissue; and the development of the lens field (Murato and Hashimoto, 2009; Maharana and Schlosser, 2018) (Table 7.10), placing *hes4* upstream of the placodal program probably at the level of NB establishment. However, additional gene cascades converge in setting this program, since other PPE markers were not affected by *hes4* knock-down (Murato and Hashimoto, 2009). Recently, a NB gene regulatory network that cross-regulates with Six1/Eya1 was proposed for controlling PPE and NCC specification. This GRN includes Hes4 and other TFs expressed in the neural and non-neural ectoderm (Maharana and Schlosser, 2018). Downstream of this GRN are *hes2*, *hes5.4*, and *hes5.6*, which are expressed in the PPE. They are presumptive direct targets of Six1/Eya1, as they were up-regulated by them in the absence of protein synthesis, and placodal *hes5.4* and *hes5.6* expression require Six1/Eya1 function (Riddiford and Schlosser, 2016).

In neurogenic placodes, Six1/Eya1 control *dll1* in a dose-dependent manner. High Six1/Eya1 levels maintain proliferating placodal precursors, but as cells delaminate from the placodes, Six/Eya1 levels are reduced and the neurogenesis program is triggered, including the onset of *dll1* expression (Schlosser et al., 2008). Notch1/RBPJ is required for *hes5.4* expression during placodal development (Tables 7.2, 7.3) (Riddiford and Schlosser, 2016). The requirement of Notch signaling for *hes2* and *hes5.6* expression in this process is currently unknown, although *hes5.6* is induced by Notch1/RBPJ during gastrulation (Tables 7.2, 7.3). *hes2* was not induced by activation of the Notch pathway in naive or neuralized animal cap explants but was moderately induced in embryos, with ectopic expression restricted to the NB (Sölter et al., 2006) (Tables 7.2, 7.3).

PPE *hes5.4* expression requires two positive regulators: (1) high Six1/Eya1 levels activate *hes5.4* independently of Notch/RBPJ and (2) Notch/RBPJ activates *hes5.4* independently of Six1/Eya1, probably through lateral inhibition (Tables 7.2, 7.3, 7.9). Subsequently, *hes5.4* maintains placodal progenitors in an undifferentiated state, restricting primary neurogenesis upstream of proneural genes (Table 7.8). As Six1/Eya1 activity declines, *hes5.4* is required at low levels to promote neuronal differentiation. Intriguingly, *hes5.4* is also required for neuronal differentiation downstream of proneural genes, as terminal differentiation markers were frequently decreased after *hes5.4* knock-down (Table 7.8). The details of the mechanism underlying these opposing roles remain unresolved, but oscillation of *hes5.4* expression might be involved since *hes5.4* represses its own transcription (Tables 7.4, 7.8) (Riddiford and Schlosser, 2017).

7.3.5.3. Other Roles for Notch Pathway in Placode Development

Other evidence further supports Notch pathway involvement in cranial placode development (Table 7.9). Potentiated by Otx2, Notch can activate *dmrta1/2* in the anterior ectoderm. These genes encode TFs expressed in the presumptive olfactory placodes and are involved in olfactory neurogenesis (Parlier et al., 2013). An RBPJ binding site was found in the main enhancer of *foxe3*, a key TF required for lens placode development (Ogino et al., 2008; Kenyon et al., 1999). *dll1* and *dlc* are expressed in the adjacent presumptive retina, from where they presumably induce *foxe3* through Notch/RBPJ. While an antimorphic *dll1* produced severe head defects, making the results difficult to interpret, the antimorphic *dlc* produced a more restricted, lens-defective phenotype, indicating that *dlc* is involved in lens development (Ogino et al., 2008).

7.3.5.4. The Midbrain/Hindbrain Boundary

The midbrain/hindbrain boundary (MHB) is considered an organizing center because signals from this region induce and pattern the adjacent mesencephalon and hindbrain (Anderson and Stern, 2016). *hes7.1* is one of the first genes to demarcate the presumptive MHB at early gastrula stages. Notably, at neural plate stages, the *hes7.1* domain coincides with a *hes5.1, hes5.2*, and *hes5.7* expression gap (Shinga et al., 2001; Takada et al., 2005) (Figure 7.2) (Table 7.11). *hes7.1* is necessary for MHB establishment through repressing, probably directly, *hes5.1, hes5.2*, and *hes5.7* in this region, whereas these *hes5* genes (which are positively regulated by Dll/Notch signaling during primary neurogenesis) are thought to restrict *hes7.1* to the MHB (Shinga et al., 2001; Takada et al., 2005) (Tables 7.4, 7.11). Strikingly, NICD1 abolished and *RBPJDBM* did not affect MHB *hes7.1* expression (Takada et al., 2005). It would be interesting to address whether *notch1* normally down-regulates *hes7.1* by a non-canonical pathway.

7.3.6. Somitogenesis

The classic Clock and Wavefront hypothesis for vertebrate somitogenesis, which involves Notch signaling, was originally postulated by experimental work based on *Xenopus* (Cooke and Zeeman, 1976; Cooke, 1981). It explains the sequential formation of vertebrate somites from the posterior presomitic mesoderm that is due to an oscillation between permissive and non-permissive phases for segmentation, the so-called "segmentation clock" that is controlled by *hes* genes. Their proteins act as pacemakers that cell-autonomously cycle on and off through an autoregulatory

TABLE 7.10

***hes* Genes in the *Xenopus* Neural Border and Its Descendants**

For the role of *hes* genes in placodal neurogenesis, see *hes2*, *hes5.4* in Table 7.8. See abbreviations in Table 7.3 legend.

Gene	Expression/Role	Gain-of-Function	Loss-of-Function (Dominant-Negative/Morpholino)
hes1	At neural plate stage, *hes1* is expressed in thin longitudinal lines corresponding to the dorsal and ventral boundaries of NCC (Vega-López et al., 2015). Promotes NCC at the expense of contiguous fates (neural plate/epidermis), independently of cell proliferation during early NCC development (Vega-López et al., 2015)	GR-*hes1* (Dex s11): ↑NCC (*snai2*), ↓neural plate (*sox2*) and non-neural ectoderm (*krt12.4*) (ISH neurula); proliferation unaffected (pH3, neurula stage) (Vega-López et al., 2015). GR-*hes1* (Dex s11) +/– HUA: ↑NCC (*foxd3*), ↓neural plate (*sox2*) (ISH neurula) (Vega-López et al., 2015).	GR-*hes1* (Dex s11): ↓NCC (*snai2*), ↑neural plate (*sox2*) and non-neural ectoderm (*krt12.4*) (ISH neurula); proliferation unaffected (pH3, neurula stage) (Vega-López et al., 2015). GR-DN-*hes1* (Dex s11) +/– HUA: ↓NCC (*foxd3*), ↑neural plate (*sox2*) (ISH neurula) (Vega-López et al., 2015).
hes2	Scattered cells in the ectoderm/neural ectoderm (mid-gastrula) Posterior PPE, including the prospective otic and lateral line placodes (neural plate) (Sölter et al., 2006; Riddiford and Schlosser, 2016).		
hes3	Strongly expressed in a domain comprising the anterior and lateral edges of the neural plate, just adjacent to the NB (Hong and Saint-Jeannet, 2018). Sufficient to promote neural plate fates at the expense of NB fates (NCC and placodes) but normal requirement still unproven. Other genes of the Hes family might compensate for *hes3* knock-down.	GR-*hes3* (Dex NF10.5): Promoted neural plate at the expense of NB fates. Blocks NCC induction by *wnt8a* DNA or β-catenin DNA injection. In animal cap assays, blocked NCC and PPE gene induction by Wnt8 and Noggin and promoted neural plate fate (Hong and Saint-Jeannet, 2018).	*hes3* MO: two translation-blocking MOs targeting *hes3.L*, one translation-blocking MO targeting *hes3.S*, and one splice-blocking MO targeting *hes3.L* and *hes3.S*, tested alone or in different combinations, did not affect the expression of gene markers that were affected by the gain of function approach (Hong and Saint-Jeannet, 2018).
hes4	NB at mid-gastrula (Tsuji et al., 2003). One of the earliest PPE markers (mid-gastrula) (Murato and Hashimoto, 2009; Maharana and Schlosser, 2018). Prospective NCC territories (neural plate stage) (Vega-López et al., 2015) *hes4* is required during several steps of NCC development (specification, maintenance, onset of migration). Only the *hes4.L* homeolog is required in *X. laevis*. *hes4* is required for the establishment of the PPE and the development of the lens field.	*hes4* overexpression*:* ↓*bmp4*, ↑NCC (*snai2, msx1*) (neural plate stage) (Glavic et al., 2004) GR-*hes4* (Dex NF11.5–12): ↓NCC (*snai2*, *foxd3*, *sox9*, *sox10*), ↑neural plate (*soxd*), ↑NB (*msx1, pax3, zic1*), ↑*dll1* ↕proliferation (pH3), ↓apoptosis (neural plate stage); ↑ and ↓ different subsets of NCC cell-types (tailbud stage) (Nichane et al., 2008b; Nichane et al., 2008a). GR-*hes4.S*, GR-*hes4.L* (Dex NF11) +/– HUA treatments, pH3; GR-*hes4.S*-EnR, GR-*hes4.L*-EnR (Dex NF12.5): Hes4 acts as a transcriptional repressor, promoting NCC specification at the expense of contiguous fates (neural plate/epider	*hes4* MO: ↓NCC markers without affecting neural plate and epidermal markers (early neurula) (Nagatomo and Hashimoto, 2007) or with ↑ of neural plate and epidermal markers (Vega-López et al., 2015). Variable changes in the expression domains of the NCC specifier *foxd3*, with slight ↑*sox3* (neural plate) (Maharana and Schlosser, 2018). ↓*six1/eya1, notch2* (PPE) (neural plate stage); other PPE markers unaffected (*foxe3, dlx5*) (Maharana and Schlosser, 2018; Murato and Hashimoto, 2009); ↓lens field (*pax6, six3, pitx1*); malformed lens (tadpoles, NF42) (Murato and

		mis) independently of cell proliferation. It is later required for NCC survival during neurulation, and cell autonomously for their initial migration (Vega-López et al., 2015).	Hashimoto, 2009). In these studies, either a mixture of *hes4.L MO* + *hes4.S* MO (Nagatomo and Hashimoto, 2007; Nichane et al., 2008b; Maharana and Schlosser, 2018), *hes4.L* MO alone (Vega-López et al., 2015; Murato et al., 2007), or *hes4.S* MO alone (Murato et al., 2007) were used. *hes4.L* MO but not *hes4.S* MO affected NCC development (Murato et al., 2007). GR-DN-*hes4.S*, GR-DN-*hes4.L* (Dex NF11) +/– HUA, pH3; GR-*hes4.S*-E1A, *GR-hes4.L-E1A* (Dex NF12.5): Hes4 acts as a transcriptional repressor, promoting NCC specification at neural plate/epidermis fates' expense, independently of cell proliferation. It is later required for NCC survival during neurulation and cell-autonomously for their initial migration (Vega-López et al., 2015). GR-*hes4DBM* (Dex NF11.5–12): same results as GR-*hes4* (Dex NF11.5–12), except that it did not affect *soxd* and *msx1* (Nichane et al., 2008b).
hes5.4	Anterior PPE (neural plate stage); otic vesicle; olfactory, epibranchial, and lateral line placodes (tailbud stage) (Riddiford and Schlosser, 2016).	See Table 7.8.	See Table 7.8.
hes5.6	Anterior PPE (neural plate stage); otic vesicle; olfactory, epibranchial, and lateral line placodes (tailbud stage) (Riddiford and Schlosser, 2016).		

TABLE 7.11
hes Genes in the Establishment of the *Xenopus* Midbrain/Hindbrain Boundary

See abbreviations in Table 7.3 legend.

Gene	Expression Role/Details	Gain-of-Function	Loss-of-Function (Dominant-Negative/Morpholino)
hes5.1	PN domains with a gap at the MHB. Restricts the MHB.	*hes5.1* overexpression: ↓MHB specification (*hes7.1* and *pax2*, ISH neural plate stage) (Takada et al., 2005)-	
hes5.2	PN domains with a gap at the MHB. Restricts the MHB.	*hes5.2* overexpression: ↓MHB specification (*pax2*, ISH at neural plate stage) (Takada et al., 2005).	
hes5.7	PN domains with a gap at the MHB. Restricts the MHB.	*hes5.7* overexpression: ↓MHB specification (*pax2*, ISH at neural plate stage) (Takada et al., 2005).	
hes7.1	Demarcates the presumptive MHB: restricted band of the inner layer in the center of the prospective neuroectoderm (onset: NF10.5) that is progressively resolved into a pair of bilateral stripes (Shinga et al., 2001). Establishes the presumptive MHB region as a prepattern gene, where it represses the putative direct target genes *hes5.1, hes5.2, hes5.7, dll1*, and *hes7.1*.	*hes7.1* overexpression: ↓MHB markers (*pax2, en2*) at neural plate stage, but ↑*en2* in some cases with lower doses, while they were unaffected at later stages (Shinga et al., 2001). ↓*hes5.1, hes5.2, hes5.7, dll1, neurog2* (neural plate stage) (Takada et al., 2005).	*hes7.1-VP16, mb-hes7.1* (basic region mutated), *hes7.1-ΔWRPW* ↓MHB markers (neural plate stage); morphologically disrupted the MHB (tailbuds) (Shinga et al., 2001). *GR-hes7.1-VP16* (Dex NF10.5–11) +/– CHX: ↑*hes5.1, hes5.2, hes5.7, dll1*, and *hes7.1* domains (neural plate stage) (Takada et al., 2005). *hes7.1* MO: filled the MHB gap with *dll1, hes5.1*, and *hes5.7* (medial stripes of PN) and anteriorly expanded their intermediate stripes (PN domains) (Takada et al., 2005).

negative feedback loop. Cell oscillations slow down towards the anterior presomitic mesoderm, generating a kinematic wave of cycling gene expression. Opposite gradients of RA from the anterior presomitic mesoderm and FGF and Wnt signaling from the tailbud region define a so-called "determination wavefront," which sweeps through the presomitic mesoderm rostro-caudally. When cycling cells at the permissive phase are reached by the determination wavefront, they stop oscillating. This results in the striped activation of *mesp* genes. Consequently, the anterior presomitic mesoderm forms whorls of "somitomeres" whose gene expression prepattern delineates the future boundaries that lead to the formation of individual somites (Figure 7.1D). During vertebrate somitogenesis, intercellular Dll/Notch signaling acts first in the posterior presomitic mesoderm to synchronize the frequencies of neighboring cell-oscillators and then in the anterior presomitic mesoderm to position the future intersomitic boundary and define the anterior-posterior polarity of the somite (Cooke, 1981; Takahashi et al., 2000; Pourquié and Tam, 2001; Moreno and Kintner, 2004; Nagano et al., 2006; Sparrow, 2008; Gomez et al., 2008; Sasaki et al., 2011; Oates et al., 2012; Hubaud and Pourquié, 2014; Wahi et al., 2016; Janesick et al., 2017; Venzin and Oates, 2020; Naoki and Matsui, 2020).

7.3.6.1. Notch Ligands and Hes Genes in Somitogenesis

While the general segmentation mechanism is conserved across vertebrates, the individual *hes* and *delta* oscillating genes involved vary between species (Oates et al., 2012). In *Xenopus*, several Notch pathway genes are expressed in discrete stripes in the presomitic mesoderm. So far, only *dlc, hes5.3, hes5.5*, and *hes5.6* were reported as oscillatory in *Xenopus* (Table 7.12, Figure 7.1D). Since a large number of embryos must be analyzed to discern a changing pattern that results from oscillatory expression (Figure 7.1D, lower panel), some genes with cycling behavior might have been overlooked (Sparrow, 2008). Interestingly, *dlc* delineates somitomeres at late gastrula (Peres et al., 2006), significantly earlier than genes involved in somite segregation (Durston et al., 2018). Notably, *hes4*, *hes5.3*, *hes5.6*, and *dlc* show a left-right asynchrony in their somitomeric pattern (Davis et al., 2001; Li et al., 2003; Blewitt, 2009; Durston et al., 2018) (Figure 7.1D, lower panel). A careful examination led to the proposal that somitogenesis waves are propagated as counter-clockwise spirals, probably linked to the mechanisms imposing left-right asymmetries (Durston et al., 2018).

The consequences of the experimental perturbation of Dlc/Notch/RBPJ signaling in *Xenopus* are consistent with a crucial role in regulating somitogenesis (Jen et al., 1997; Sparrow et al., 1998; Peres et al., 2006) (Table 7.12). Although *dll1* is expressed in the tailbud in a poorly described segmental prepattern (Table 7.12), its possible role in somitogenesis has been overlooked. *notch1* shows continuous expression throughout the tailbud presomitic mesoderm but is restricted to one-half of mature somites, whereas *jag2* is expressed in the opposite pattern (Table 7.12), suggesting an interplay between *notch1* and *jag2* after somite segregation.

Among *hes* genes for which there is a precise description of their somitomeric expression pattern, *hes4* is restricted to posterior compartments, and others, including *dlc*, are restricted to anterior compartments (Figure 7.1D) (Jen et al., 1997). A paired RBPJ motif in the proximal promoter of *hes4*, including the intervening hexamer, is necessary for its somitomeric pattern together with its 3'UTR, which confers mRNA instability except in its striped domains in the presomitic mesoderm. Since the 3'UTR of *hes5.6* can impose this striped pattern on *hes4*, cyclic *hes5.6* expression might also be regulated by mRNA decay (Davis et al., 2001). The results summarized in Table 7.12 indicate that spatially controlled *dlc* expression is necessary for *Xenopus* somitogenesis and for setting the normal segmental prepattern of Notch targets related to the segmentation program (*hes7.2, hes7.3/esr5*, *hes4*). Notch/RBPJ represses *dlc* and *mespa*, whereas Dlc from the anterior half of somitomeres activates *hes4* in the posterior half through Notch/RBPJ.

hes7.3/esr5 is necessary for proper somitogenesis, including the refinement of *dlc, hes7.2*, and *mespa* expression into stripes in the so-called "transition zone" between the somitomeric and tailbud regions (Table 7.12) (Figure 7.1D) (Jen et al., 1999). It was proposed that the Notch pathway uniformly activates targets like *hes7.3/esr5* in the tailbud region. Then, a mechanism requiring *de novo* protein synthesis and HDAC represses *dlc*, *hes7.2*, and *hes7.3/esr5* in the transition zone, which introduces an expression gap that generates an on/off periodicity that is stably maintained in the somitomeres. *hes7.3/esr5* participates in a negative feedback loop, repressing *dlc* and *hes7.2* in posterior half-segments in the transition zone from where somitomeres arise. In contrast, rostral to the transition zone, *hes7.3/esr5* participates in a positive feedback loop, maintaining the segmental *dlc* prepattern in the somitomeric region (Jen et al., 1999).

hes6.1 shows a broad tailbud expression domain and a segmental prepattern in somitomeres (Table 7.12). Overexpression of *hes6.1* or a mutant DNA binding form severely disrupted somitogenesis and molecular markers (Cossins et al., 2002), suggesting that *hes6.1* must be spatially regulated in the presomitic mesoderm for proper segmentation, perhaps by protein-protein interactions rather than DNA binding. Interestingly, *hes6.1* is negatively regulated by Notch/RBPJ in the neural plate (Koyano-Nakagawa et al., 2000), so it will be interesting to study a possible interplay between *hes6.1* and the Notch pathway in somitogenesis.

7.3.6.2. Interplay between Notch and Other Genes and Pathways in Somitogenesis

Somite boundary formation is also regulated by the Notch pathway via repression of *protocadherin 8* (*pcdh8*) in the posterior half of somitomeres. Pcdh8, which is expressed in their anterior half, in turn regulates differential cell adhesion and prevents the intermingling of anterior and posterior cells between somitomeres, contributing to maintaining

TABLE 7.12
Notch Pathway Genes Expressed during *Xenopus* Somitogenesis

See abbreviations in Table 7.3 legend.

Gene	Expression Related to Somitogenesis and Mature Somites	Functional Evidence Related to Somitogenesis
notch1	Continuous in PSM and TBD. One-half of mature somites (Chitnis et al., 1995; McLaughlin et al., 2000; Rones et al., 2002; Xenbase, community submitted images: www.xenbase.org/, RRID:SCR_003280; Bowes et al., 2010).	**Gain-of-function:** *NICD1:* expanded *hes7.2* and *hes7.3/esr5* domains into the gaps between stripes in the somitomeric region (Jen et al., 1999; Peres et al., 2006); expanded *rnd1*, ↓*rnd3* (Goda et al., 2009). *notch1-ΔE:* ↓*ripply2.2* in the PSM (Kondow et al., 2006). GR-*NICD1;* Dex NF11 or 19: ↑*hey1* in somites, global disorganization of somite borders (Rones et al., 2002).
RBPJ		**Gain-of-function:** *RBPJ-Ank:* ↓*dlc* along the PSM (Sparrow et al., 1998); expanded the *hes7.2* and *hes7.3/esr5* domains into the gaps between stripes in the somitomeric region (Jen et al., 1999; Peres et al., 2006). GR-*RBPJ*-VP16 (Dex NF11–13, Dex NF15–19, ISH NF24–30): ↑*hey1* in somites, global disorganization of somite borders (Rones et al., 2002). **Loss-of-function:** *RBPJDBM*: expanded *dlc* domains into the gaps between somitomeric stripes without affecting *dlc* in the TBD (Jen et al., 1997; Sparrow et al., 1998); ↓*hes4* in somitomeres (Jen et al., 1997); ↓*hes7.2* along the PSM (Jen et al., 1999; Peres et al., 2006); ↓*hes7.3/esr5* in the somitomeric and TZ regions (Jen et al., 1999; Peres et al., 2006); produced a fusion of both *ripply2.2* somitomeric stripes (Kondow et al., 2006); ↓*ripply2.1* in the PSM (Chan et al., 2006); disrupted *rnd3* expression (Goda et al., 2009). GR-*RBPJDBM* (Dex NF11–13, Dex NF15–19, ISH NF24–30): ↓*hey1* in somites (Rones et al., 2002). ***RBPJ* regulation:** Celf1 controls somitogenesis through *RBPJ* mRNA decay (see main text for details) (Gautier-Courteille et al., 2004; Cibois et al., 2010; Cibois et al., 2013).
dll1	More restricted than *dlc*. Circumblastoporal collar/TBD. Two somitomeric stripes (from NF12): stronger in the posterior than in the anterior one (Chitnis et al., 1995; McLaughlin et al., 2000; Rones et al., 2002; Lamar and Kintner, 2005; Dingwell and Smith, 2006; Kondow et al., 2007; Wang et al., 2007).	***dll1* regulation:** *ripply2.1* overexpression: slight posterior shift of *dll1* in the PSM (Chan et al., 2006). *ripply2.1* MO: anterior shift of *dll1* in the PSM (Chan et al., 2006). *ripply2.2* MO: ↓*dll1* stripes in the PSM (Kondow et al., 2007).

dlc	Anterior part of prospective somites SO, S-I, S-II (somitomeres), and S-III (TZ), with spatial refinement: stripes progressively thinner from caudal to rostral PSM. Expression in somitomeres first appears at late gastrula (NF12). Broad domain in TBD. Oscillatory behavior in TZ and TBD. Left-right asynchrony in somitomeres, with the right side relatively more advanced (Jen et al., 1997; Sparrow et al., 1998; Jen et al., 1999; Moreno and Kintner, 2004; Peres et al., 2006; Sparrow, 2008; Durston et al., 2018).	**Gain-of-function:** *dlc* overexpression: segmentation defects (Jen et al., 1997; Peres et al., 2006); expanded *hes7.2* and *hes7.3/esr5* expression into the gaps between stripes in the somitomeric region (ISH NF20–22, late neurula/early tailbud stages) (Jen et al., 1999; Peres et al., 2006); did not affect *hoxc6* and *hoxd1* in the paraxial mesoderm (ISH, tailbud stage) (Peres et al., 2006) **Loss-of-function:** DN-*dlc*: segmentation defects (Jen et al., 1997); expanded the *dlc* domains into the gaps between somitomeric stripes, without affecting *dlc* in the TBD (Jen et al., 1997; Sparrow et al., 1998); ↓*hes4* in somitomeres (Jen et al., 1997); disrupted and ↓*rnd1* and *rnd3* expression domains (Goda et al., 2009). *dlc* MO: segmentation defects (Peres et al., 2006); ↓*hes7.2* in somitomeres (Jen et al., 1999; Peres et al., 2006) and *hoxb4* and *hoxc6* in the paraxial mesoderm during somitogenesis (ISH tailbud stage, NF21) (Peres et al., 2006). ***dlc* regulation:** *RBPJ-Ank:* ↓*dlc* along the PSM (Sparrow et al., 1998). *RBPJDBM*: expanded the *dlc* domains into the gaps between somitomeric stripes, without affecting *dlc* in the TBD (Jen et al., 1997; Sparrow et al., 1998). Knock-down of the whole *hox* paralogous group 1: disrupted somitogenesis and ↓*dlc* in the PSM (Peres et al., 2006). *mespa* overexpression: segmental pattern of *dlc* lost, ↓*dlc* in somitomeres; expression in TBD unaffected (Sparrow et al., 1998). *ripply2.1* overexpression: slight posterior shift of *dlc* in the PSM (Chan et al., 2006). *ripply2.1* MO: anterior shift of *dlc* in the PSM (Chan et al., 2006). *ripply2.2* overexpression: ↓*dlc* in the PSM through recruitment of the TLE4 co-repressor (Kondow et al., 2006). *ripply2.2* MO: ↑*dlc* expression in S0 and S-I and anteriorly shifted these domains (Kondow et al., 2007). *myod1* MO: ↓*dlc* in PSM stripes at early neurula (NF13); anteriorly shifted *dlc* stripes around the onset of somitogenesis (NF19) (Maguire et al., 2012). CHX treatment: continuous *dlc* expression in the PSM (Jen et al., 1999; Kim et al., 2000). RA or SU5402 (inhibitor of FGF signaling) treatments: caudal shift of the *dlc* TBD domain (Moreno and Kintner, 2004).
dll4	Intersomitic vessels (sprouting from the dorsal aorta) (NF39). Image from Kirmizitas et al. (2017), description from Xenbase (Bowes et al., 2010).	
jag2	One-half of mature somites. Xenbase, community submitted images (Bowes et al., 2010).	
hes1	Similar to *hes4* pattern, but with much lower expression (Davis et al., 2001).	***hes1* regulation:** GR-*NICD1*, GR-*RBPJ*-VP16 (Dex NF11–13, Dex NF15–19, ISH NF24–30): ↑*hey1* in somites, global disorganization of somite borders (Rones et al., 2002). GR-*RBPJDBM* (Dex NF11–13, Dex NF15–19, ISH NF24–30): ↓*hey1* in somites (Rones et al., 2002).

(*Continued*)

TABLE 7.12 (Continued)
Notch Pathway Genes Expressed during *Xenopus* Somitogenesis

Gene	Expression Related to Somitogenesis and Mature Somites	Functional Evidence Related to Somitogenesis
hes4	Posterior part of S-I and S-II (somitomeres), complementary to *dlc*. Left-right asynchrony in somitomeres observed from NF18–19, with the right side relatively more advanced. Very low expression in mature somites (Jen et al., 1997; Davis et al., 2001).	***hes4* regulation:** Segmental *hes4* prepattern requires a paired RBPJ motif (including the intervening hexamer) present in the proximal promoter of *hes4* and the 3' UTR, which confers general mRNA instability (Davis et al., 2001). *RBPJDBM* or DN-*dlc:* ↓*hes4* in somitomeres (Jen et al., 1997). *dlc* MO: ↓*hes4* (Peres et al., 2006). *ripply2.1* overexpression: slight posterior shift of *hes4* in the PSM. *ripply2.1* MO: anterior shift of *hes4* in the PSM (Chan et al., 2006). *ripply2.2* MO ↓*hes4* in the PSM (Kondow et al., 2007). CHX treatment: ↓*hes4* in the PSM (Kim et al., 2000).
hes5.3	1–2 somitomeric stripes. Broad domain in TZ+TBD. Oscillatory behavior in the PSM, with left-right asynchrony (Blewitt, 2009).	Microarray analysis showed that manipulating RA signaling significantly changed *hes5.3* levels (Janesick et al., 2017).
hes5.5	Anterior part of prospective somite S-II. Broad domain in TZ+TBD. Oscillatory behavior in TZ and TBD. (Li et al., 2003).	
hes5.6	Anterior part of prospective somite S-II. Broad domain in TZ+TBD. Oscillatory behavior in TZ and TBD. Left-right asynchrony in somitomeres, with the right side relatively more advanced (Li et al., 2003).	***hes5.6* regulation:** *hes5.6* 3' UTR can replace *hes4* 3´UTR to generate a striped pattern (Davis et al., 2001). CHX treatments (Li et al., 2003): 30 or 60 min (comprising the approximate time of formation of 1 somite): ↑*hes5.6*. *De novo* protein synthesis is not required for cyclic expression. CHX 120 min: *de novo* protein synthesis required for *hes5.6* repression to generate the typical striped pattern RA or SU5402 (inhibitor of FGF signaling) treatment: caudal shift of the *hes5.6* TBD domain (Moreno and Kintner, 2004).
hes6.1	Broad domain in TBD. 2–3 stripes in prospective somites (Koyano-Nakagawa et al., 2000; Cossins et al., 2002; Moreno and Kintner, 2004).	**Gain-of-function:** *hes6.1* overexpression: expanded the myotome (*myod1*+ cells) at neural plate stage, inhibited terminal myogenic differentiation (Ab 12/101), and severely disrupted somitogenesis (Cossins et al., 2002). **Loss-of-function:** *hes6.1DBM*: same effects as *hes6.1* overexpression, indicating that DNA binding is not required for these activities (Cossins et al., 2002). ***hes6.1* regulation:** RA or SU5402 (inhibitor of FGF signaling) treatment: caudal shift of the *hes6.1* TBD domain (Moreno and Kintner, 2004).

hes7.2	Anterior part of prospective somites S-II (somitomere) and S-III (TZ). Broad domain in TBD (Jen et al., 1999).	***hes7.2* regulation:** *dlc* overexpression, *RBPJ-Ank*, or *NICD1:* expanded the *hes7.2* domains into the gaps between stripes in the somitomeric region (Jen et al., 1999; Peres et al., 2006). *RBPJDBM:* ↓*hes7.2* throughout the PSM (Jen et al., 1999; Peres et al., 2006). CHX treatment: continuous *hes7.2* expression in the PSM (Jen et al., 1999).
hes7.3/esr5	Anterior part of prospective somites S-II (somitomere) and S-III (TZ). Broad domain in TBD. Segmented prepattern already detected at late gastrula (NF12) (Sparrow et al., 1998; Jen et al., 1999)	**Gain-of-function:** *hes7.3/esr5* overexpression: ↓*dlc* and *hes7.2* in the somitomeric region but activated *dlc* more anteriorly, with a net result of a rostral shift of the *dlc* domain (Jen et al., 1999). **Loss-of-function:** DN-*hes7.3/esr5:* impaired segmentation and expanded *dlc, hes7.2*, and *mespa* expression into the gaps between stripes in the TZ (Jen et al., 1999). ***hes7.3/esr5* regulation:** *dlc* overexpression, *RBPJ-Ank* or *NICD1:* expanded *hes7.3/esr5* domains into the gaps between stripes in the somitomeric region (Jen et al., 1999; Peres et al., 2006). *RBPJDBM:* ↓*hes7.3/esr5* in the somitomeric and TZ regions (Jen et al., 1999; Peres et al., 2006). CHX treatment: continuous *hes7.2* expression in the PSM (Jen et al., 1999). *mespa* overexpression: segmental *hes7.3/esr5* pattern lost. *hes7.3/esr5* in TBD unaffected (Sparrow et al., 1998). RA or SU5402 (inhibitor of FGF signaling) treatment: caudal shift of the *hes7.3/esr5* TBD domain (Moreno and Kintner, 2004). DN-RARα: rostral shift of the *hes7.3/esr5* TBD domain (Moreno and Kintner, 2004). RARβ2 MO: ↓somite number, ↑somite size, and rostrally expanded PSM markers, including *hes7.3/esr5* (Janesick et al., 2017). *ripply2.1* overexpression: slight posterior shift of *hes7.3/esr5* expression in the PSM (Chan et al., 2006). *ripply2.1* MO: anterior shift of *hes7.3/esr5* expression in the PSM (Chan et al., 2006).
hey1	Mature somites (apparently in the caudal half), from NF17 (Rones et al., 2002; Pichon et al., 2002).	

a segmental boundary (Kim et al., 2000). *ripply2.2*, which encodes a WRPW-containing protein, is also required for the formation of somite boundaries. While *ripply2.2* is required for *dll1* and *hes4* expression in their proper position in the presomitic mesoderm (Kondow et al., 2007) (Table 7.12), Notch/RBPJ signaling localizes *ripply2.2* in the anterior halves of somitomeres (Kondow et al., 2006) (Figure 7.1D), which in turn further restricts *dlc* to the anterior border of the most anterior somitomeres by recruiting the TLE4 co-repressor (Kondow et al., 2006). It was proposed that Tbx6 acts as a transcriptional activator of segmental target genes in posterior somitomeres but changes to a transcriptional repressor through binding to a Ripply2.2/TLE4 complex when Ripply2.2 accumulates above a threshold level in the most anterior somitomeres. In this way, Ripply2.2 and Tbx6 contribute to terminate the segmentation program in the anterior presomitic mesoderm (Kondow et al., 2007; Hitachi et al., 2008). Interestingly, the related *ripply2.1*, whose striped expression in the anterior presomitic mesoderm is also dependent on Notch/RBPJ signaling (Figure 7.1D) (Table 7.12), is not required for segmentation but for positioning the segmentation front via RA signaling (Chan et al., 2006). The Dlc/Notch/RBPJ pathway is also necessary for striped *rnd1* and *rnd3* expression in somitomeres (Figure 7.1D) (Table 7.12). They encode GTP binding proteins required for segmentation independently of *hes7.3/esr5*. *rnd1* is expressed in the anterior half of somitomeres, whereas *rnd3* is expressed in the boundary between the anterior and posterior halves, suggesting different roles in segmentation (Goda et al., 2009).

hox genes are necessary for somitogenesis and establish a reciprocal positive regulation with *dlc* in the paraxial mesoderm (Tables 7.15, 7.12). *dlc* might regulate the timer for temporal collinearity of *hox* gene expression, which in turn controls somite anterior-posterior identity (Peres et al., 2006; Durston et al., 2012).

The Notch pathway also is regulated during somitogenesis at other levels. For example, *celf1*, which encodes an RNA-binding protein that mediates sequence-specific mRNA deadenylation, binds the 3'UTR of *RBPJ* mRNA promoting its degradation; this is required to control the interplay between FGF and RA signaling that governs the determination front (Gautier-Courteille et al., 2004; Cibois et al., 2010; Cibois et al., 2013). RA treatments or FGF pathway blockade repressed *dlc, hes5.6, hes6.1*, and *hes7.3/esr5* in the tailbud, shifting their expression domain caudally (Moreno and Kintner, 2004). RARβ2 knock-down reduced somite number, increased somite size, and rostrally expanded presomitic mesoderm markers, including *hes7.3/esr5*. Microarray analysis showed that manipulating RA signaling significantly changed *hes5.3* levels (Janesick et al., 2017) (Table 7.12).

7.4. FUTURE DIRECTIONS

Work in *Xenopus* frequently has led the field in addressing the role of *notch1* and *dll1* in several developmental programs, as well as *dlc* in somitogenesis, but there is much less information about other Notch receptors and ligands during frog development. Expression patterns for some are available in limited types of tissues. For example, *notch2* is expressed in the PPE and during lens development, where it is positively controlled by *hes4* (Ogino et al., 2008; Murato and Hashimoto, 2009); *notch1*, *notch2*, *jag1*, and *jag2* are expressed in the liver during metamorphosis (Ueno et al., 2015), whereas *notch4* and *dll4* are implicated in the arterial endothelial program (Ciau-Uitz et al., 2010; Leung et al., 2013; Nimmo et al., 2013; Kirmizitas et al., 2017). RNAseq data (Session et al., 2016) (Figure 7.1C, right column) suggest that *notch3*, *jag1*, *jag2*, and *dll4* might have roles during embryogenesis, but we need to know their spatial distributions at different developmental timepoints. Finally, since the *notch4* gene model was not available at the time of the RNAseq study, a developmental expression profile is not yet available.

To dissect Notch signaling involvement in developmental processes more precisely, a combination of strategies will be necessary. For example, experiments employing *RBPJDBM*, *psen* MO, or γ-Secretase inhibitors impair the function of every *notch* paralogue; knock-down/knock-out strategies are needed to provide results specific for each paralogue. Strikingly, only *notch1* has been knocked down so far, both in studies by our group concerning germ layers, DML, and DV axis, and by others concerning ciliogenesis in the epidermis, GRP and left-right patterning (Sakano et al., 2010; Tözser et al., 2015; Tomankova et al., 2017). Since there is growing evidence of *RBPJ*-independent Ligand/Notch functions in several biological contexts (Hayward et al., 2005), including various aspects of *Xenopus* development (Revinski et al., 2010; Peres et al., 2006; Acosta et al., 2011), knock-down/knock-out approaches next need to address both canonical and non-canonical functions. As RBPJ has dual properties, activating or repressing Notch-targets depending on the ON/OFF status of Notch signaling, it might not always be straightforward to interpret the results of RBPJ blockade in complex contexts, including those in which multiple inputs from different ligands might take place. For example, in some studies, *RBPJDBM* produced milder or more variable effects in comparison to the blockade of one ligand or the receptor (Revinski et al., 2010) or did not affect the process under study (Takada et al., 2005; Peres et al., 2006; Nichane et al., 2008a). The effects of protecting *RBPJ* mRNA from Celf1-mediated degradation were compatible with a Notch/RBPJ gain-of-function in the posterior presomitic mesoderm and with a Notch/RBPJ loss-of-function in the anterior presomitic mesoderm (Cibois et al., 2013). In addition, the response to perturbing Notch signaling can change abruptly at certain developmental transitions (Contakos et al., 2005; Revinski et al., 2010), thus requiring a more detailed analysis of gene markers and phenotypes by time-controlled manipulations.

Work from different animal models and cell types show that the number of direct Notch/RBPJ targets outside the *hes/hey* families is constantly growing, including genes

involved in proliferation, apoptosis, cell-fate choice, signaling pathways, metabolism, and cytoskeletal regulators (Bray and Bernard, 2010; Meier-Stiegen et al., 2010). The discovery of new targets and modulators in *Xenopus* will be essential to building Notch-regulated GRNs that control different developmental processes. microRNAs regulate Notch signaling during multiciliogenesis in the epidermis (Marcet et al., 2011), and RITA (RBPJ-interacting and tubulin-associated protein) negatively modulates Notch signaling through nuclear export of RBPJ during primary neurogenesis (Wacker et al., 2011). It will be exciting to extend the study of such modulations to the different contexts in which Notch signaling operates.

REFERENCES

Acosta, H., López, S.L., Revinski, D.R., Carrasco, A.E., 2011. Notch destabilises maternal beta-catenin and restricts dorsal-anterior development in Xenopus. *Development* 138, 2567–2579. https://doi.org/10.1242/dev.061143

Aguirre, C.E., Murgan, S., Carrasco, A.E., López, S.L., 2013. An intact brachyury function is necessary to prevent spurious axial development in *Xenopus laevis*. *PLoS One* 8, e54777. https://doi.org/10.1371/journal.pone.0054777

Ali, F.R., Cheng, K., Kirwan, P., Metcalfe, S., Livesey, F.J., Barker, R.A., Philpott, A., 2014. The phosphorylation status of Ascl1 is a key determinant of neuronal differentiation and maturation in vivo and in vitro. *Development* 141, 2216–2224. https://doi.org/10.1242/dev.106377

Anderson, C., Stern, C.D., 2016. Organizers in development. *Curr. Top. Dev. Biol*. 117, 435–454. https://doi.org/10.1016/BS.CTDB.2015.11.023

Andreazzoli, M., Gestri, G., Cremisi, F., Casarosa, S., Dawid, I.B., Barsacchi, G., 2003. Xrx1 controls proliferation and neurogenesis in Xenopus anterior neural plate. *Development* 130, 5143–5154. https://doi.org/10.1242/dev.00665

Artavanis-Tsakonas, S., Grimwade, B.G., Harrison, R.G., Markopoulou, K., Muskavitch, M.A.T., Schlesinger-Bryant, R., Wharton, K., Yedvobnick, B., 1983. The Notch locus of *Drosophila melanogaster*: A molecular analysis. *Dev. Genet*. 4, 233–254. https://doi.org/10.1002/dvg.1020040403

Artinger, M., Blitz, I., Inoue, K., Tran, U., Cho, K.W., 1997. Interaction of goosecoid and brachyury in Xenopus mesoderm patterning. *Mech. Dev*. 65, 187–196.

Beck, C., Slack, J.M., 1998. Analysis of the developing Xenopus tail bud reveals separate phases of gene expression during determination and outgrowth. *Mech. Dev*. 72, 41–52. https://doi.org/10.1016/S0925-4773(98)00015-X

Bellefroid, E.J., Bourguignon, C., Hollemann, T., Ma, Q., Anderson, D.J., Kintner, C., Pieler, T., 1996. X-MyT1, a Xenopus C2HC-type zinc finger protein with a regulatory function in neuronal differentiation. *Cell* 87, 1191–1202.

Bertrand, N., Castro, D.S., Guillemot, F., 2002. Proneural genes and the specification of neural cell types. *Nat. Rev. Neurosci*. 3, 517–530. https://doi.org/10.1038/nrn874

Blewitt, R., 2009. Enhancer of split-related-2 mRNA shows cyclic expression during somitogenesis in *Xenopus laevis*. *Biosci. Horizons* 2, 22–31. https://doi.org/10.1093/biohorizons/hzp006

Bonev, B., Pisco, A., Papalopulu, N., 2011. microRNA-9 reveals regional diversity of neural progenitors along the anterior-posterior axis. *Dev. Cell* 20, 19–32. https://doi.org/10.1016/j.devcel.2010.11.018

Bouwmeester, T., Kim, S., Sasai, Y., Lu, B., De Robertis, E.M., 1996. Cerberus is a head-inducing secreted factor expressed in the anterior endoderm of Spemann's organizer. *Nature* 382, 595–601. https://doi.org/10.1038/382595a0

Bowes, J.B., Snyder, K.A., Segerdell, E., Jarabek, C.J., Azam, K., Zorn, A.M., Vize, P.D., 2010. Xenbase: Gene expression and improved integration. *Nucleic Acids Res* 38, D607–D612. https://doi.org/10.1093/nar/gkp953

Bray, S.J., 2016. Notch signalling in context. *Nat. Rev. Mol. Cell Biol*. 17, 722–735. https://doi.org/10.1038/nrm.2016.94

Bray, S.J., Bernard, F., 2010. Notch targets and their regulation. *Curr. Top. Dev. Biol*. 92, 253–275. https://doi.org/10.1016/S0070-2153(10)92008-5

Brewster, R., Lee, J., Ruiz i Altaba, A., 1998. Gli/Zic factors pattern the neural plate by defining domains of cell differentiation. *Nature* 393, 579–583. https://doi.org/10.1038/31242

Bridges, C.B., Morgan, T.H., 1916. *Sex-Linked Inheritance in Drosophila*. Carnegie Institution of Washington, Washington. https://doi.org/10.5962/bhl.title.22854

Brugmann, S.A., Pandur, P.D., Kenyon, K.L., Pignoni, F., Moody, S.A., 2004. Six1 promotes a placodal fate within the lateral neurogenic ectoderm by functioning as both a transcriptional activator and repressor. *Development* 131, 5871–5881. https://doi.org/10.1242/dev.01516

Campos-Ortega, J.A., 1985. Genetics of early neurogenesis in *Drosophila melanogaster*. *Trends Neurosci* 8, 245–250. https://doi.org/10.1016/0166-2236(85)90097-9

Castro Colabianchi, A.M., Revinski, D.R., Encinas, P.I., Baez, M.V., Monti, R.J., Rodríguez Abinal, M., Kodjabachian, L., Franchini, L.F., López, S.L., 2018. Notch1 is asymmetrically distributed from the beginning of embryogenesis and controls the ventral center. *Development* 145, dev159368. https://doi.org/10.1242/dev.159368

Chalmers, A.D., Welchman, D., Papalopulu, N., 2002. Intrinsic differences between the superficial and deep layers of the Xenopus ectoderm control primary neuronal differentiation. *Dev. Cell* 2, 171–182.

Chan, T., Satow, R., Kitagawa, H., Kato, S., Asashima, M., 2006. Ledgerline, a novel *Xenopus laevis* gene, regulates differentiation of presomitic mesoderm during somitogenesis. *Zoolog. Sci*. 23, 689–697. https://doi.org/10.2108/zsj.23.689

Chen, J.-A., Voigt, J., Gilchrist, M., Papalopulu, N., Amaya, E., 2005. Identification of novel genes affecting mesoderm formation and morphogenesis through an enhanced large scale functional screen in Xenopus. *Mech. Dev*. 122, 307–331. https://doi.org/10.1016/J.MOD.2004.11.008

Chitnis, A., Henrique, D., Lewis, J., Ish-Horowicz, D., Kintner, C., 1995. Primary neurogenesis in Xenopus embryos regulated by a homologue of the Drosophila neurogenic gene Delta. *Nature* 375, 761–766. https://doi.org/10.1038/375761a0

Chitnis, A., Kintner, C., 1996. Sensitivity of proneural genes to lateral inhibition affects the pattern of primary neurons in Xenopus embryos. *Development* 122, 2295–2301.

Ciau-Uitz, A., Pinheiro, P., Gupta, R., Enver, T., Patient, R., 2010. Tel1/ETV6 specifies blood stem cells through the agency of VEGF signaling. *Dev. Cell* 18, 569–578. https://doi.org/10.1016/j.devcel.2010.02.009

Cibois, M., Gautier-Courteille, C., Kodjabachian, L., Paillard, L., 2013. A gene regulation network controlled by Celf1 protein-rbpj mRNA interaction in Xenopus somite segmentation. *Biol. Open* 2, 1078–1083. https://doi.org/10.1242/bio.20135629

Cibois, M., Gautier-Courteille, C., Vallée, A., Paillard, L., 2010. A strategy to analyze the phenotypic consequences of inhibiting the association of an RNA-binding protein with

a specific RNA. *RNA* 16, 10–15. https://doi.org/10.1261/rna.1742610

Coffman, C.R., Harris, W., Kintner, C., 1990. Xotch, the Xenopus homolog of Drosophila notch. *Science* 249, 1438–1441.

Coffman, C.R., Skoglund, P., Harris, W.A., Kintner, C.R., 1993. Expression of an extracellular deletion of Xotch diverts cell fate in Xenopus embryos. *Cell* 73, 659–671.

Contakos, S.P., Gaydos, C.M., Pfeil, E.A., McLaughlin, K.A., 2005. Subdividing the embryo: A role for Notch signaling during germ layer patterning in *Xenopus laevis*. *Dev. Biol*. 288, 294–307. https://doi.org/10.1016/j.ydbio.2005.09.015

Cooke, J., 1981. The problem of periodic patterns in embryos. *Philos. Trans. R. Soc. Lond. B. Biol. Sci*. 295, 509–524. https://doi.org/10.1098/rstb.1981.0157

Cooke, J., Zeeman, E.C., 1976. A clock and wavefront model for control of the number of repeated structures during animal morphogenesis. *J. Theor. Biol*. 58, 455–476. https://doi.org/10.1016/S0022-5193(76)80131-2

Cossins, J., Vernon, A.E., Zhang, Y., Philpott, A., Jones, P.H., 2002. Hes6 regulates myogenic differentiation. *Development* 129, 2195–207.

Cui, Y., 2005. Hairy is a cell context signal controlling Notch activity. *Dev. Growth Differ*. 47, 609–625. https://doi.org/10.1111/j.1440-169X.2005.00823.x

Dale, L., Slack, J.M., 1987. Fate map for the 32-cell stage of *Xenopus laevis*. *Development* 99, 527–551.

Davis, R.L., Turner, D.L., 2001. Vertebrate hairy and enhancer of split related proteins: Transcriptional repressors regulating cellular differentiation and embryonic patterning. *Oncogene* 20, 8342–8357. https://doi.org/10.1038/sj.onc.1205094

Davis, R.L., Turner, D.L., Evans, L.M., Kirschner, M.W., 2001. Molecular targets of vertebrate segmentation: Two mechanisms control segmental expression of Xenopus hairy2 during somite formation. *Dev. Cell* 1, 553–565.

Deblandre, G.A., Wettstein, D.A., Koyano-Nakagawa, N., Kintner, C., 1999. A two-step mechanism generates the spacing pattern of the ciliated cells in the skin of Xenopus embryos. *Development* 126, 4715–4728.

De Robertis, E.M., 2009. Spemann's organizer and the self-regulation of embryonic fields. *Mech. Dev*. 126, 925–941. https://doi.org/10.1016/j.mod.2009.08.004

Dexter, J.S., 1914. The analysis of a case of continuous variation in Drosophila by a study of its linkage relations. *Am. Nat*. 48, 712–758.

Dingwell, K.S., Smith, J.C., 2006. Tes regulates neural crest migration and axial elongation in Xenopus. *Dev. Biol*. 293, 252–267. https://doi.org/10.1016/j.ydbio.2006.02.004

D'Souza, B., Meloty-Kapella, L., Weinmaster, G., 2010. Canonical and non-canonical Notch ligands. *Curr. Top. Dev. Biol*. 92, 73–129. https://doi.org/10.1016/S0070-2153(10)92003-6

Dubois, L., Bally-Cuif, L., Crozatier, M., Moreau, J., Paquereau, L., Vincent, A., 1998. XCoe2, a transcription factor of the Col/Olf-1/EBF family involved in the specification of primary neurons in Xenopus. *Curr. Biol*. 8, 199–209. https://doi.org/10.1016/S0960-9822(98)70084-3

Durston, A.J., Peres, J., Cohen, M.H., 2018. Spiral waves and vertebrate embryonic handedness. *J. Biosci*. 43, 375–390.

Durston, A.J., Wacker, S., Bardine, N., Jansen, H.J., 2012. Time space translation: A hox mechanism for vertebrate A-P patterning. *Curr. Genomics* 13, 300–307. https://doi.org/10.2174/138920212800793375

Favarolo, M.B., López, S.L., 2018. Notch signaling in the division of germ layers in bilaterian embryos. *Mech. Dev*. 154, 122–144. https://doi.org/10.1016/j.mod.2018.06.005

Fortini, M.E., 2009. Notch signaling: The core pathway and its posttranslational regulation. *Dev. Cell* 16, 633–647. https://doi.org/10.1016/j.devcel.2009.03.010

Gautier-Courteille, C., Le Clainche, C., Barreau, C., Audic, Y., Graindorge, A., Maniey, D., Osborne, H.B., Paillard, L., 2004. EDEN-BP-dependent post-transcriptional regulation of gene expression in Xenopus somitic segmentation. *Development* 131, 6107–6117. https://doi.org/10.1242/dev.01528

Gawantka, V., Pollet, N., Delius, H., Vingron, M., Pfister, R., Nitsch, R., Blumenstock, C., Niehrs, C., 1998. Gene expression screening in Xenopus identifies molecular pathways, predicts gene function and provides a global view of embryonic patterning. *Mech. Dev*. 77, 95–141. https://doi.org/10.1016/S0925-4773(98)00115-4

Gazave, E., Lapébie, P., Richards, G.S., Brunet, F., Ereskovsky, A. V., Degnan, B.M., Borchiellini, C., Vervoort, M., Renard, E., 2009. Origin and evolution of the Notch signalling pathway: An overview from eukaryotic genomes. *BMC Evol. Biol*. 9, 249. https://doi.org/10.1186/1471-2148-9-249

Glavic, A., Silva, F., Aybar, M.J., Bastidas, F., Mayor, R., 2004. Interplay between Notch signaling and the homeoprotein Xiro1 is required for neural crest induction in Xenopus embryos. *Development* 131, 347–359. https://doi.org/10.1242/dev.00945

Goda, T., Takagi, C., Ueno, N., 2009. Xenopus Rnd1 and Rnd3 GTP-binding proteins are expressed under the control of segmentation clock and required for somite formation. *Dev. Dyn*. 238, 2867–2876. https://doi.org/10.1002/dvdy.22099

Gomez, C., Özbudak, E.M., Wunderlich, J., Baumann, D., Lewis, J., Pourquié, O., 2008. Control of segment number in vertebrate embryos. *Nature* 454, 335–339. https://doi.org/10.1038/nature07020

Grocott, T., Tambalo, M., Streit, A., 2012. The peripheral sensory nervous system in the vertebrate head: A gene regulatory perspective. *Dev. Biol*. 370, 3–23. https://doi.org/10.1016/j.ydbio.2012.06.028

Groot, A.J., Vooijs, M.A., 2012. The role of Adams in notch signaling. *Adv. Exp. Med. Biol*. 727, 15–36. https://doi.org/10.1007/978-1-4614-0899-4_2

Hardwick, L.J.A., Philpott, A., 2015. Multi-site phosphorylation regulates NeuroD4 activity during primary neurogenesis: A conserved mechanism amongst proneural proteins. *Neural Dev*. 10, 15. https://doi.org/10.1186/s13064-015-0044-8

Hardwick, L.J.A., Philpott, A., 2019. N-terminal phosphorylation of xHes1 controls inhibition of primary neurogenesis in Xenopus. *Biochem. Biophys. Res. Commun*. 509, 557–563. https://doi.org/10.1016/J.BBRC.2018.12.135

Hayata, T., Blitz, I.L., Iwata, N., Cho, K.W.Y., 2009. Identification of embryonic pancreatic genes using Xenopus DNA microarrays. *Dev. Dyn*. 238, 1455–1466. https://doi.org/10.1002/dvdy.21868

Hayward, P., Brennan, K., Sanders, P., Balayo, T., DasGupta, R., Perrimon, N., Martinez Arias, A., 2005. Notch modulates Wnt signalling by associating with Armadillo/beta-catenin and regulating its transcriptional activity. *Development* 132, 1819–1830. https://doi.org/10.1242/dev.01724

Hayward, P., Kalmar, T., Martinez Arias, A., 2008. Wnt/Notch signalling and information processing during development. *Development* 135, 411–424. https://doi.org/10.1242/dev.000505

Heeg-Truesdell, E., LaBonne, C., 2006. Neural induction in Xenopus requires inhibition of Wnt-beta-catenin signaling. *Dev. Biol*. 298, 71–86. https://doi.org/10.1016/j.ydbio.2006.06.015

Hein, K., Mittler, G., Cizelsky, W., Kühl, M., Ferrante, F., Liefke, R., Berger, I.M., Just, S., Sträng, J.E., Kestler, H.A., Oswald, F., Borggrefe, T., 2015. Site-specific methylation of Notch1 controls the amplitude and duration of the Notch1 response. *Sci. Signal*. 8, ra30. https://doi.org/10.1126/scisignal.2005892

Heitzler, P., 2010. Biodiversity and noncanonical Notch signaling. *Curr. Top. Dev. Biol*. 92, 457–481. https://doi.org/10.1016/S0070-2153(10)92014-0

Hindley, C., Ali, F., McDowell, G., Cheng, K., Jones, A., Guillemot, F., Philpott, A., 2012. Post-translational modification of Ngn2 differentially affects transcription of distinct targets to regulate the balance between progenitor maintenance and differentiation. *Development* 139, 1718–1723. https://doi.org/10.1242/dev.077552

Hitachi, K., Danno, H., Tazumi, S., Aihara, Y., Uchiyama, H., Okabayashi, K., Kondow, A., Asashima, M., 2009. The Xenopus Bowline/Ripply family proteins negatively regulate the transcriptional activity of T-box transcription factors. *Int. J. Dev. Biol*. 53, 631–639. https://doi.org/10.1387/ijdb.082823kh

Hitachi, K., Kondow, A., Danno, H., Inui, M., Uchiyama, H., Asashima, M., 2008. Tbx6, Thylacine1, and E47 synergistically activate bowline expression in Xenopus somitogenesis. *Dev. Biol*. 313, 816–828. https://doi.org/10.1016/J.YDBIO.2007.10.015

Hong, C.-S., Saint-Jeannet, J.-P., 2018. The b-HLH transcription factor Hes3 participates in neural plate border formation by interfering with Wnt/β-catenin signaling. *Dev. Biol*. 442, 162–172. https://doi.org/10.1016/j.ydbio.2018.07.011

Howell, M., Inman, G.J., Hill, C.S., 2002. A novel Xenopus Smad-interacting forkhead transcription factor (XFast-3) cooperates with XFast-1 in regulating gastrulation movements. *Development* 129, 2823–2834.

Huang, C., Chan, J.A., Schuurmans, C., 2014. Proneural bHLH genes in development and disease. *Curr. Top. Dev. Biol*. 110, 75–127. https://doi.org/10.1016/B978-0-12-405943-6.00002-6

Hubaud, A., Pourquié, O., 2014. Signalling dynamics in vertebrate segmentation. *Nat. Rev. Mol. Cell Biol*. 15, 709–721. https://doi.org/10.1038/nrm3891

Hufton, A.L., Vinayagam, A., Suhai, S., Baker, J.C., 2006. Genomic analysis of Xenopus organizer function. *BMC Dev. Biol*. 6, 27. https://doi.org/10.1186/1471-213X-6-27

Imayoshi, I., Kageyama, R., 2014. Oscillatory control of bHLH factors in neural progenitors. *Trends Neurosci* 37, 531–538. https://doi.org/10.1016/j.tins.2014.07.006

Ito, M., Katada, T., Miyatani, S., Kinoshita, T., 2007a. XSu(H)2 is an essential factor for gene expression and morphogenesis of the Xenopus gastrula embryo. *Int. J. Dev. Biol*. 51, 27–36. https://doi.org/10.1387/ijdb.062211mi

Ito, M., Nishitani, E., Kinoshita, T., 2007b. Xenopus suppressor of Hairless 2 is involved in the cell fate decision during gastrulation through the transcriptional regulation of Xoct25/91. *Biochem. Biophys. Res. Commun*. 353, 644–649. https://doi.org/10.1016/j.bbrc.2006.12.087

Janesick, A., Tang, W., Nguyen, T.T.L., Blumberg, B., 2017. RARβ2 is required for vertebrate somitogenesis. *Development* 144, 1997–2008. https://doi.org/10.1242/dev.144345

Jen, W.C., Gawantka, V., Pollet, N., Niehrs, C., Kintner, C., 1999. Periodic repression of Notch pathway genes governs the segmentation of Xenopus embryos. *Genes Dev*. 13, 1486–1499. https://doi.org/10.1101/gad.13.11.1486

Jen, W.C., Wettstein, D., Turner, D., Chitnis, A., Kintner, C., 1997. The Notch ligand, X-Delta-2, mediates segmentation of the paraxial mesoderm in Xenopus embryos. *Development* 124, 1169–1178.

Jorissen, E., De Strooper, B., 2010. Gamma-secretase and the intramembrane proteolysis of Notch. *Curr. Top. Dev. Biol*. 92, 201–230. https://doi.org/10.1016/S0070-2153(10)92006-1

Kageyama, R., Ohtsuka, T., Kobayashi, T., 2007. The Hes gene family: Repressors and oscillators that orchestrate embryogenesis. *Development* 134, 1243–1251. https://doi.org/10.1242/dev.000786

Kao, H.Y., Ordentlich, P., Koyano-Nakagawa, N., Tang, Z., Downes, M., Kintner, C.R., Evans, R.M., Kadesch, T., 1998. A histone deacetylase corepressor complex regulates the Notch signal transduction pathway. *Genes Dev*. 12, 2269–2277. https://doi.org/10.1101/gad.12.15.2269

Karimi, K., Fortriede, J.D., Lotay, V.S., Burns, K.A., Wang, D.Z., Fisher, M.E., Pells, T.J., James-Zorn, C., Wang, Y., Ponferrada, V.G., Chu, S., Chaturvedi, P., Zorn, A.M., Vize, P.D., 2018. Xenbase: A genomic, epigenomic and transcriptomic model organism database. *Nucleic Acids Res* 46, D861–D868. https://doi.org/10.1093/nar/gkx936

Katada, T., Kinoshita, T., 2003. XMam1, the Xenopus homologue of mastermind, is essential to primary neurogenesis in *Xenopus laevis* embryos. *Int. J. Dev. Biol*. 47, 397–404. https://doi.org/10.1387/IJDB.14584777

Keller, R., Danilchik, M., 1988. Regional expression, pattern and timing of convergence and extension during gastrulation of *Xenopus laevis*. *Development* 103, 193–209.

Kenyon, K.L., Moody, S.A., Jamrich, M., 1999. A novel fork head gene mediates early steps during Xenopus lens formation. *Development* 126, 5107–5116.

Kiecker, C., Niehrs, C., 2001. The role of prechordal mesendoderm in neural patterning. *Curr. Opin. Neurobiol*. 11, 27–33.

Kim, S.H., Jen, W.C., De Robertis, E.M., Kintner, C., 2000. The protocadherin PAPC establishes segmental boundaries during somitogenesis in xenopus embryos. *Curr. Biol*. 10, 821–830.

Kinoshita, T., Haruta, Y., Sakamoto, C., Imaoka, S., 2011. Antagonistic role of XESR1 and XESR5 in mesoderm formation in *Xenopus laevis*. *Int. J. Dev. Biol*. 55, 25–31. https://doi.org/10.1387/ijdb.092990tk

Kirby, M.L., Lawson, A., Stadt, H.A., Kumiski, D.H., Wallis, K.T., McCraney, E., Waldo, K.L., Li, Y.-X., Schoenwolf, G.C., 2003. Hensen's node gives rise to the ventral midline of the foregut: Implications for organizing head and heart development. *Dev. Biol*. 253, 175–188. https://doi.org/10.1016/S0012-1606(02)00024-6

Kirmizitas, A., Meiklejohn, S., Ciau-Uitz, A., Stephenson, R., Patient, R., 2017. Dissecting BMP signaling input into the gene regulatory networks driving specification of the blood stem cell lineage. *Proc. Natl. Acad. Sci. U. S. A*. 114, 5814–5821. https://doi.org/10.1073/pnas.1610615114

Kiyota, T., Jono, H., Kuriyama, S., Hasegawa, K., Miyatani, S., Kinoshita, T., 2001. X-Serrate-1 is involved in primary neurogenesis in *Xenopus laevis* in a complementary manner with X-Delta-1. *Dev. Genes Evol*. 211, 367–376. https://doi.org/10.1007/s004270100165

Kiyota, T., Kinoshita, T., 2004. The intracellular domain of X-Serrate-1 is cleaved and suppresses primary neurogenesis in *Xenopus laevis*. *Mech. Dev*. 121, 573–585. https://doi.org/10.1016/j.mod.2004.03.034

Kjolby, R.A.S., Harland, R.M., 2017. Genome-wide identification of Wnt/β-catenin transcriptional targets during Xenopus gastrulation. *Dev. Biol*. 426, 165–175. https://doi.org/10.1016/j.ydbio.2016.03.021

Kondow, A., Hitachi, K., Ikegame, T., Asashima, M., 2006. Bowline, a novel protein localized to the presomitic mesoderm,

interacts with Groucho/TLE in Xenopus. *Int. J. Dev. Biol*. 50, 473–479. https://doi.org/10.1387/ijdb.052138ak

Kondow, A., Hitachi, K., Okabayashi, K., Hayashi, N., Asashima, M., 2007. Bowline mediates association of the transcriptional corepressor XGrg-4 with Tbx6 during somitogenesis in Xenopus. *Biochem. Biophys. Res. Commun*. 359, 959–964. https://doi.org/10.1016/j.bbrc.2007.05.211

Kopan, R., Ilagan, M.X.G., 2009. The canonical Notch signaling pathway: Unfolding the activation mechanism. *Cell* 137, 216–233. https://doi.org/10.1016/j.cell.2009.03.045

Kopan, R., Nye, J.S., Weintraub, H., 1994. The intracellular domain of mouse Notch: A constitutively activated repressor of myogenesis directed at the basic helix-loop-helix region of MyoD. *Development* 120, 2385–2396.

Kovall, R.A., Blacklow, S.C., 2010. Mechanistic insights into Notch receptor signaling from structural and biochemical studies. *Curr. Top. Dev. Biol*. 92, 31–71. https://doi.org/10.1016/S0070-2153(10)92002-4

Koyano-Nakagawa, N., Kim, J., Anderson, D., Kintner, C., 2000. Hes6 acts in a positive feedback loop with the neurogenins to promote neuronal differentiation. *Development* 127, 4203–4216.

Kurata, T., Ueno, N., 2003. Xenopus Nbx, a novel NK-1 related gene essential for neural crest formation. *Dev. Biol*. 257, 30–40. https://doi.org/10.1016/s0012-1606(03)00060-5

Kuriyama, S., Lupo, G., Ohta, K., Ohnuma, S., Harris, W.A., Tanaka, H., 2006. Tsukushi controls ectodermal patterning and neural crest specification in Xenopus by direct regulation of BMP4 and X-delta-1 activity. *Development* 133, 75–88. https://doi.org/10.1242/dev.02178

Kuroda, H., Wessely, O., De Robertis, E.M., 2004. Neural induction in Xenopus: Requirement for ectodermal and endomesodermal signals via Chordin, Noggin, beta-Catenin, and Cerberus. *PLoS Biol*. 2, E92. https://doi.org/10.1371/journal.pbio.0020092

Kwon, C., Cheng, P., King, I.N., Andersen, P., Shenje, L., Nigam, V., Srivastava, D., 2011. Notch post-translationally regulates β-catenin protein in stem and progenitor cells. *Nat. Cell Biol*. 13, 1244–1251. https://doi.org/10.1038/ncb2313

Lahaye, K., Kricha, S., Bellefroid, E.J., 2002. XNAP, a conserved ankyrin repeat-containing protein with a role in the Notch pathway during Xenopus primary neurogenesis. *Mech. Dev*. 110, 113–124. https://doi.org/10.1016/S0925-4773(01)00570-6

Lai, E.C., 2004. Notch signaling: Control of cell communication and cell fate. *Development* 131, 965–973. https://doi.org/10.1242/dev.01074

Lamar, E., Deblandre, G., Wettstein, D., Gawantka, V., Pollet, N., Niehrs, C., Kintner, C., 2001. Nrarp is a novel intracellular component of the Notch signaling pathway. *Genes Dev*. 15, 1885–1899. https://doi.org/10.1101/gad.908101

Lamar, E., Kintner, C., 2005. The Notch targets Esr1 and Esr10 are differentially regulated in Xenopus neural precursors. *Development* 132, 3619–3630. https://doi.org/10.1242/dev.01937

Layden, M.J., Martindale, M.Q., 2014. Non-canonical Notch signaling represents an ancestral mechanism to regulate neural differentiation. *Evodevo* 5, 30. https://doi.org/10.1186/2041-9139-5-30

Lee, J., Platt, K.A., Censullo, P., Ruiz i Altaba, A., 1997. Gli1 is a target of Sonic hedgehog that induces ventral neural tube development. *Development* 124, 2537–2552.

Lehmann, R., Jiménez, F., Dietrich, U., Campos-Ortega, J.A., 1983. On the phenotype and development of mutants of early neurogenesis in *Drosophila melanogaster*: Wilhelm Roux's Arch. *Dev. Biol*. 192, 62–74. https://doi.org/10.1007/BF00848482

Leung, A., Ciau-Uitz, A., Pinheiro, P., Monteiro, R., Zuo, J., Vyas, P., Patient, R., Porcher, C., 2013. Uncoupling VEGFA functions in arteriogenesis and hematopoietic stem cell specification. *Dev. Cell* 24, 144–158. https://doi.org/10.1016/j.devcel.2012.12.004

Lewis, J., 1998. Notch signalling and the control of cell fate choices in vertebrates. *Semin. Cell Dev. Biol*. 9, 583–589. https://doi.org/10.1006/scdb.1998.0266

Li, Y., Fenger, U., Niehrs, C., Pollet, N., 2003. Cyclic expression of esr9 gene in Xenopus presomitic mesoderm. *Differentiation* 71, 83–89. https://doi.org/10.1046/j.1432-0436.2003.700608.x

López, S.L., Carrasco, A.E., 2006. Sonic hedgehog signalling in dorsal midline and neural development. In: Fisher, C.E., Howie, S.E.M. (Eds.), *Shh and Gli Signalling and Development*. Landes Biosciences and Springer New York, New York, NY, pp. 12–22.

López, S.L., Paganelli, A.R., Rosato Siri, M. V, Ocaña, O.H., Franco, P.G., Carrasco, A.E., 2003. Notch activates Sonic hedgehog and both are involved in the specification of dorsal midline cell-fates in Xenopus. *Development* 130, 2225–2238. https://doi.org/10.1242/dev.00443

López, S.L., Rosato-Siri, M. V, Franco, P.G., Paganelli, A.R., Carrasco, A.E., 2005. The Notch-target gene hairy2a impedes the involution of notochordal cells by promoting floor plate fates in Xenopus embryos. *Development* 132, 1035–1046. https://doi.org/10.1242/dev.01659

Ma, Q., Kintner, C., Anderson, D.J., 1996. Identification of neurogenin, a vertebrate neuronal determination gene. *Cell* 87, 43–52.

Maguire, R.J., Isaacs, H. V., Pownall, M.E., 2012. Early transcriptional targets of MyoD link myogenesis and somitogenesis. *Dev. Biol*. 371, 256–268. https://doi.org/10.1016/j.ydbio.2012.08.027

Maharana, S.K., Schlosser, G., 2018. A gene regulatory network underlying the formation of pre-placodal ectoderm in *Xenopus laevis*. *BMC Biol*. 16, 79. https://doi.org/10.1186/s12915-018-0540-5

Marcet, B., Chevalier, B., Luxardi, G., Coraux, C., Zaragosi, L.-E., Cibois, M., Robbe-Sermesant, K., Jolly, T., Cardinaud, B., Moreilhon, C., Giovannini-Chami, L., Nawrocki-Raby, B., Birembaut, P., Waldmann, R., Kodjabachian, L., Barbry, P., 2011. Control of vertebrate multiciliogenesis by miR-449 through direct repression of the Delta/Notch pathway. *Nat. Cell Biol*. 13, 694–701. https://doi.org/10.1038/ncb2241

Marine, J.-C., Bellefroid, J.E., Pendeville, H., Martial, J.A., Pieler, T., 1997. A role for Xenopus Gli-type zinc finger proteins in the early embryonic patterning of mesoderm and neuroectoderm. *Mech. Dev*. 63, 211–225. https://doi.org/10.1016/S0925-4773(97)00050-6

McLaughlin, K.A., Rones, M.S., Mercola, M., 2000. Notch regulates cell fate in the developing pronephros. *Dev. Biol*. 227, 567–580. https://doi.org/10.1006/dbio.2000.9913

Meier-Stiegen, F., Schwanbeck, R., Bernoth, K., Martini, S., Hieronymus, T., Ruau, D., Zenke, M., Just, U., 2010. Activated Notch1 target genes during embryonic cell differentiation depend on the cellular context and include lineage determinants and inhibitors. *PLoS One* 5, e11481. https://doi.org/10.1371/journal.pone.0011481

Miazga, C.M., McLaughlin, K.A., 2009. Coordinating the timing of cardiac precursor development during gastrulation: A new role for Notch signaling. *Dev. Biol*. 333, 285–296. https://doi.org/10.1016/j.ydbio.2009.06.040

Michiue, T., Yamamoto, T., Yasuoka, Y., Goto, T., Ikeda, T., Nagura, K., Nakayama, T., Taira, M., Kinoshita, T., 2017. High

variability of expression profiles of homeologous genes for Wnt, Hh, Notch, and Hippo signaling pathways in *Xenopus laevis*. *Dev. Biol*. 426, 270–290. https://doi.org/10.1016/j.ydbio.2016.12.006

Milet, C., Maczkowiak, F., Roche, D.D., Monsoro-Burq, A.H., 2013. Pax3 and Zic1 drive induction and differentiation of multipotent, migratory, and functional neural crest in Xenopus embryos. *Proc. Natl. Acad. Sci. U. S. A*. 110, 5528–5533. https://doi.org/10.1073/pnas.1219124110

Minsuk, S.B., Keller, R.E., 1997. Surface mesoderm in Xenopus: A revision of the stage 10 fate map. *Dev. Genes Evol*. 207, 389–401. https://doi.org/10.1007/s004270050128

Mir, A., Kofron, M., Heasman, J., Mogle, M., Lang, S., Birsoy, B., Wylie, C., 2008. Long- and short-range signals control the dynamic expression of an animal hemisphere-specific gene in Xenopus. *Dev. Biol*. 315, 161–172. https://doi.org/10.1016/j.ydbio.2007.12.022

Mohr, O.L., 1919. Character changes caused by mutation of an entire region of a chromosome in Drosophila. *Genetics* 4, 275–282.

Moody, S.A., 1987a. Fates of the blastomeres of the 16-cell stage Xenopus embryo. *Dev. Biol*. 119, 560–578. https://doi.org/10.1016/0012-1606(87)90059-5

Moody, S.A., 1987b. Fates of the blastomeres of the 32-cell-stage Xenopus embryo. *Dev. Biol*. 122, 300–319. https://doi.org/10.1016/0012-1606(87)90296-x

Moreno, T.A., Kintner, C., 2004. Regulation of segmental patterning by retinoic acid signaling during Xenopus somitogenesis. *Dev. Cell* 6, 205–218. https://doi.org/10.1016/S1534-5807(04)00026-7

Morgan, T.H., 1917. The theory of the gene. *Am. Nat*. 51, 513–544. https://doi.org/10.1086/279629

Muñoz-Descalzo, S., Sanders, P.G.T., Montagne, C., Johnson, R.I., Balayo, T., Martinez Arias, A., 2010. Wingless modulates the ligand independent traffic of Notch through Dishevelled. *Fly (Austin)*. 4, 182–193. https://doi.org/10.4161/fly.4.3.11998

Murai, K., Philpott, A., Jones, P.H., 2011. Hes6 is required for the neurogenic activity of neurogenin and NeuroD. *PLoS One* 6, e27880. https://doi.org/10.1371/journal.pone.0027880

Murai, K., Vernon, A.E., Philpott, A., Jones, P., 2007. Hes6 is required for MyoD induction during gastrulation. *Dev. Biol*. 312, 61–76. https://doi.org/10.1016/j.ydbio.2007.09.011

Murato, Y., Hashimoto, C., 2009. Xhairy2 functions in Xenopus lens development by regulating p27(xic1) expression. *Dev. Dyn*. 238, 2179–2192. https://doi.org/10.1002/dvdy.21883

Murato, Y., Nagatomo, K., Yamaguti, M., Hashimoto, C., 2007. Two alloalleles of *Xenopus laevis* hairy2 gene: Evolution of duplicated gene function from a developmental perspective. *Dev. Genes Evol*. 217, 665–673. https://doi.org/10.1007/s00427-007-0176-x

Murato, Y., Yamaguti, M., Katamura, M., Cho, K.W.Y., Hashimoto, C., 2006. Two modes of action by which Xenopus hairy2b establishes tissue demarcation in the Spemann-Mangold organizer. *Int. J. Dev. Biol*. 50, 463–471. https://doi.org/10.1387/ijdb.052106ym

Murgan, S., Castro Colabianchi, A.M., Monti, R.J., Boyadjián López, L.E., Aguirre, C.E., Stivala, E.G., Carrasco, A.E., López, S.L., 2014. FoxA4 favours notochord formation by inhibiting contiguous mesodermal fates and restricts anterior neural development in Xenopus embryos. *PLoS One* 9, e110559. https://doi.org/10.1371/journal.pone.0110559

Nagano, T., Takehara, S., Takahashi, M., Aizawa, S., Yamamoto, A., 2006. Shisa2 promotes the maturation of somitic precursors and transition to the segmental fate in Xenopus embryos. *Development* 133, 4643–4654. https://doi.org/10.1242/dev.02657

Nagatomo, K., Hashimoto, C., 2007. Xenopus hairy2 functions in neural crest formation by maintaining cells in a mitotic and undifferentiated state. *Dev. Dyn*. 236, 1475–1483. https://doi.org/10.1002/dvdy.21152

Nakata, K., Nagai, T., Aruga, J., Mikoshiba, K., 1998. Xenopus Zic family and its role in neural and neural crest development. *Mech. Dev*. 75, 43–51. https://doi.org/10.1016/S0925-4773(98)00073-2

Naoki, H., Matsui, T., 2020. Somite boundary determination in normal and clock-less vertebrate embryos. *Dev. Growth Differ*. 62, 177–187. https://doi.org/10.1111/dgd.12655

Nichane, M., de Crozé, N., Ren, X., Souopgui, J., Monsoro-Burq, A.H., Bellefroid, E.J., 2008a. Hairy2-Id3 interactions play an essential role in Xenopus neural crest progenitor specification. *Dev. Biol*. 322, 355–367. https://doi.org/10.1016/j.ydbio.2008.08.003

Nichane, M., Ren, X., Bellefroid, E.J., 2010. Self-regulation of Stat3 activity coordinates cell-cycle progression and neural crest specification. *EMBO J*. 29, 55–67. https://doi.org/10.1038/emboj.2009.313

Nichane, M., Ren, X., Souopgui, J., Bellefroid, E.J., 2008b. Hairy2 functions through both DNA-binding and non DNA-binding mechanisms at the neural plate border in Xenopus. *Dev. Biol*. 322, 368–380. https://doi.org/10.1016/j.ydbio.2008.07.026

Nieber, F., Hedderich, M., Jahn, O., Pieler, T., Henningfeld, K.A., 2013. NumbL is essential for Xenopus primary neurogenesis. *BMC Dev. Biol*. 13, 36. https://doi.org/10.1186/1471-213X-13-36

Nimmo, R., Ciau-Uitz, A., Ruiz-Herguido, C., Soneji, S., Bigas, A., Patient, R., Enver, T., 2013. MiR-142–3p controls the specification of definitive hemangioblasts during ontogeny. *Dev. Cell* 26, 237–249. https://doi.org/10.1016/j.devcel.2013.06.023

Oates, A.C., Morelli, L.G., Ares, S., 2012. Patterning embryos with oscillations: Structure, function and dynamics of the vertebrate segmentation clock. *Development* 139, 625–639. https://doi.org/10.1242/dev.063735

Ogino, H., Fisher, M., Grainger, R.M., 2008. Convergence of a head-field selector Otx2 and Notch signaling: A mechanism for lens specification. *Development* 135, 249–258. https://doi.org/10.1242/dev.009548

Olson, E.C., Schinder, A.F., Dantzker, J.L., Marcus, E.A., Spitzer, N.C., Harris, W.A., 1998. Properties of ectopic neurons induced by Xenopus neurogenin1 misexpression. *Mol. Cell. Neurosci*. 12, 281–299. https://doi.org/10.1006/mcne.1998.0712

Onai, T., Aramaki, T., Inomata, H., Hirai, T., Kuratani, S., 2015. On the origin of vertebrate somites. *Zool. Lett*. 1, 33. https://doi.org/10.1186/s40851-015-0033-0

Oswald, F., Rodriguez, P., Giaimo, B.D., Antonello, Z.A., Mira, L., Mittler, G., Thiel, V.N., Collins, K.J., Tabaja, N., Cizelsky, W., Rothe, M., Kühl, S.J., Kühl, M., Ferrante, F., Hein, K., Kovall, R.A., Dominguez, M., Borggrefe, T., 2016. A phospho-dependent mechanism involving NCoR and KMT2D controls a permissive chromatin state at Notch target genes. *Nucleic Acids Res*. 44, 4703–4720. https://doi.org/10.1093/nar/gkw105

Paganelli, A.R., Ocaña, O.H., Prat, M.I., Franco, P.G., López, S.L., Morelli, L., Adamo, A.M., Riccomagno, M.M., Matsubara, E., Shoji, M., Affranchino, J.L., Castaño, E.M., Carrasco, A.E., 2001. The Alzheimer-related gene presenilin-1 facilitates Sonic hedgehog expression in Xenopus primary neurogenesis. *Mech. Dev*. 107, 119–131. https://doi.org/10.1016/s0925-4773(01)00458-0

Papalopulu, N., Kintner, C., 1996. A posteriorising factor, retinoic acid, reveals that anteroposterior patterning controls the timing of neuronal differentiation in Xenopus neuroectoderm. *Development* 122, 3409–3418.

Parlier, D., Moers, V., Van Campenhout, C., Preillon, J., Leclère, L., Saulnier, A., Sirakov, M., Busengdal, H., Kricha, S., Marine, J.-C., Rentzsch, F., Bellefroid, E.J., 2013. The Xenopus doublesex-related gene Dmrt5 is required for olfactory placode neurogenesis. *Dev. Biol*. 373, 39–52. https://doi.org/10.1016/J.YDBIO.2012.10.003

Pegoraro, C., Monsoro-Burq, A.H., 2013. Signaling and transcriptional regulation in neural crest specification and migration: Lessons from Xenopus embryos. *WIREs Dev. Biol*. 2, 247–259. https://doi.org/10.1002/wdev.76

Peres, J.N., Durston, A.J., 2006. Role of X-Delta-2 in the early neural development of *Xenopus laevis*. *Dev. Dyn*. 235, 802–810. https://doi.org/10.1002/dvdy.20677

Peres, J.N., McNulty, C.L., Durston, A.J., 2006. Interaction between X-Delta-2 and Hox genes regulates segmentation and patterning of the anteroposterior axis. *Mech. Dev*. 123, 321–333. https://doi.org/10.1016/j.mod.2006.03.001

Perron, M., Opdecamp, K., Butler, K., Harris, W.A., Bellefroid, E.J., 1999. X-ngnr-1 and Xath3 promote ectopic expression of sensory neuron markers in the neurula ectoderm and have distinct inducing properties in the retina. *Proc. Natl. Acad. Sci. U. S. A*. 96, 14996–15001. https://doi.org/10.1073/PNAS.96.26.14996

Peyrot, S.M., Wallingford, J.B., Harland, R.M., 2011. A revised model of Xenopus dorsal midline development: Differential and separable requirements for Notch and Shh signaling. *Dev. Biol*. 352, 254–266. https://doi.org/10.1016/j.ydbio.2011.01.021

Pichon, B., Taelman, V., Bellefroid, E.J., Christophe, D., 2004. Transcriptional repression by the bHLH-Orange factor XHRT1 does not involve the C-terminal YRPW motif. *Biochim. Biophys. Acta-Gene Struct. Expr*. 1680, 46–52. https://doi.org/10.1016/j.bbaexp.2004.08.010

Pichon, B., Taelman, V., Kricha, S., Christophe, D., Bellefroid, E.J., 2002. XHRT-1, a hairy and enhancer of split related gene with expression in floor plate and hypochord during early Xenopus embryogenesis. *Dev. Genes Evol*. 212, 491–495. https://doi.org/10.1007/s00427-002-0270-z

Pla, P., Monsoro-Burq, A.H., 2018. The neural border: Induction, specification and maturation of the territory that generates neural crest cells. *Dev. Biol*. 444, S36–S46. https://doi.org/10.1016/j.ydbio.2018.05.018

Pollet, N., Muncke, N., Verbeek, B., Li, Y., Fenger, U., Delius, H., Niehrs, C., 2005. An atlas of differential gene expression during early Xenopus embryogenesis. *Mech. Dev*. 122, 365–439. https://doi.org/10.1016/j.mod.2004.11.009

Poulson, D.F., 1937. Chromosomal deficiencies and the embryonic development of *Drosophila melanogaster*. *Proc. Natl. Acad. Sci. U. S. A*. 23, 133–137.

Pourquié, O., Tam, P.P.L., 2001. A nomenclature for prospective somites and phases of cyclic gene expression in the presomitic mesoderm. *Dev. Cell* 1, 619–620. https://doi.org/10.1016/s1534-5807(01)00082-x

Revinski, D.R., Paganelli, A.R., Carrasco, A.E., López, S.L., 2010. Delta-Notch signaling is involved in the segregation of the three germ layers in *Xenopus laevis*. *Dev. Biol*. 339, 477–492. https://doi.org/10.1016/j.ydbio.2010.01.010

Riddiford, N., Schlosser, G., 2016. Dissecting the pre-placodal transcriptome to reveal presumptive direct targets of Six1 and Eya1 in cranial placodes. *Elife* 5. https://doi.org/10.7554/eLife.17666

Riddiford, N., Schlosser, G., 2017. Six1 and Eya1 both promote and arrest neuronal differentiation by activating multiple Notch pathway genes. *Dev. Biol*. 431, 152–167. https://doi.org/10.1016/J.YDBIO.2017.09.027

Roberts, A., 1989. The neurons that control axial movements in a frog embryo. *Am. Zool*. 29, 53–63. https://doi.org/10.1093/icb/29.1.53

Rones, M.S., Woda, J., Mercola, M., McLaughlin, K.A., 2002. Isolation and characterization of Xenopus Hey-1: A downstream mediator of notch signaling. *Dev. Dyn*. 225, 554–560. https://doi.org/10.1002/dvdy.10192

Saint-Jeannet, J.-P., Moody, S.A., 2014. Establishing the preplacodal region and breaking it into placodes with distinct identities. *Dev. Biol*. 389, 13–27. https://doi.org/10.1016/j.ydbio.2014.02.011

Sakano, D., Kato, A., Parikh, N., McKnight, K., Terry, D., Stefanovic, B., Kato, Y., 2010. BCL6 canalizes Notch-dependent transcription, excluding Mastermind-like1 from selected target genes during left-right patterning. *Dev. Cell* 18, 450–462. https://doi.org/10.1016/j.devcel.2009.12.023

Sanalkumar, R., Dhanesh, S.B., James, J., 2010. Non-canonical activation of Notch signaling/target genes in vertebrates. *Cell. Mol. Life Sci*. 67, 2957–2968. https://doi.org/10.1007/s00018-010-0391-x

Sanders, P.G.T., Muñoz-Descalzo, S., Balayo, T., Wirtz-Peitz, F., Hayward, P., Martinez Arias, A., 2009. Ligand-independent traffic of Notch buffers activated Armadillo in Drosophila. *PLoS Biol*. 7, e1000169. https://doi.org/10.1371/journal.pbio.1000169

Sasaki, N., Kiso, M., Kitagawa, M., Saga, Y., 2011. The repression of Notch signaling occurs via the destabilization of mastermind-like 1 by Mesp2 and is essential for somitogenesis. *Development* 138, 55–64. https://doi.org/10.1242/dev.055533

Schlosser, G., Awtry, T., Brugmann, S.A., Jensen, E.D., Neilson, K., Ruan, G., Stammler, A., Voelker, D., Yan, B., Zhang, C., Klymkowsky, M.W., Moody, S.A., 2008. Eya1 and Six1 promote neurogenesis in the cranial placodes in a SoxB1-dependent fashion. *Dev. Biol*. 320, 199–214. https://doi.org/10.1016/J.YDBIO.2008.05.523

Schneider, M.L., Turner, D.L., Vetter, M.L., 2001. Notch signaling can inhibit Xath5 function in the neural plate and developing retina. *Mol. Cell. Neurosci*. 18, 458–472. https://doi.org/10.1006/mcne.2001.1040

Seo, S., Lim, J.-W., Yellajoshyula, D., Chang, L.-W., Kroll, K.L., 2007. Neurogenin and NeuroD direct transcriptional targets and their regulatory enhancers. *EMBO J*. 26, 5093–5108. https://doi.org/10.1038/sj.emboj.7601923

Session, A.M., Uno, Y., Kwon, T., Chapman, J.A., Toyoda, A., Takahashi, S., Fukui, A., Hikosaka, A., Suzuki, A., Kondo, M., van Heeringen, S.J., Quigley, I., Heinz, S., Ogino, H., Ochi, H., Hellsten, U., Lyons, J.B., Simakov, O., Putnam, N., Stites, J., Kuroki, Y., Tanaka, T., Michiue, T., Watanabe, M., Bogdanovic, O., Lister, R., Georgiou, G., Paranjpe, S.S., van Kruijsbergen, I., Shu, S., Carlson, J., Kinoshita, T., Ohta, Y., Mawaribuchi, S., Jenkins, J., Grimwood, J., Schmutz, J., Mitros, T., Mozaffari, S. V., Suzuki, Y., Haramoto, Y., Yamamoto, T.S., Takagi, C., Heald, R., Miller, K., Haudenschild, C., Kitzman, J., Nakayama, T., Izutsu, Y., Robert, J., Fortriede, J., Burns, K., Lotay, V., Karimi, K., Yasuoka, Y., Dichmann, D.S., Flajnik, M.F., Houston, D.W., Shendure, J., DuPasquier, L., Vize, P.D., Zorn, A.M., Ito, M., Marcotte, E.M., Wallingford, J.B., Ito, Y., Asashima, M., Ueno, N., Matsuda, Y., Veenstra, G.J.C., Fujiyama, A., Harland, R.M., Taira, M., Rokhsar, D.S., 2016.

Genome evolution in the allotetraploid frog *Xenopus laevis*. *Nature* 538, 336–343. https://doi.org/10.1038/nature19840

Shinga, J., Itoh, M., Shiokawa, K., Taira, S., Taira, M., 2001. Early patterning of the prospective midbrain: Hindbrain boundary by the HES-related gene XHR1 in Xenopus embryos. *Mech. Dev*. 109, 225–239. https://doi.org/10.1016/S0925-4773(01)00528-7

Shook, D.R., Majer, C., Keller, R., 2004. Pattern and morphogenesis of presumptive superficial mesoderm in two closely related species, *Xenopus laevis* and *Xenopus tropicalis*. *Dev. Biol*. 270, 163–185. https://doi.org/10.1016/j.ydbio.2004.02.021

Sjöqvist, M., Andersson, E.R., 2019. Do as I say, Not(ch) as I do: Lateral control of cell fate. *Dev. Biol*. 447, 58–70. https://doi.org/10.1016/j.ydbio.2017.09.032

Sölter, M., Locker, M., Boy, S., Taelman, V., Bellefroid, E.J., Perron, M., Pieler, T., 2006. Characterization and function of the bHLH-O protein XHes2: Insight into the mechanisms controlling retinal cell fate decision. *Development* 133, 4097–4108. https://doi.org/10.1242/dev.02567

Souopgui, J., Sölter, M., Pieler, T., 2002. XPak3 promotes cell cycle withdrawal during primary neurogenesis in *Xenopus laevis*. *EMBO J*. 21, 6429–6439.

Sparrow, D.B., 2008. Old wares and new: Five decades of investigation of somitogenesis in *Xenopus laevis*. *Adv. Exp. Med. Biol*. 638, 73–94. https://doi.org/10.1007/978-0-387-09606-3_4

Sparrow, D.B., Jen, W.C., Kotecha, S., Towers, N., Kintner, C., Mohun, T.J., 1998. Thylacine 1 is expressed segmentally within the paraxial mesoderm of the Xenopus embryo and interacts with the Notch pathway. *Development* 125, 2041–2051.

Steventon, B., Mayor, R., 2012. Early neural crest induction requires an initial inhibition of Wnt signals. *Dev Biol* 365, 196–207. https://doi.org/10.1016/j.ydbio.2012.02.029

Steventon, B., Mayor, R., Streit, A., 2014. Neural crest and placode interaction during the development of the cranial sensory system. *Dev. Biol*. 389, 28–38. https://doi.org/10.1016/j.ydbio.2014.01.021

Stuhlmiller, T.J., García-Castro, M.I., 2012. Current perspectives of the signaling pathways directing neural crest induction. *Cell. Mol. Life Sci*. 69, 3715–3737. https://doi.org/10.1007/s00018-012-0991-8

Taelman, V., Van Campenhout, C., Sölter, M., Pieler, T., Bellefroid, E.J., 2006. The Notch-effector HRT1 gene plays a role in glomerular development and patterning of the Xenopus pronephros anlagen. *Development* 133, 2961–2971. https://doi.org/10.1242/dev.02458

Taelman, V., Van Wayenbergh, R., Sölter, M., Pichon, B., Pieler, T., Christophe, D., Bellefroid, E.J., 2004. Sequences downstream of the bHLH domain of the Xenopus hairy-related transcription factor-1 act as an extended dimerization domain that contributes to the selection of the partners. *Dev. Biol*. 276, 47–63. https://doi.org/10.1016/j.ydbio.2004.08.019

Takada, H., Hattori, D., Kitayama, A., Ueno, N., Taira, M., 2005. Identification of target genes for the Xenopus Hes-related protein XHR1, a prepattern factor specifying the midbrain-hindbrain boundary. *Dev. Biol*. 283, 253–267. https://doi.org/10.1016/j.ydbio.2005.04.020

Takahashi, Y., Koizumi, K.I., Takagi, A., Kitajima, S., Inoue, T., Koseki, H., Saga, Y., 2000. Mesp2 initiates somite segmentation through the Notch signalling pathway. *Nat. Genet*. 25, 390–396. https://doi.org/10.1038/78062

Tanigaki, K., Honjo, T., 2010. Two opposing roles of RBP-J in Notch signaling. *Curr. Top. Dev. Biol*. 92, 231–252. https://doi.org/10.1016/S0070-2153(10)92007-3

Taverner, N. V., Kofron, M., Shin, Y., Kabitschke, C., Gilchrist, M.J., Wylie, C., Cho, K.W.Y., Heasman, J., Smith, J.C., 2005. Microarray-based identification of VegT targets in Xenopus. *Mech. Dev*. 122, 333–354. https://doi.org/10.1016/J.MOD.2004.10.010

Thisse, B., Thisse, C., 2015. Formation of the vertebrate embryo: Moving beyond the Spemann organizer. *Semin. Cell Dev. Biol*. 42, 1–9. https://doi.org/10.1016/j.semcdb.2015.05.007

Thurmond, J., Goodman, J.L., Strelets, V.B., Attrill, H., Gramates, L.S., Marygold, S.J., Matthews, B.B., Millburn, G., Antonazzo, G., Trovisco, V., Kaufman, T.C., Calvi, B.R., Perrimon, N., Gelbart, S.R., Agapite, J., Broll, K., Crosby, L., Dos Santos, G., Emmert, D., Falls, K., Jenkins, V., Sutherland, C., Tabone, C., Zhou, P., Zytkovicz, M., Brown, N., Garapati, P., Holmes, A., Larkin, A., Pilgrim, C., Urbano, P., Czoch, B., Cripps, R., Baker, P., 2019. FlyBase 2.0: The next generation. *Nucleic Acids Res*. 47, D759–D765. https://doi.org/10.1093/nar/gky1003

Tomankova, S., Abaffy, P., Sindelka, R., 2017. The role of nitric oxide during embryonic epidermis development of *Xenopus laevis*. *Biol. Open* 6, 862–871. https://doi.org/10.1242/bio.023739

Tözser, J., Earwood, R., Kato, A., Brown, J., Tanaka, K., Didier, R., Megraw, T.L., Blum, M., Kato, Y., 2015. TGF-β signaling regulates the differentiation of motile cilia. *Cell Rep*. 11, 1000–1007. https://doi.org/10.1016/j.celrep.2015.04.025

Tsuji, S., Cho, K.W.Y., Hashimoto, C., 2003. Expression pattern of a basic helix-loop-helix transcription factor Xhairy2b during *Xenopus laevis* development. *Dev. Genes Evol*. 213, 407–411. https://doi.org/10.1007/s00427-003-0338-4

Turner, D.L., Weintraub, H., 1994. Expression of achaete-scute homolog 3 in Xenopus embryos converts ectodermal cells to a neural fate. *Genes Dev*. 8, 1434–1447. https://doi.org/10.1101/gad.8.12.1434

Ueno, T., Ishihara, A., Yagi, S., Koike, T., Yamauchi, K., Shiojiri, N., 2015. Histochemical analyses of biliary development during metamorphosis of *Xenopus laevis* tadpoles. *Zool. Sci*. 32, 88–96. https://doi.org/10.2108/zs140104

Umbhauer, M., Boucaut, J.C., Shi, D.L., 2001. Repression of XMyoD expression and myogenesis by Xhairy-1 in Xenopus early embryo. *Mech. Dev*. 109, 61–68.

Vasiliu, D., Clamons, S., McDonough, M., Rabe, B., Saha, M., 2015. A regression-based differential expression detection algorithm for microarray studies with ultra-low sample size. *PLoS One* 10. https://doi.org/10.1371/journal.pone.0118198

Vega-López, G.A., Bonano, M., Tríbulo, C., Fernández, J.P., Agüero, T.H., Aybar, M.J., 2015. Functional analysis of Hairy genes in Xenopus neural crest initial specification and cell migration. *Dev. Dyn*. 244, 988–1013. https://doi.org/10.1002/dvdy.24295

Venzin, O.F., Oates, A.C., 2020. What are you synching about? Emerging complexity of Notch signaling in the segmentation clock. *Dev. Biol*. 460, 40–54. https://doi.org/10.1016/j.ydbio.2019.06.024

Vernon, A.E., Movassagh, M., Horan, I., Wise, H., Ohnuma, S., Philpott, A., 2006. Notch targets the Cdk inhibitor Xic1 to regulate differentiation but not the cell cycle in neurons. *EMBO Rep*. 7, 643–648. https://doi.org/10.1038/sj.embor.7400691

Wacker, S.A., Alvarado, C., von Wichert, G., Knippschild, U., Wiedenmann, J., Clauss, K., Nienhaus, G.U., Hameister, H., Baumann, B., Borggrefe, T., Knöchel, W., Oswald, F., 2011. RITA, a novel modulator of Notch signalling, acts via

nuclear export of RBP-J. *EMBO J*. 30, 43–56. https://doi.org/10.1038/emboj.2010.289

Wahi, K., Bochter, M.S., Cole, S.E., 2016. The many roles of Notch signaling during vertebrate somitogenesis. *Semin. Cell Dev. Biol*. 49, 68–75. https://doi.org/10.1016/j.semcdb.2014.11.010

Wang, J., Li, S., Chen, Y., Ding, X., 2007. Wnt/β-catenin signaling controls Mespo expression to regulate segmentation during Xenopus somitogenesis. *Dev. Biol*. 304, 836–847. https://doi.org/10.1016/j.ydbio.2006.12.034

Wardle, F.C., Smith, J.C., 2004. Refinement of gene expression patterns in the early Xenopus embryo. *Development* 131, 4687–4696. https://doi.org/10.1242/dev.01340

Watanabe, M., Yasuoka, Y., Mawaribuchi, S., Kuretani, A., Ito, M., Kondo, M., Ochi, H., Ogino, H., Fukui, A., Taira, M., Kinoshita, T., 2017. Conservatism and variability of gene expression profiles among homeologous transcription factors in *Xenopus laevis*. *Dev. Biol*. 426, 301–324. https://doi.org/10.1016/j.ydbio.2016.09.017

Wessely, O., Agius, E., Oelgeschläger, M., Pera, E.M., De Robertis, E.M., 2001. Neural induction in the absence of mesoderm: Beta-catenin-dependent expression of secreted BMP antagonists at the blastula stage in Xenopus. *Dev. Biol*. 234, 161–173. https://doi.org/10.1006/dbio.2001.0258

Wettstein, D.A., Turner, D.L., Kintner, C., 1997. The Xenopus homolog of Drosophila suppressor of Hairless mediates Notch signaling during primary neurogenesis. *Development* 124, 693–702.

Wittenberger, T., Steinbach, O.C., Authaler, A., Kopan, R., Rupp, R.A., 1999. MyoD stimulates delta-1 transcription and triggers notch signaling in the Xenopus gastrula. *EMBO J*. 18, 1915–1922. https://doi.org/10.1093/emboj/18.7.1915

Yamaguti, M., Cho, K.W.Y., Hashimoto, C., 2005. Xenopus hairy2b specifies anterior prechordal mesoderm identity within Spemann's organizer. *Dev. Dyn*. 234, 102–113. https://doi.org/10.1002/dvdy.20523

Yan, B., Moody, S.A., 2007. The competence of Xenopus blastomeres to produce neural and retinal progeny is repressed by two endo-mesoderm promoting pathways. *Dev. Biol*. 305, 103–119. https://doi.org/10.1016/J.YDBIO.2007.01.040

Yan, B., Neilson, K.M., Moody, S.A., 2009. Notch signaling downstream of foxD5 promotes neural ectodermal transcription factors that inhibit neural differentiation. *Dev. Dyn*. 238, 1358–1365. https://doi.org/10.1002/dvdy.21885

Zhou, M., Yan, J., Ma, Z., Zhou, Y., Abbood, N.N., Liu, J., Su, L., Jia, H., Guo, A.-Y., 2012. Comparative and evolutionary analysis of the HES/HEY gene family reveal exon/intron loss and teleost specific duplication events. *PLoS One* 7, e40649. https://doi.org/10.1371/journal.pone.0040649

Zimmerman, K., Shih, J., Bars, J., Collazo, A., Anderson, D.J., 1993. XASH-3, a novel Xenopus achaete-scute homolog, provides an early marker of planar neural induction and position along the mediolateral axis of the neural plate. *Development* 119, 221–232.